LAKE SEDIMENT RECORDS OF ENVIRONMENTAL AND CLIMATIC CHANGES FROM NORTHERN ETHIOPIA (LAKE ASHANGE)

A THESIS

SUBMITTED TO THE SCHOOL OF GRADUATE STUDIES

ADDIS ABABA UNIVERSITY

IN PARTIAL FULFILMENT OF THE REQUIRMENT FOR THE DEGREE OF MASTER OF SCIENCE IN GEOLOGY

BY ZELALEM KUBSA

JANUARY 2005

ADDIS ABABA UNIVERSITY
SCHOOL OF GRADUATE STUDIES

Lake Sediment Records of Environmental and Climatic changes from Northern Ethiopia (Lake Ashange)

A THESIS
SUBMITTED TO THE SCHOOL OF GRADUATE STUDIES ADDIS ABABA UNIVERSITY

IN PARTIAL FULFILMENT OF THE REQUIRMENT FOR THE DEGREE OF MASTER OF SCIENCE IN GEOLOGY

Department of Geology and Geophysics

By ZELALEM KUBSA

JANUARY 2005

ADDIS ABABA UNIVERSITY
SCHOOL OF GRADUATE STUDIES

LAKE SEDIMENT RECORDS OF ENVIRONMENTAL AND CLIMATIC CHANGES FROM NORTHERN ETHIOPIA (LAKE ASHANGE)

By

Zelalem Kubsa

Department of Geology and Geophysics

Faculty of Science

Approved by Board of Examiners: **Signature**

Dr. Dereje Ayalew (Chairman/Examiner)

Dr. Mohammed Umer (Advisor)

Prof. Getaneh Assefa (Examiner)

Dr.Dagnachew Legesse(Examiner)

Dr. Tamrat Endale

Examiner (External)

ACKNOWLEDGMENT

My sincere thanks go to Mekelle and Addis Ababa Universities (particularly the respective departments of applied geology and geology & geophysics) for allowing and supporting this work to be done. I would like to give my deepest gratitude to Dr. Henry Lamb for facilitating the field trip to Ashange, for helping me to acquire the material upon which the study has been conducted and for arranging my laboratory work in The University of Wales, Aberystwyth. The Deutscher Akademischer Austauschdienst (DAAD) provided me with financial and logistic supports through in-country scholarship and sponsored my laboratory work in the Technical University of Berlin under the supervision of Dr. Robert Bussert. I appreciate his consistent help in guiding the laboratory work and in obtaining quality results as well as for correcting the thesis.

I am greatly indebted to my Advisor Dr Mohammed Umer for his guidance and instructive supervision of this thesis at its various stages. His close follow up, review and comments on the manuscript are highly appreciated. Moreover, the discussions I made with him on the results of this thesis and their interpretation were very important. I duly acknowledge his contributions to realize this study.

I am also grateful to all staff members of the Department of Geology and Geophysics for their various support. Special thanks goes to Dr. Dereje Ayalew, the head, whose assistance in helping me to acquire financial and logistic support was crucial and to Prof. Getaneh Assefa whose instruction in the basic sciences of sdimentology/stratigraphy and paleontology were paramount. Dr. Dagnachew Legesse, and Dr. Seifu Kebede provided valuable suggestions on the subject matter Ato Khalid Adem for his friendly help. W/o

Aynalem Gebeyehu and W/o Tsilat Adenew were kind in helping with matters of administrative and secretarial services.

I would like to extend my gratitude to Dr. Paul Comb and Mikael Henry Marshall for their friendly help in the field and in Wales.

I would like to thank Ato Hailu Dibbe for a comfortable drive to the field and Ato Weldeselassie for technical assistance. My friends Ato Zeleke kebebew, W/t Hamelmal Hagos, W/t Yodit Ayalew, and others whose list would be long to mentioned for all their friendly support and encouragement during my study period.

Special thanks to my mother W/O Aynalem Berhanu, My father Kubsa Bedaso and my great grand mother who thought me the principles of life. My father, who died in 1998, was the source of my ultimate strength in every aspect of life. I would also like to extend special thanks to my sisters Yemesrach, Selamawit, Webesh, Tigist and Rahel my brothers Gultie, Ermias and Dereje, who gave me all the encouragement I needed to accomplish my study.

Finally, yet most importantly, I offer my deepest gratitude to my wife Hanna Endale. She is the source of my strength and inspiration. Her encouragement, support and love were the pillars of my achievements. I would like to dedicate this work to my Wife.

Table of contents

ABSTRACT

Lacustrine sediments can be used to study the palaeoenvironmental evolution of a particular catchment. This is because they reflect developments in the Lake Ecosystem and productivity as well as changes in the rate and type of processes of the catchment such as weathering, erosion and sediment transport. Moreover, they are often deposited in undisturbed sedimentary environments and give time-integrated information on the evolution of the basin and its surroundings.

The aim of the present work is to contribute to the understanding of the Holocene evolution of climate variability and environmental changes due to both climatic and human causes in Northern Ethiopia from the sediments of lake cores and shorelines as well as from sections collected in and around Lake Ashange in the year 2003 under the Lake Tana project.

The studied core is dominantly organic and measures 8.1m and is recovered under 9m of water depth. The basal radiocarbon age shows a date of 11,920 $\pm$ 40 years BP. More radiocarbon dates, from samples corresponding to important shifts in the studied proxies, are under analysis. Because of this, linear extrapolation of age versus sediment depth has been applied in this study by considering the top of the core as modern.

Sediments were also analyzed for lithology, magnetic susceptibility, X-ray diffraction [(XRD) Mineralogy] and X-ray fluorescence [(XRF) (Elemental analysis)]. Moreover water samples were collected for chemical analysis and secondary information was also gathered from hydrometeorological data as well as from aerial photographs of 1965, 1980 and 1986. The integrated analyses gave the first evidences of continuous and high resolution climatic and environmental changes for the late Pleistocene and Holocene of Northern Ethiopia. The core was subdivided into four zones corresponding to important changes relative to the studied parameters.

Zone I is the basal zone and lies between 810 cm-650 cm, having an estimated age of 13,047-10,470 ^{14}C yr BP. It is characterized by a high sediment yield, by signals of low chemical weathering and low lake level. The climate in this zone is interpreted as cold and dry.

Zone II lies between 650 cm-425 cm and has an estimated age of 10,470-6,845 ^{14}C yr BP. The interval is characterized by low sediment yield, signals of strong chemical weathering and high lake level. The climate in this zone is interpreted to be more stable, wet and warm. At an estimated age of ~ 7425^{14}C yr BP an arid interval is documented within a generally wet and warm Early Holocene.

Zone III lies between 425 cm -180 cm with an estimated age of 6,848- 2,899 ^{14}C yr BP. The interval is characterized by low sediment yield at the base increasing higher up, by signals of low productivity at the base and at the top with higher productivity sub-zone in the middle. The climate in the zone is then interpreted as dry except at an estimated age of 4,317 ^{14}C yr BP in the middle.

Zone IV is the upper most zone between 180 cm-0 cm with an estimated age of 2,899 ^{14}C yr BP and modern. The zone is characterized by a high sediment yield from the catchment signals of low chemical weathering and low productivity. It is more generally interpreted as a dry interval with some signals indicative of wet pulses.

List of Figures

List of Tables

List of Plates

List of Annex

CHAPTER ONE
INTRODUCTION

1.1 Background and Objective

At present the study area is sensitive to climatic changes, as shown by the frequently recurring droughts, may be as a result of its geographical position at the proximity of the northern limit of the Inter Tropical Convergence Zone (ITCZ) (Griffith, 1972; Gamachu, 1977). The region also has a long standing history of human cultural development as evidenced by archaeological and historical records (Butzer, 1980; Phillipson, 1985). There is therefore a need to provide a long term pattern of environmental changes as well as their causes. The aim of the present work is to contribute to the understanding of the Late Pleistocene/Holocene environmental changes in the lake Ashange region due to both climatic and human factors. The information has been obtained from sedimentary records of lacustrine cores and shoreline as well as section evidences collected in and around Lake Ashange (= Ashenge and Ashangi).

In Ethiopia, most of the lakes are situated in the Main Ethiopian and the Afar Rifts. Morphogenic, stratigraphic, sedimentologic, limnological paleontological and geochemical evidences of several late Quaternary lake level fluctuations were obtained over the last decades, with support from extensive radiocarbon dating (Grove and Goudine, 1971; Grove et al., 1975; Geze, 1975; Laury and Albritton, 1975; Williams et al., 1980; Gasse, 1977;; Gasse and Street, 1978; Street, 1979; Gillespie et al., 1983; Street et al., 1990; Gasse and Van Campo, 1994; Telford et al., 1999; Lamb et al., 2000; Lamb et al., 2002; Dagnachew et al., 2002; Chalié et

al., 2002) making the lake region a reference site for paleoclimate reconstruction in the tropics (Street and Street-Perrot, 1990; Gasse and Van Campo, 1994).

On the other hand, in Northern Ethiopia Holocene sequences have been obtained from buried soils (Berakhi et al. 1998; Dramis et al., 2002) and from sequences of several in-filled valley deposits (Machado et al., 1998). These records are discontinuous and with low resolution. It is also difficult to find, in them multiple proxies of environmental changes. Recently however Lakes Hayke and Hardibo in Wollo have provided short-term data of the last 3000 years indicating the impacts of climate and man on the environment (Darbyshire et al., 2003).

Lake Ashange, located on the Northwestern Ethiopian plateau margin within the escarpment zone of the Afar Rift in the Danakil basin, is one of the few sites with a potential to provide a long term and continuous evidences of environmental changes. It is also one of the least studied of the Ethiopian lakes from a limnological, hydrologiccal and hydrogeologiccal points of view.

In this work data for the reconstruction of lake levels have been obtained from two principal environments: (a) the shore and near shore environments and (b) the main lake water body. The shore environments provide the best information on the paleo-lake area and elevation, while the deep-water environments provide long and continuous information on the chronology and paleoliminology but with limited information on the absolute magnitude of lake-level changes. Complementary studies from both environments are desirable because together they can provide a comprehensive understanding of the lake basin history. However, this combination is seldom achieved.

This study tries to combine data from both the shore and near shore environments as well as the deep water environment, from the cores.

1.2 Literature Review (Mainly based on Mohammed et al., 2004)

1.2.1 Climate changes during the last glaciations

1.2.1.1 Main Ethiopia Rift and the Afar

The longest and most continuous sedimentary sequence so far obtained is from Lake Abhé, the terminal lake of Awash river in central Afar. A 50 m- long sediment core reveals the major lacustrine episodes over at least 70,000 years Gasse, 1977; Gasse et al., 1980, (Figure 1.1) but only the upper section is supported by ^{14}C dating. Reconstruction of lake levels and salinity fluctuations over the past 40,000 years was based on sedimentary and diatom studies of the core and numerous outcrops, and paleo-beaches (Gasse, 1977), Gasse et al., (1980, 1998). Following shallow, saline-alkaline conditions around 31 ^{14}C Kyr BP, Lake Abhé became a large (6,000 km^2), deep, fresh Water Lake between 27 and 23 ^{14}C Kyr BP. A step wise fall to the modern lake level occurred between ca. 23 and 17.1 ^{14}C Kyr BP. A paleosol, with in situ grass remains, dated to between 17.1 and 16.1 ^{14}C Kyr BP. then developed at the core site. The lake was dry, or nearly so, during the Last Glacial Maximum (LGM). Traces of this wet Late Pleistocene episodes and arid LGM are found in all the main grabens in central Afar. Lake Abhé and the neighboring basins filled up again rapidly in Late-glacial and at the on set of the Holocene period.

The Main Ethiopian Rift experienced a comparable climate evolution, as shown by geomorphic and sedimentological studies of outcropping sequences and shorelines in the Ziway-Shala basins (Street 1979a; Gasse and Street 1978; Gasse et al., 1980; Sagri et al., 1999; Le Turdu et al., 1999). Today, this internal drainage basin

contains four lakes of decreasing altitude and increasing salinity: L. Ziway, L. Langano, L.Abyata and L. Shala. A highstand, at least 83 m above the modern lake Shala, occurred between ca. 26.5 and 22 ^{14}C Kyr BP Street (1979a). The lake then fell dramatically to levels at or below present, and remains low until about 12.5 ^{14}C Kyr BP. Assuming temperatures 3 to 6 °C lower than today, water balance calculation suggest a decrease in annual precipitation of 9 to 32 % compared to modern during the LGM (Street 1979a; 1979b). The consistent regional LGM aridity is also reflected in significant reductions in the seasonal discharge of Blue Nile River (Said 1993).

Late Pleistocene climate changes as inferred from lake records can be accounted for by orbital forcing, which predict enhanced monsoon rainfall, and thus high lake levels, during periods of increased summer insolation, around 35-30 cal kyr BP, and dry climates during the LGM in the northern tropics (Kutzbach et al., 1993).

None of the Ethiopian Mountains are glaciated today, but traces of Pleistocene glaciations on the Bale, Arssi and Semain Mountains have long been identified (Nillson 1940). The age of the most recent glacial advance is unknown. As glacial development requires both cold and wet climatic conditions, the last advance may have taken place during the 35-30 cal. kyr BP wet phase, rather than during the dry LGM (Gasse et al., 1980). The age of the last deglaciation has been indirectly inferred from the study of high altitude peat- bogs. In the Arssi Mountains, a peat core from a small cirque at 4070 meters suggests that the Mt Badda ice-cap had totally disappeared by at least 11.5 ^{14}C Kyr (Street 1979a; Hamilton 1982). An age for deglaciation of about 13-14 ^{14}C Kyr BP was proposed from pollen analysis in the Bale Mountains (Mohammed and Bonnefille, 1998).

1.2.2 Climate changes over the past 15,000 cal. years

Much wetter conditions than today prevailed during the early-mid Holocene in response to an orbitally –induced increase monsoon strength. It has long been apparent that the modern vegetation altitudinal belts began to establish during the Holocene in response to both wetter and warmer climatic conditions (Hamilton 1982; Lézine and Bonnefille 1982; Mohammed and Bonnefille 1982). The lakes experienced early-mid Holocene high stands followed by generally low water levels during the past 5000 cal. yr (e.g. Butzer et al. (1972), Fontes and Pouchan (1975), Street and Grove (1979), Street (1979a), Williams et al. (1977), Gasse (1977), Gasse and Street (1978), Gasse and Descourtieux (1979), Owen et al. (1982)). However, most records show that vegetation and hydrological changes did not respond to the smooth sinusoidal waves of orbital forcing alone.

1.2.2.1 Lake records

1.2.2.1a Reconstruction of ancient shore lines

The Ziway-Shala lake level record (Street, 1979a; Gillespie et al., 1983) shows that the re-establishment of wet conditions after LGM occurred in two phases, at 14.5 and 11.5 cal. Kyr BP. These two steps were thought to match the two major de-glacial warming events separated by the younger dryas cold event observed in high northern altitude (Street, Perrott and Perrott 1990). The second step was by far the most significant; the lakes of the Ziway-Shala basin merged to form a single lake that reached an outlet level and over flowed northward towards the Awash River, probably between ca.9.5 and 8.5 14C Kyr BP and from ca. 5.5 to 4.5 14C Kyr BP when its surface was 112 meters above the modern Lake Shall level. During the intervals, Lake Abhé in the Afar depression received water from both the modern drainage areas of the Awash River and the Ziway-Shala overflow. Lake Abhé was

a large, closed, fresh water lake (Gasse 1977). The lake level reconstruction of both the Lake Ziway-Shala and Abhé (Street 1979a, Gasse and Street 1978; Gasse et al. 1980; Gillespie et al. 1983; Gasse 2000) shows a large but short-term water-level lowering culminating at 7.8-7.2 ^{14}C Kyr BP, and a minor one around 5.9 ^{14}C Kyr BP. The first of these dry events, recorded in the lake levels, has been correlated with a stratigraphical level devoid of pollen in a core from Lake Abiyata (Léziane and Bonnefille 1982).

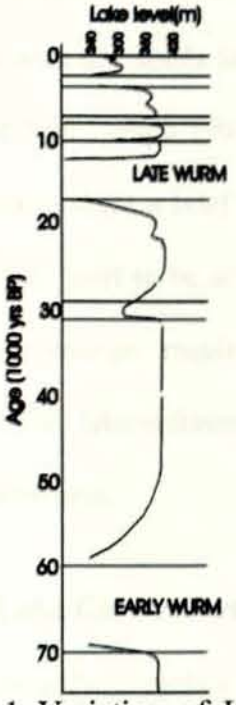

Figure 1.1 Variation of Lake Abhé level during the late Pleistocene and Holocene (Gasse, 1977)

Lake Ziway-Shala fell drastically after ca.5-4.5 ^{14}C Kyr BP and Lake Abhé after 4.5-4.1 ^{14}C Kyr BP. Fluctuations of moderate amplitudes have been recorded during the late Holocene. Rise of 42 meters above the present-day Lake Shala level was placed around 2-1.5 ^{14}C Kyr BP but with large dating uncertainties (Gillespie et al. 1983). A rise of 70 meters was dated between 3.5 and 1.6 ^{14}C Kyr BP at Lake Abhé (Gasse 1977; fonts et al. 1985). Street (1979b) estimated that mean annual precipitation in the Early Holocene was 28-47% higher than modern rainfall in the

Ziway-Shala basin. For the entire catchment area of the early Holocene Lake Abhé, water salt balance calculations suggest an increase in Precipitation-Evaporation (P-E) of 25% compared to the present day (Gasse et al., 1980).

Quantitative reconstructions of water-level fluctuations of the Afar and Main Ethiopian Rift Valley lakes were among the first evidences that arid intervals interrupted generally by humid early-mid Holocene climate. Although the rapid regressive events around 8.7-8.1, 6.7, and 5.5-4.5 cal. kyr BP appears roughly coincident with dry spells in the other regions of the northern monsoon domain (Gasse and Van Campo 1994), no satisfactory explanation has been proposed for these events, and for a brief return to wetter conditions during the late Holocene, which are too short to be accounted for by orbital forcing. The understanding of these abrupt changes requires more precise data on their timing, duration and intensity. Detail lake sediment core studies have recently complimented and refined these older records.

1.2.2.1b Lake Core records in the Main Ethiopian Rift

Three lakes without surface outlets have been recently investigated in the Main Ethiopia Rift Valley: (i) Lake Abijata I the tectonic, internal drainage Ziway-Shall basin; (ii) lake Tilo, a small crater lake lying south west of the

Ziway-Shala basin and (iii) Lake Awassa, which occupies a caldera in the southern part of the Main Ethiopian Rift. These three lakes partly depend on ground water inflows. The same diatom- based transfer functions (Gasse et al., 1995) were used to infer salinity changes, which enclosed lakes can reflect changes in P-E, provided that the signal is not biased by local hydrological factors (Gasse et al. 1997) while diatom records from Lake Tilo and Abijata can be interpreted in terms of climate

changes, observed changes from diatom records in Lake Awassa are believed to be primarily due to pulsed input of saline ground water independent of climate (Telford et al., 1999).

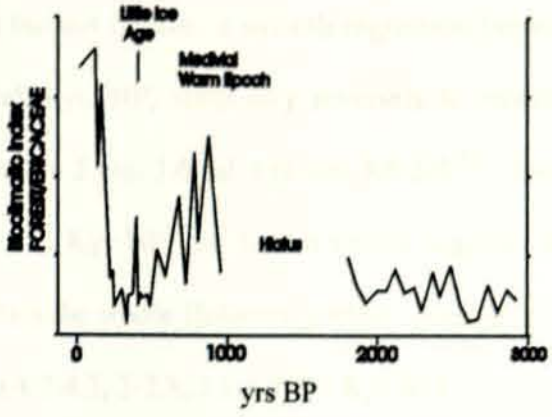

Figure 1.2 Bioclimatic index (ratio between arboreal and Ericaceae Pollen). During the "Little Ice Age cold periods" the forest limit is lower and Ericaceae dominate (Bonnefille and Mohammed (1994)).

The 6.5 ^{14}C Kyr BP $\delta^{18}O$ record from carbonates in Lake Awassa does, however, show broad regional climate changes (Lamb A.L. et al., 2002). Co-varying and increasing $\delta^{18}O$ and $\delta^{13}O$ varying from ~ 4.8 ^{14}C Kyr BP suggests an aridification of climate after the early Holocene insolation maximum. After 4.0 ^{14}C Kyr BP when $\delta^{18}O$ increases again, reflecting drier condition.

Lake Abiyata is currently closed, saline- alkaline lake, mainly supplied by the outflow of the upstream Lakes Ziway and Langano. Although sub-surface water contributes significantly to the water supply (Gibert et al., 1999), lake-level and salinity are very sensitive to P-E balance in the surrounding Plateaux (Vallet-Coulomb et al. 2001; Daganachew Legesse et al., 2003). A 12.6 m–long sediment core taken in the deepest part of the lake presents the past 13,500 years. Diatom-inferred changes in water level and chemistry (Chalié and Gasse 2002) confirm the conditions generally much wetter than today prevailed from ca. 11 to 5.7 cal. kyr.

There were rapid shifts toward an overall Late Holocene water deficit between 5.7 and 5 cal. kyr (ca. 5-4.4 ^{14}C Kyr BP. The short-term regressions reconstructed by Gillespie et al., (1983) at 8.8-8.5 and 6.7 cal. kyr BP are not apparent in the diatom records, which instead indicate a smooth regression between 9.3 and 7.3 cal. kyr. BP. After 5 cal. kyr. BP, temporary reversals to relatively wet conditions are observed between 4.3 and 3.6 cal. kyr (ca. 3.6-3.2 ^{14}C Kyr BP) and at 2.9-2.6 cal. kyr (ca.2.8-2.5 ^{14}C Kyr BP) the diatom record suggests that events of maximum water deficit from the whole Holocene period occurred at 5.3-4.9, 3.2-3, and 2-1.8 cal. kyr. BP (ca.4.7-4.3, 3-2.8, 2.1-1.9 ^{14}C Kyr BP)

Lake Tilo is supplied by direct precipitation and by ground water inflow, and is currently saline-alkaline. A 23 m sediment core taken from this lake covers the past 10,000 cal. years. The cores were analyzed for diatoms (Telford and Lamb, 1999) and stable isotopes of carbonates (Lamb et al., 2000). The diatom record shows that deep, fresh water conditions prevailed until about 4.5 ^{14}C Kyr BP. A marked change in diatom assemblages and in calcite and silica deposition rates at 5.5 ^{14}C Kyr BP was attributed to a decline in geothermal ground water inflow (Telford et al., 1999). Lake salinity began to increase about 4.5 ^{14}C Kyr BP in response to decreasing P-E, and reached approximately its present state ca.2.5 ^{14}C Kyr BP. There is, however, a temporary reversal to lower salinity at 3.8-3.5 ^{14}C Kyr BP. The isotope record (Lamb et al. 2000) shows low δ^{18}O values until 5.5 ^{14}C Kyr BP reflecting combinations of higher precipitation, greater spring inflow and less evaporation from the lake surface than today. This wet phase was interrupted by short periods of aridity from 7.9 to 7.6 ^{14}C Kyr BP (8.8-8.5 cal. kyr) and at 5.9 ^{14}C Kyr BP (6.7 cal. kyr). These events are not recorded by the diatom but are in good agreement with the reconstructed lake Ziway-Shala and Lake Abhé lake-levels. An

abrupt increase in $\delta^{18}O$ values at 4.2 ^{14}C Kyr BP (4.7 cal. kyr reflects a sharp fall in P-E which was maintained up to 3.7 ^{14}C Kyr BP (4.1 cal. kyr) it was followed by a wetter episode that lasted for at least 300 years, in agreement with the diatom record. Over the last 2.5 ^{14}C Kyr BP (2.6 cal. kyr), large swings in isotope values and the occurrence of varied laminations are interpreted in terms of anoxic bottom-water conditions. An intermittent carbonate diagenesis possibly linked to irregular over turning of the lake.

Spring-fed lakes in the Afar, e.g., Lake Afrera, did not record the 7.8-7.2^{14}C Kyr BP and 5.9 ^{14}C Kyr BP arid intervals (Gasse and Street, 1978). Presumably, the aquifer that feeds them with water from the highlands has a residence time longer than the duration of the arid intervals (Lezine and Bonnefille, 1982), with no record change attributed to the increase in aridity at 5 kyr BP, instead a rise in *Podocarpus* pollen occurs at 3 kyr BP, but it is not fully understood (Figure 1.2).

1.2.1.2 Northern Ethiopia

Although up to now there is no research work done in the catchment in general and on Lake Ashenge in particular, lots of relevant researches were conducted on different aspects in the north and north-western highlands of Ethiopia.

A geomorphic-stratigraphic analysis of a travertine dammed lacustrine-swampy sedimentary sequences in the highlands of Tigray (Northern Ethiopia) allows to establish that the travertine dams have developed at least between 7,310 ±90 yr BP and 5,160±80 yr BP indicating a wetter climatic condition than present (Baraki et al., 1998), and it is a reference for environmental evolution, climate changes and human impact in Northern Ethiopia.

In Northern Ethiopia the aggradations of travertine dams started at the beginning of Holocene. In the first stage the deposition rates were quite rapid, giving rise to relatively swampy areas upstream. Subsequently, since ca.4,700 ^{14}C yr BP, periods of alternating stages of dam incision and aggradations occurred, followed by a more recent phase of general incision which deeply cut the travertine dams.

Paleoenvironmental reconstruction based on several infilled valley sequences suggests that the past 4000 yr comprised three major wetter periods (ca. 4000-3500 yr BP., 2500-1500 yr BP and 1000-960 yr BP), during which soils were formed, and two degradation episodes (ca. 3500-2500 yr BP and 1500-1000 yr BP) happened and there was sediment yield increase from slope into the valleys. For the past 1000 yr, and in particular since the early 17th century, stratigraphic records together with historic chronicles suggest increasing aridity. At about 500 BC following Semitic immigration to northern Ethiopia, the forests were cleared and replaced by secondary vegetation of Dodonaes scrub and grassland that persisted for 1800 years. Pollen and charcoal analysis of (Darbyshire et al., 2003) sediment cores from two lakes (Hayk and Hardibo) in the highlands of northern Ethiopia provide evidences that the vegetation has changed in response to human impact during the last 3000 years. Since forest regrowth was possible after 1800 years of human impact northern Ethiopia should again be capable of supporting forest under appropriate land management.

1.3 Objectives and scope of the present work

1.3.1 Main objective

- To reconstruct the paleoenvironmental and paleoclimatic conditions of Northern Ethiopia from Lake sediment records during the last ~12,000 years.

1.3.2 Specific objectives

- To reconstruct recent changes in land use and land cover as well as in the lake level
- To Map the basin to show the distribution of the lake margin sediments and to study them to infer long term lake level fluctuations.
- To analyze changes in sediment type of the studied core (e.g. terrestrial versus lake productivity changes) as well as sediment composition (geochemistry and mineralogy) over time in order to understand environmental implications.
- To reconstruct fluctuations in the rate of sedimentation of the core (sediment yield from the catchment).
- To reconstruct environmental changes in the catchment and in the lake
- To correlate the results with previous data from Ethiopia and elsewhere in tropical Africa in order to understand implications of climate and/or human impact on the environment in order to evaluate to what extent the present landscape of Northern Ethiopia represents a product of the Holocene history of anthropogenic and/or climatic stress.

1.4 Materials and Methods

To attain the above objectives different materials and methods were employed Figure 1.3

1.4.1 Material

- Topographic maps (1996 E.C.) and aerial photographs (1965 E.C., 1980 E.C. and 1986 E.C.) of 1: 50,000 scale were used as bases to map drainage pattern, land use-land cover, slope, soil and to produce geological and structural maps of the catchment.
- A GPS was used for positioning the studied sections, sampling locations on the lake and during the bathymetric survey.
- Water quality kits (EC and pH meters) were used to measure the electrical conductivity (Eh) and pH of the lake water to check the lateral and vertical variation of these parameters.
- An eco-sounder was used to measure the depth of the lake and to decide on the location for coring.
- Two hand-operated piston corers were used: Kullumberg type to sample sediments of the sediment-water interface and Livingstone type to sample deep lake sediments. A grab sampler was applied for sampling modern sediments; gauge corers were used for the consolidated sediments in the lake.
- Gully sections were studied, sediments described and sections measured using measuring tape.

1.4.2 Methods

1.4.2.1 Field methods

A) Coring

Cores were recovered from Lake Ashenge in October 2003 with Kullunberg and Livingston piston samplers (Wright et al., 1989), with a barrel 1 meter long and 5 cm in diameter, operated on a raft supported by two securely anchored inflatable boats in 8.9 m water. A total of 9 m core was recovered (03AL1-03AL5; see appendix). Depths were measured from a datum level on the raft and recalculated both from the water surface and the sediment surface.

Cores were extruded into labeled sections of polyvinylchloride (PVC) guttering wrapped with cling-film and sealed in plastic tubing. The cores were stored at Aberystwyth, University of Wales, at 4 °C.

B) Sections

Sections exposed in the catchment are cut by gulling and streams. These were measured using measuring tape. Lake sediments distributed outside of the lake area are located on the base map using GPS. (See appendix A).

The main problem with section evidence is the fragmentary nature of deposits in the Quaternary due to the restless nature of the climate, which affects the deposits trough erosion.

"Trying to reconstruct environmental changes from terrestrial evidences is like trying to assemble a jigsaw puzzle and make sense of the picture where more than 90% of the pieces are missing" (Lowe and Walker, 1995).

1.4.2.2 Laboratory Methods

A) Sediment lithology and Radiocarbon dating

The core is sub-divided into five major lithological units (figure 5.1) based on color, sedimentary structures and proportion of the different organic and inorganic components using the method described by Tröels-Smith (1955), using munsell color chart and slide smears.

The Basal age at 1630 m from the water surface (740 cm sediment depth) is dated to 11,920±40 ^{14}C yrs BP by Beta-Analitic Inc. The date was obtained from the bulk organic fraction of the sediments pretreated with acid, using conventional radiocarbon dating technique. By international conventions, the modern reference standard was 95 % of C^{14} content of National Bureaus of Standards' Oxalic acid and calculated using the Libby C^{14} half life (5568 yrs).

Because only one date at the base of the core is obtained linear interpolation, assuming the top of the core as modern, was used to estimate the age of the upper levels.

B) Loss on Ignition

One cm^3 sediment was sub-sampled from the core using a brass sampler at 5 cm intervals for the determination of Loss On Ignition (LOI) of both organic matter and carbonates. The method for loss on ignition is modified from Dean (1974). Diffraction thermal analysis (DTA) shows that when a dried, powdered sample containing organic material and calcium carbonate is heated in a muffle furnace, the organic material begins to ignite at about 200 °C and completely ignited by the furnace temperature has reached approximately 550 °C. Evolution of CO_2 from the

calcium carbonate will begin at about 800 °C and proceed rapidly so that most of the CO_2 has been evolved by the time the furnace has reached 850 °C.

Samples were placed in pre-weighted porcelain crucibles and weighted before drying, then were dried for at least 12 hrs at 105 ° C. After cooling in a desiccators, the samples were reweighed.

The samples were then heated to 550° C for at least 2 hrs, and then to 950° C for at least 1 hr. and were respectively cooled in a desiccators and weighted

The mass loss, after heating up to 105 ° C, is assumed to be the moisture content. The dry weight of the sample is the basis for all weight loss calculations.

The mass loss between 105° C and 550 ° C is assumed to be due to ignition of organic matter (organic carbon through CO_2 emission).The mass loss between 550°C and 950°C is the amount of carbon dioxide (CO_2) evolved from carbonate minerals when thermally decomposed. If a significant amount of clay is present in the clastic fraction, the 550°C -1000°C ignition loss would contain a significant amount of lattice water in samples which are low in carbonate and high in clays as the water in clays is not removed until heated to 550° C-1000 ° C.

As noted in Dean, (1974) to obtain the organic carbon and the actual percentage of calcium carbonate from the loss on ignition at 550° C and between 550°C-950°C respectively, a correction factors should be used.

$$\%OM=[(A-B)/A]*100*R^{OC}$$

$$\%CO_3=[(B-C)/B]*100*R^{IC}$$

Where: A- Sample dried at 105 °C
B-Sample weight at 550 °C
C-sample weight at 950 °C

With correction factors R^{OC} of 0.40 and R^{IC} of 0.12 (Zilifi and Eagle, 2000 Nyanza Report)

C) Magnetic Susceptibility

Whole core magnetic susceptibility was measured with a Barrington Instruments MS2 meter with a typical MS2c sensor at an interval of 2 cms, while they were still in the PVC guttering. (Appendix C)

D) X-ray diffraction (XRD): Mineralogy

The whole length of the core was re-sampled at 16 cm interval. A total of 51 samples were analyzed using X-ray diffractometry (Cu Kα radiation) for whole powder mineralogy using a Philips PW 1710; PW 1729 (X-ray generator); Digital professional 380 (computer) and APD 17000(program) at the Technical Universtät of Berlin in the Institute für Angewandte Geowissenschaften using the procedures described by Moore and Reynolds (1997).

12 samples were selected for clay mineral separation in settling tubes/ Atterberg cylinders. The samples were pretreated with a flocculent ($Na_2P_2O_7.1H_2O$) and with H_2O_2 to free them from organic matter which helps to get better defined peaks in the diffractogram. The suspended particles were let to settle for about 17 to 18 hours depending on the temperature. The separated, <2μm size fraction was

concentrated by centrifugation for about 30 minutes at 3500 revolution/ minutes and mounted on glass slides according to Gibbs (1965; 1968).The mounts were analyzed for clay minerals in three stages: untreated air dried, solvated for at least 24 hours with ethylene glycol vapors at 60 ° C and heated to 550 ° C for 2 hours. The XRD analysis was performed after mounting, solvation and heating.

E) X-ray fluorescence (XRF): Elemental analysis

The same samples which were analyzed by XRD were further analyzed for elemental composition using the X-ray fluorescence technique on fused pellets after the methods described by Norish and Chappel (1977), using a Philips PW 1404/10 automatic sequential wavelength dispersive X-ray spectrometer.

A careful mixture of 0.6 g of the ignited powdered sample and of 3.600 g of $LiBO_2$-flux was prepared to make the fused glass discs. On the bases of these fused glass discs a total of 37 major oxides, major, minor and trace elements were determined with the Oxiquant program using 82 international rock standards and artificial standards for calibration. The analytical errors of this method are + 3-5 % for major and +10% for trace elements.

Samples were ignited at 1000°C for at least 1 hour to measure the total loss on ignition. The quality of the element analyzed is checked by adding the loss on ignition (mainly H_2O and CO_2) and the percentage of the respective elements analyzed, which should be in the range of 99 to 101%.

F) Biogenic silica

Normative biogenic silica was calculated from the geochemical data obtained from the XRF results. Normative biogenic silica values (Sibio nor =SiO_2-2.8*Al_2O_3;

Robinson et al., 1993) sited in (N. Calanchi et al., 1996) is used to evaluate the diatom productivity.

G) Water Chemistry and hydrometeorology

Water samples from the lake and inflows to the lake in the north, northwest, south and southwest of the catchment were analyzed for major cations and anions (i.e. Cl^-, NO_3^-, PO_4^{3-}, SO_4^{2-}, Na^+, K^+, Mg_2^+ and Ca_2^+) with a Dionex using Atomic Absorption Spectrometry.

Hydrometeorological data of four stations (Maychew, Korem, Mehoney and Alamata) were collected from the Ethiopian Meteorological Service Agency (EMSA) to compute the water balance of Lake Ashange.

In addition, lake level measurements between 1975 and 2001 were obtained from the Minstery of Water Resources to characterize the seasonal variability and yearly fluctuation and trend.

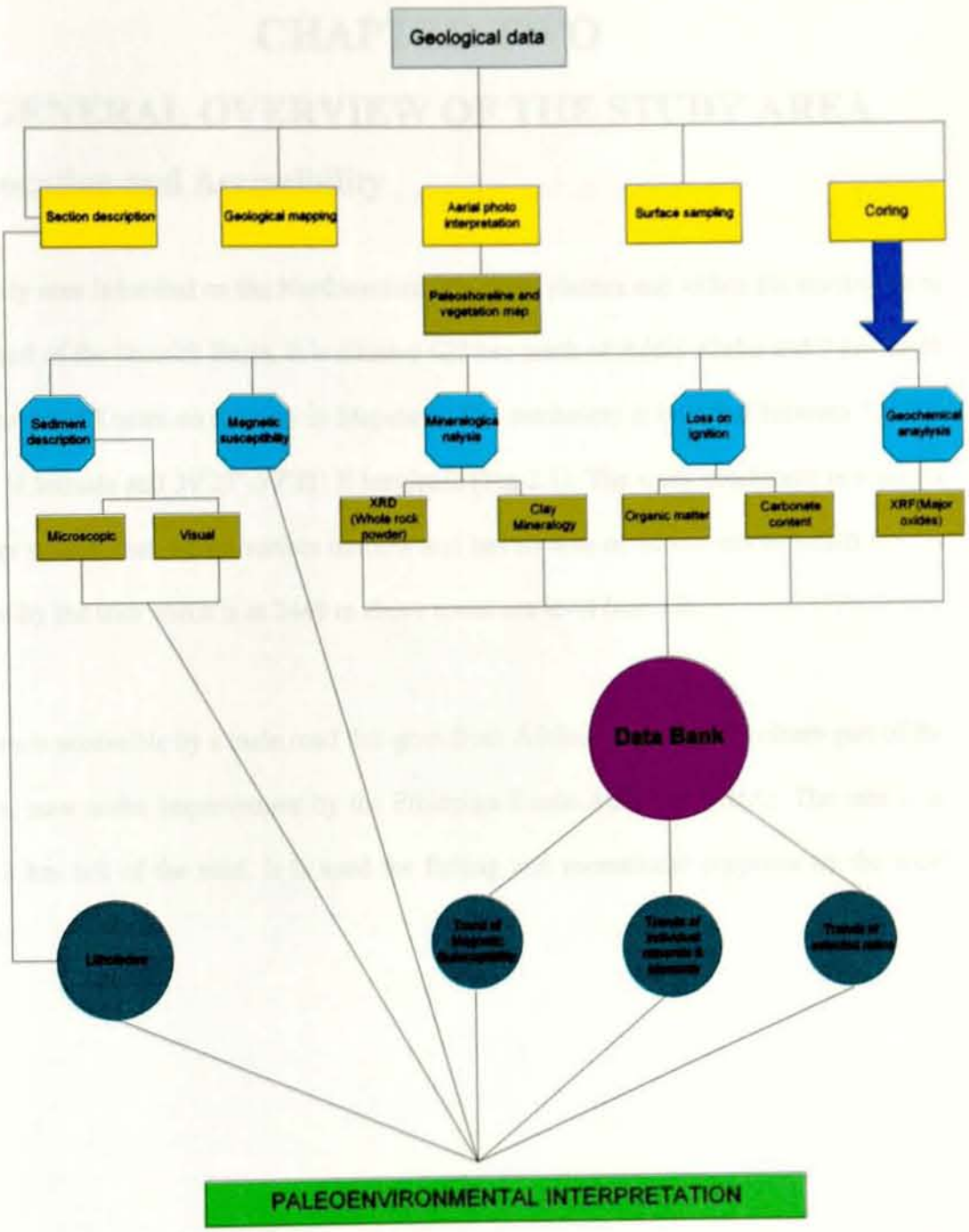

Figure 1.3 Summary of the methods and approaches to achieve the aim of this study

CHAPTER TWO

GENERAL OVERVIEW OF THE STUDY AREA

2.1 Location and Accessibility

The study area is located on the Northwestern Ethiopian plateau and within the northwestern watershed of the Danakil Basin. It is situated 622 km north of Addis Ababa and 7 km north of the town of Korem on the way to Maychew. The catchment is bounded between 12°32'-12°39' N latitude and 39°27'-39°32' E longitude (Fig 2.1). The study catchment is a closed drainage system that has no surface outflow and has an area of 82 km^2 out of which $1/5^{th}$ is covered by the lake which is at 2440 m above mean sea level (a.m.s.l)

The area is accessible by a main road that goes from Addis Ababa to the northern part of the country, now under improvement by the Ethiopian Roads Authority (ERA). The lake is at about 2 km left of the road. It is used for fishing and recreational purposes by the local people.

Figure 2.1 Location map of the Study Catchment

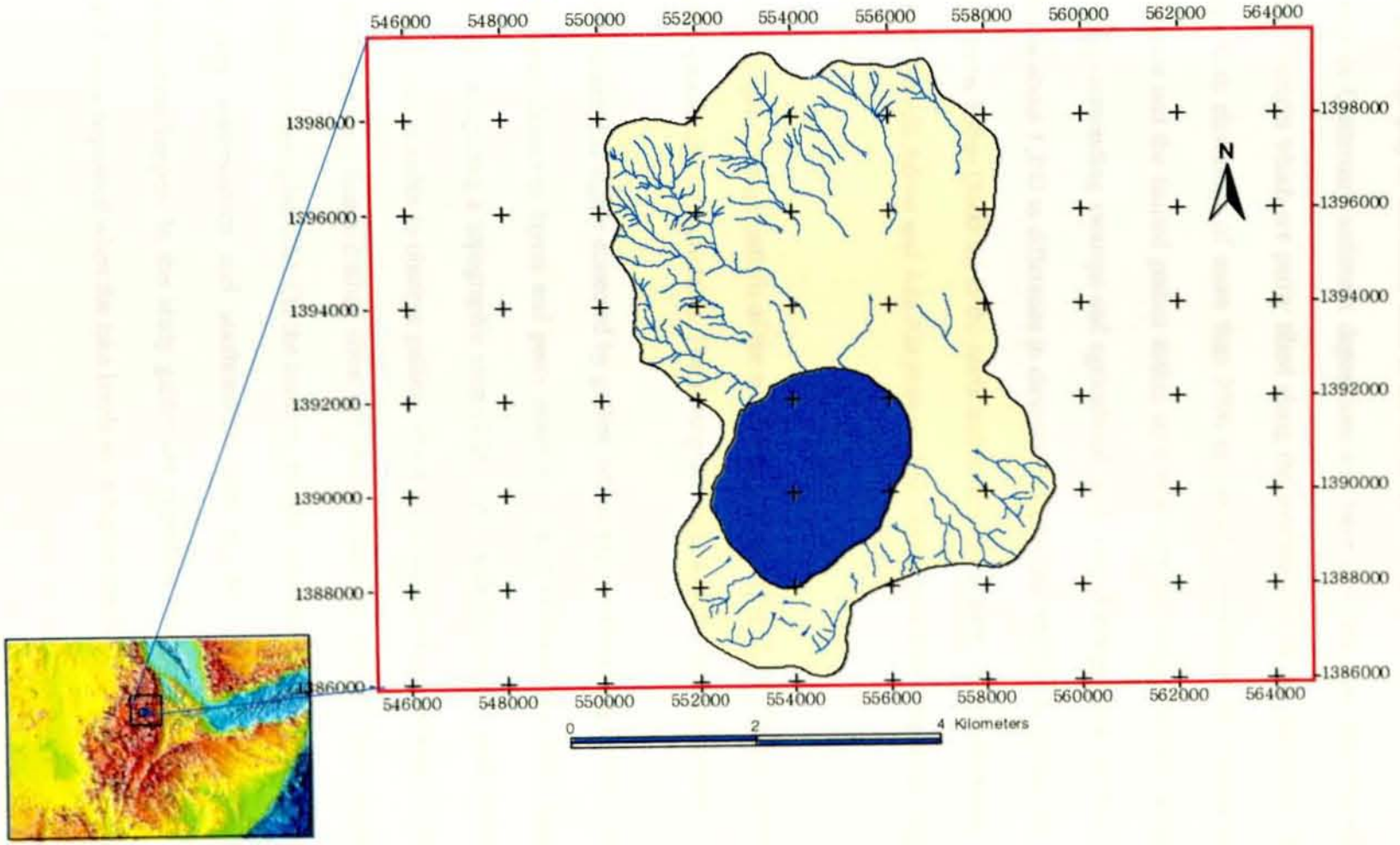

2.2 Physiography and Drainage

The physiography of the study area is the result of Tertiary volcanic and tectonic activities as well as Quaternary sediment depositions and later erosions. The exposed rocks are of volcanic origin which are partly tilted along the western side of the catchment. Steep fault scarps with elevations of more than 3500 m a.m.s.l. characterize the morphology of the catchment and the faulted graben makes up a relatively flat low lying area comprising the lake the surrounding swamps and agricultural lands (i.e. Ashange plain north of the lake). There is about 1,200 m difference in elevation between the lake (2400 m) and the top of the Tikur Imba Ridge (3600 m) in the north and northwestern parts of the catchment. Chegwar, Haynet, Shanfa Adewt and Ada Ala streams drain water from this ridge to the flat lands and the lake.

The principal drainage pattern of the catchment is radial (Fig. 2.2). The flat area around the lake is surrounded by mountains. The swamp serves as a buffer to the sediment.

The catchment is highly dissected by gullies, which expose alternating layers of fine grained sediments, diatomite layers and peaty materials, which indicate lake level changes in the past. By comparing a topographic map of the 1996 with the ground truth during the field visits, it was possible to observe gullies, which were not traced on the map or even if some were traced they then had small sizes, implying the land has severely been degraded during the last 10 years (plate 2A). On the contrary, people are rehabilitating some of the gullies in the very southwestern and southeastern parts of the catchment showing a reverse phenomenon happen. In this study gullies are important in exposing paleo-lake sediments, which were deposited when the lake levels were higher than today.

Figure 2.2 Drainage map of Lake Ashange Catchment

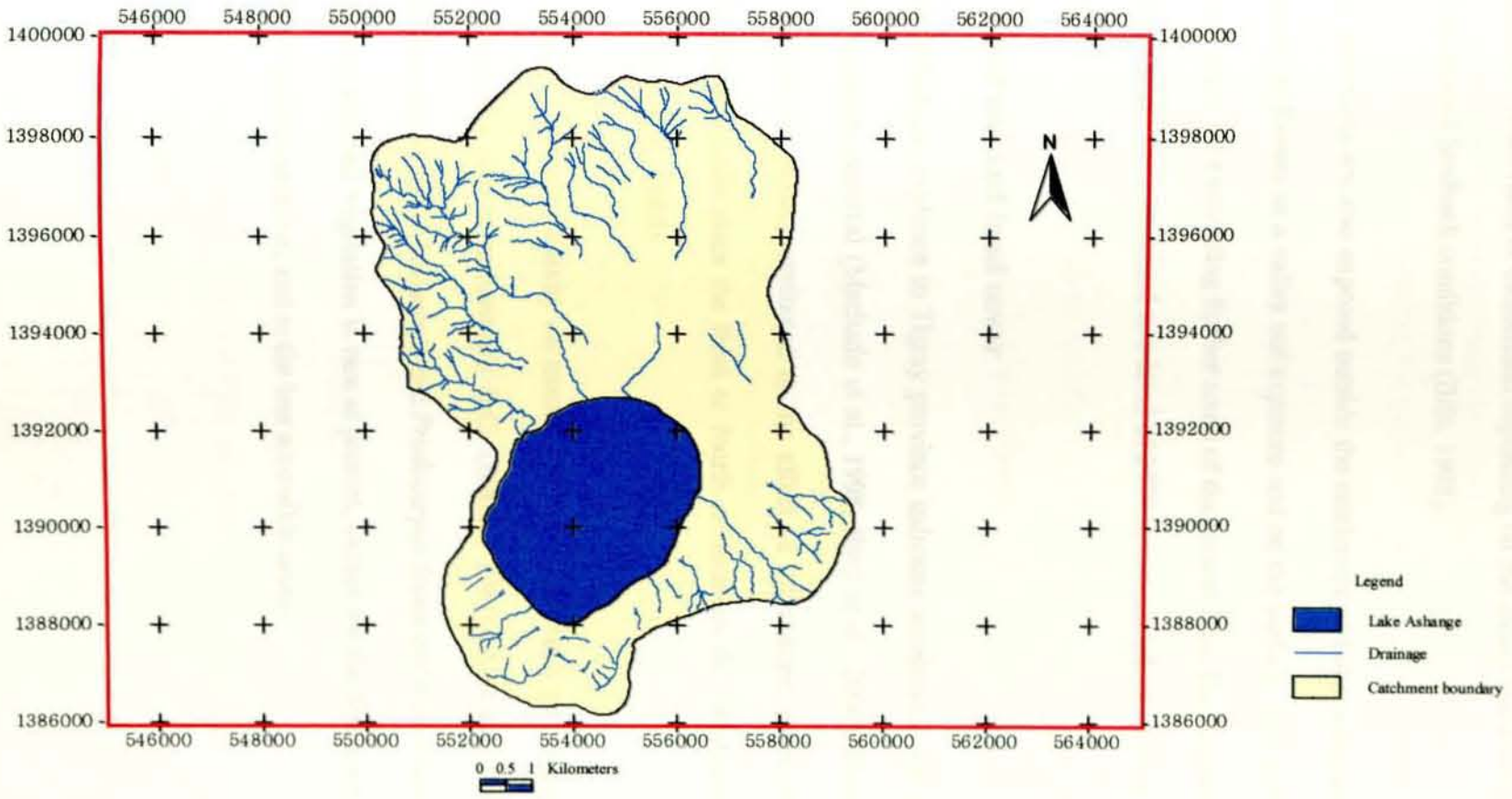

Gulley erosion has been variously ascribed to climate change, land use change, or variation in geomorphological processes involving extrinsic and intrinsic threshold conditions. It can be initiated, reactivated or established depending on the nature and extent of the disturbance and the related feedback conditions (Billi, 1998).

Lake sediments are also exposed outside the catchment of Lake Ashenge along the road to the town of Korem in a valley cut exposure and on the surface. This probably indicates an ancient paleo-lake extending further south of the present lake. During the above wet periods the lake might have increased to a level of 2470 m a.m.s.l. which is 30 m above the present level.

2.3 Land use and land cover

Geomorphologic evidence in Tigray province indicates accelerated soil erosion associated with vegetation removal (Machado et al., 1998; Bard et al., 2000). Deforestation and soil degradation are widely attributed to the effect of agriculture, practiced in the northern Ethiopian highlands since the third or fourth millennium BC (Phillipson, 1985) sited in (Darbyshire et al., 2003).

The impact of human activity on natural vegetation has been particularly effective in the area since the second millennium B.C. (Butzer, 1981). Although the present climatic conditions would allow *Juniprerus* and *Prodocarpus* forest and mixed deciduous *Juniprerus* woodland, arboreal vegetation is rare at present, except for the few trees, clustered around churches and monasteries, and in the less accessible areas.

In the study area, the main land use/ land cover classes are (Figure 2.3, Table 2.1):

1. Scattered trees and shrubs covering the steeper escarpments, hilltops and some of the flat lands where there are settlements.
2. Cultivated land covering the gently sloping and flat lands that are not covered by swamp.
3. Grass land covering the swampy areas.
4. The area covered by the lake.

The major crops grown are cereals: Barley (Hordeum vulgare L.), Maize (Zea mays L.) and Sorghum (Sorghum bicolor (L.) Moench); Pulse and vegetables: Beans (Phaseolus spp.,Vigna spp.) and wood/timber: Eucalyptus (Eucalyptus spp.).

No town is present in the catchment area. The main towns in the vicinity are Korem, Gumbrda and Shinko Majo.

Land use/Land cover	Area proportion (km^2)	Area coverage (%)
Trees and shrubs	38.5	46.8
Cultivated land	23.1	28.1
Grass land	6.7	8.1
Lake surface	14.0	17.0

Table 2.1 Proportion of Land use land cover in the Lake Ashange catchment (December 2003)

Figure 2.3 Land use-Land cover of Lake Ashange Catchment

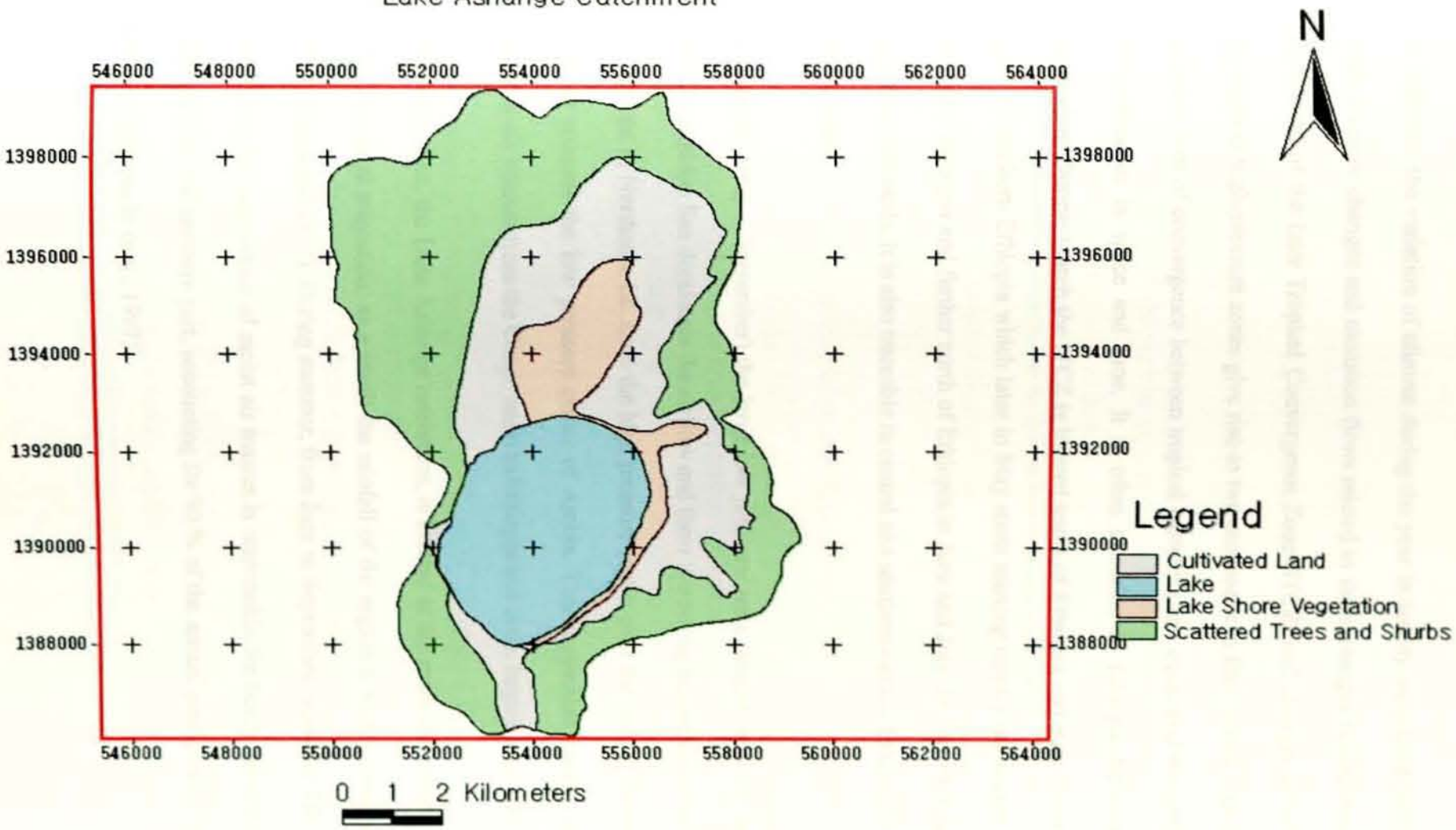

2.4 Climate

In Ethiopia, the variation of climate during the year is largely associated with the macro-scale pressure changes and monsoon flows related to these changes (Gamachu, 1977). The movement of the Inter Tropical Convergence Zone (ITCZ) and changes in the location of the tropical high-pressure zones give rise to two monsoons in East Africa. The ITCZ, a low pressure area of convergence between tropical easterlies and equatorial westerlies, may not be continuous in space and time. It is often traceable in Ethiopia between May and November. During March the ITCZ is located south of Ethiopia and moves further north in April to southern Ethiopia which later in May starts moving rapidly northward and reaches Northern Ethiopia and further north of Ethiopia in June and July. In August it starts moving rapidly southwards. It is also traceable in central and southern-central Ethiopia in September and October.

In summer (July – September) the large low pressure zone located over the Indian Ocean and the Arabian Sea dominates the airflow and there is a strong movement of moist air from Southwest to Northeast, i.e. from the high pressure center over the Gulf of Guinea (Atlantic Ocean) towards the low pressure center of Arabia. This movement carries warm, moist, unstable air masses from the Congo basin to Ethiopia and is the largest source of rainwater.

The study area, the Lake Ashange catchment, is located at the extreme northern limit of the ITCZ seasonal migration; as a result the rainfall of the region is highly seasonal (Griffths, 1972; Gamachu, 1977). During summer, from June to September, when the ITCZ lies north of Eritrea, the convection of moist air masses is responsible for heavy rainfall in Ethiopia, especially in the northern part, accounting for 90 % of the annual precipitation (Said, 1993) sited in (Marchado et al., 1997)

2.4.1 Rainfall and Temperature

Rainfall is one of the most important elements in characterizing the climate of a region. In Northern Ethiopia the main dry season is longer (November - February) unlike in southern Ethiopia (December – February); and, conversely the main rainy season is longer in the south (May – November) and shorter in the north (June – August) (Suzuki, 1967).

In Ethiopia, fourteen rainfall regions are recognized based on whether the rain months are continuously distributed (type I) or there are two rainy "seasons" (type II) (Gemechu, 1977). Different rain types are recognized in the northwestern plateau, in the rift valley and near the rift margins and the southeastern plateau. Figure 2.4

The study area is characterized by two rainy seasons (i.e. Type II rainfall region). Like most of the regions on the western escarpment of the Rift system the Lake Ashange catchment is located in regime IID. Regime IID is characterized by six rainy months from March to April and June to September. The small rains are in March, April and June and the big rains are from July to September with very high concentrations in July and August (Gamachu, 1977).

In order to compare the monthly distribution of rainfall at various stations with different rainfall amounts, the following "rainfall coefficient" method from data for the Awash River basin (UNFAO, 1965, P.20) has been applied:

$$\textbf{Rainfall coefficient} = \frac{\textbf{mean monthly rainfall}}{\textbf{1/12 Annual mean}}$$

In the Awash River Basin method a month is designated as "rainy" when the monthly rainfall coefficient reaches 0.6 (60%of the rainfall module) and as "dry" when it is below this value. Moreover it becomes distinctly rainy when it exceeds 0.8. Extremely rainy

months have a coefficient of more than 1(that is, the rainfall exceeds the module value)

(UNFAO, 1965, p.20)

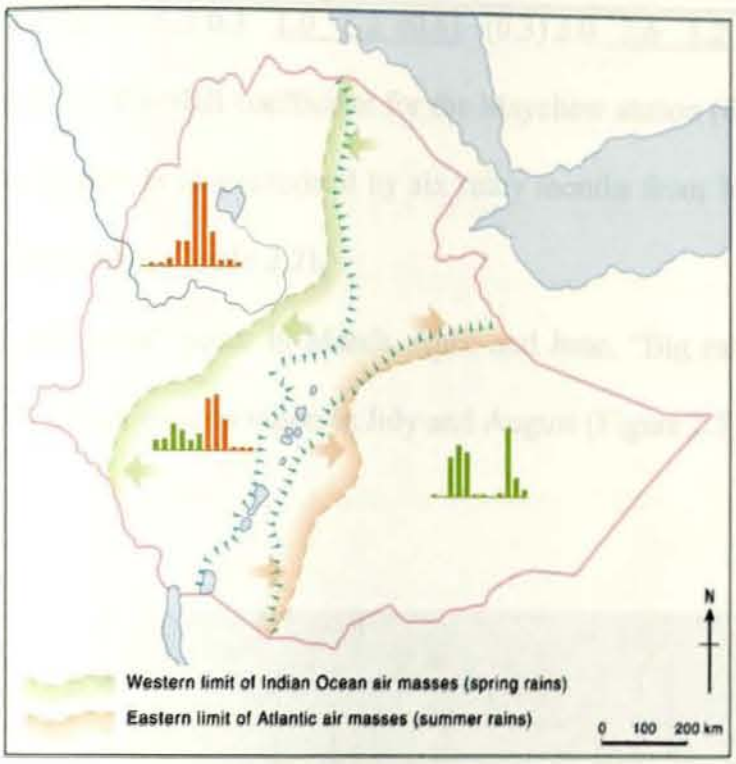

Figure 2.4 Types of rain and their distribution in Ethiopia (on Northwestern and Southeastern plateaus and in Rift and Rift margin areas)

Classification sachem of monthly rainfall coefficient value

Designation	**Rf coefficient**
Dry months	< 0.6
Rainy months	0.6 and over
Small rains	0.6 - 0.9
Big rains	1.0 and over
Moderate concentration	1.0 – 1.9
High concentration	2.0 – 2.9
Very high concentration	3.0 and over

Rainfall coefficient

Station	J	F	M	A	M	J	J	A	S	O	N	D	Annual (mm)
Maychew	0.3	0.3	1.0	1.2	(0.6)	(0.3)	3.0	3.6	1.2	0.4	0.1	0.1	817.6

Table 2.2 Rainfall coefficient for the Maychew station (Gemechu, 1977)

The station is characterized by six rainy months from March to May and from June to September (Table 2.2).

"Small rains" occur in March, April and June, "Big rains" from July to September with a high concentration in July and August (Figure 2.5).

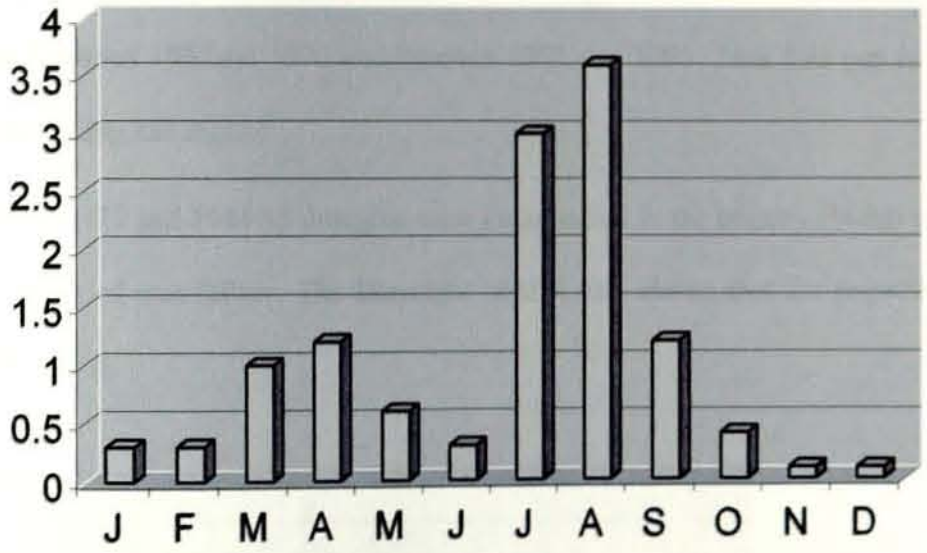

Figure 2.5 Rainfall coefficient of Maychew station

The regional variation in the amount of rainfall in Ethiopia is determined by two factors: the direction of moisture bearing seasonal air currents and elevation. Variability of rainfall is higher where the total amounts are lower and vise versa (Gamachu, 1977).

Rainfall intensities are high in the lowlands of Ethiopia, reaching up to 1400 mm a day such as in the lower Awash valley; low on the highlands (less than 50mm a day). However,

relatively low intensity of rainfall on the highlands doesn't prevent fast rates of runoff and accelerated soil erosion due to steep slopes.

2.4.1.1 Rainfall

The average annual rainfall of the study area in the region is 817.6 mm (Gemechu, 1977).

From the long-term rainfall data of the study area the trend of precipitation and extreme wet /extreme dry years are observed. The general trend of precipitation is a decrease until 1960, with a little increase up to 1965 then a decreases up to the early 1970s, (the driest year), followed by an increase in 1974 (the wettest). The second dry year is 1984 followed by an increase until 1992 and a decrease to the present. (Figure 2.6)

Although rainfall data is available from 1953 to 2003, the record is not complete. Data were missing between 1967and 1970 and between 1983 and 1991. This data gap is due to the civil war during last regime.

During 1971-75 and 1984-85 droughts were documented in the country (Webb et al., 1989) due to years of rain failure. The Maychew station also shows that the respective periods were the driest.

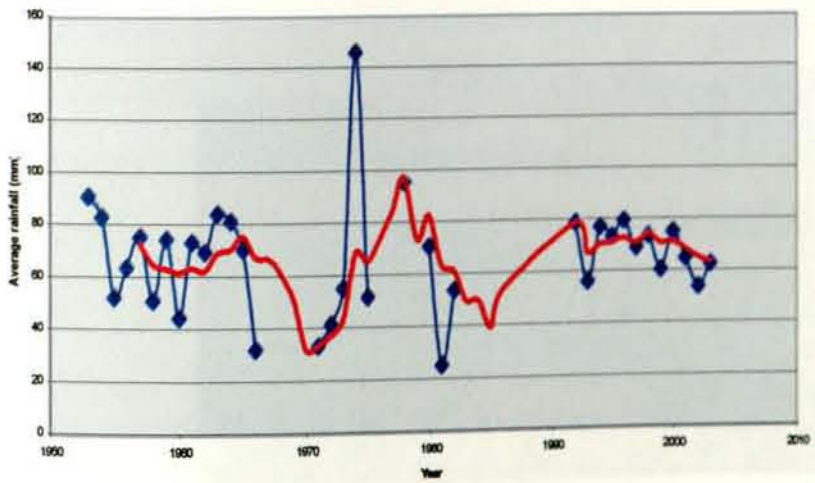

Figure 2.6 Long-term rainfalls (blue line) with Five years moving average (red line) of the study area (Source: Ethiopian meteorology Agency)

2.4.1.2 Temperature

Mean monthly average temperature values for the Maychew station are shown in figure 2.7. Generally, the months of May, June, July, August and September have the highest average temperatures while December, January and February have the lowest. The maximum temperature reaches as high as 27 °C, in June while the minimum temperature gets as low as 4°C, in December.

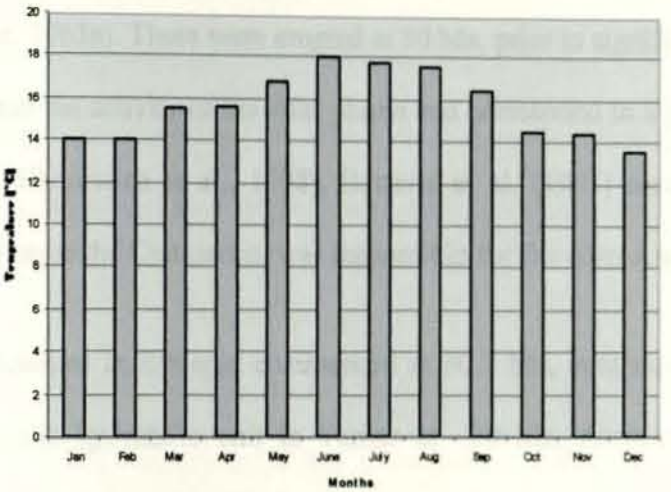

Figure 2.7 Long-term mean monthly temperature of the study area (Source: Ethiopian Meteorological Agency)

Plate 2A Gully formation in the Ashange Plain

2.5 Regional Geological Setting

The Cenozoic Ethiopian continental flood basalt province is located at the junction of three rifts: the oceanic rifts of the Red Sea, the Gulf of Aden and the East African continental rift. The main part of the province crops out in Ethiopia, whereas the rest is located on the eastern side of the Red sea, in Yemen. In Ethiopia, a huge volume of lava (about 350,000 Km^3) forms a pile up to 2,000 m thick, and covers more than 600,000 Km^2 (Mohr and Zanettin, 1978) (~ 750,000 km^2 before erosion) (Mohr, 1963a). These were erupted at 30 Ma, prior to significant extension. They result from the activity of the Afar plume and correspond to a pre–Oligocene hotspot track (Chorowicz et al., 1998). Bonavia et al. (1995) assumes that this hotspot, active since the Cretaceous, was responsible for the Afro-Arabian swell.

Rhyolitic volcanism in Ethiopia commenced at 30.2 Ma, contemporaneous with the first rhyolitic ignimbrite unit in Yemen at ~30 Ma. Accurate and precise $^{40}Ar/^{39}Ar$ dates on initial rhyolitic ignimbrite eruptions suggest that silicic flood volcanism in Afro-Arabia post-dates the Oligocene Oi2 global cooling event, ruling out a causative link between these explosive silicic eruptions (with individual volumes ~200 km^3) and climatic cooling which produced the first major expansion of the Antarctic ice sheets. Ethiopian olcanism shows a progressive and systematic younging from north to south along the escarpment and parallel to the rifted margin, from pre-rift flood volcanics in the north to syn-rift northern Main Ethiopian Rift volcanism in the south. A dramatic decrease in volcanic activity in Ethiopia between 25 and 20 Ma correlates with a prominent break-up unconformity in Yemen (26-19 Ma), both of which mark the transition from pre- to syn-rift volcanism (~25-26 Ma) triggered by the separation of Africa and

Arabia (Ingrid et al., 2002). A second magmatic hiatus and angular unconformity in the northern Main Ethiopian Rift is evident at 10.6-3.2 Ma,

The flood basalts of the Ethiopian Traps are transitional between tholeiitic and alkaline in composition. They form three distinct magma groups, which show geographical rather than temporal variation in their major and trace element composition (5). The LT basalts, which occupy the north-western part of the plateau, show consistently low TiO_2 contents and considerable heterogeneity in their trace element geochemistry. Marked troughs for Th and Ta-Nb, and variable LREE enrichment may suggest that they have undergone extensive lithospheric contamination, and that they are derived from a LREE depleted garnet free source.

The Maichew volcanics represent the thickest and most complete pre-rift plateau flood volcanics (comprising Ashangi Basalt, Amba Aiba Basalts, and Amba Alaji Basalts and Ignimbrites/Rhyolites), which occur within at the eastern-most margin of the western Ethiopian plateau volcanics (Zanettin and Justin-Visentin 1974; Mohr, 1980 and references therein).

Seven stratigraphic sequences (bottom to top) are identified in Maichew area:
1. a deeply weathered and often tilted basalts (phyric and aphyric) with intercalations of basaltic agglomerates (~1900-2500 m); 2. an ankaramitic to phyric and aphyric basalts and agglomerates (~2500-2700 m); 3. a cliff forming aphyric basalts and intercalations of basaltic agglomerates (~2700-2900 m); 4. an unconsolidated lithic tuff with minor phyric basalt intercalations (~2900-3000!m); 5. an ankaramitic and phyric basalt with ~20-40 m thick ignimbrite and unconsolidated tuff (~3000-3200 m); 6. an intercalations of ankaramite and phyric

basalt (~3200-3450 m); and 7. an aphyric and phyric basalt intercalations with 20-40 m thick ignimbrite (~3450-3870 m) Kabeto et al., 2004.

2.6 Regional Geologic Structures

The evolution of the area is controlled by up-lifting and up-warping (Meral 1963; Azzaroli, 1968). At the beginning of each stage volcanism occurred within a large, and elongated basin. Then, the outer part of the basin was uplifted and volcanism died out on the uplifted areas. In this way the escarpment was formed and volcanism was confined to the rifts. Afterwards, strips of the escarpment and the outer zone of the rift were in turn lifted up forming intervening marginal grabens and lead to a further narrowing the rift. In some cases (Afar) the shifting of the escarpment towards the axis of the rift, matched by a widening of the rift, caused regional extension. Sometimes the general uplift of the whole area, involving a stage of volcanism and tectonism, could have caused the termination of the stage itself.

The most important of the volcanic and tectonic stages noted in the Ethiopian plateau have been tentatively correlated with the main episodes of the evolution of the red Sea and the Gulf of Aden (Zanettin and Justine-Vesentin, 1975).

The pre-Oligocene escarpment (which later was dated as Oligocene) was formed immediately after the extrusion of the Ashangi basalts. This is thought to be the western extension of the Upper-Eocene South-Arabian downwarp (Baydoun, 1970) which delimitates the Gulf of Aden on its northern side. The emplacement of the Aiba flood basalt can be correlated with the first important separation of Arabia

from Africa. Alaji rhyolite and basalts and the formation of the western Afar margin coincided with the beginning of the formation of the Red Sea.

2.7 Local Geology

2.7.1 General

The Ashenge lake basin is comprised of highly fractured and weathered basaltic rocks: olivin basalt, pyroxen basalt and amygdaloidal basalt. Based on the work of Zanettin Jestin (1978) the rocks in the catchment correlate with the pre-Oligocene Ashange Formation of basalts with transitional tholeiitic affinity and/ or alkaline basalts which are low in Al_2O_3 and high in TiO_2 and the Oligocene Aiba Formation, whose composition is very homogeneous, transitional between tholeiitic and alkaline basalt (Zanetiin et al., 1974a; 1975).

A 1: 50,000 topographic map (1996 E.C.) and aerial photographs of 1980 E.C and 1986 E.C have been used to map the structures and to identify the different lithologic units prior to field work.

The basin floor is dominantly covered by Quaternary deposits from alluvial, colluvial and lacustrine sources. They are exposed along gulley cuts at the southern, south-eastern and south-western lake shore areas.

The rocks in the catchment are grouped into five units: alluvial/ colluvial sediments, basalt-pyroclastic intercalations, pyroclastic rocks, ultramafic rocks and lacustrine deposits. (Figure 2.8)

2.7.2 Alluvial and Colluvial sedimentary unit

This is the most extensive unit in the catchment, covering approximately 26.2 km^2. It is found in the low lying plane surrounding the lake, mostly in the northern part. Both alluvium and colluvium are included in the unit, with the exception of the swampy area. People depend on this part of the catchment for agriculture. Thick piles of the unit are exposed by the gullies, especially in the South and South-Eastern part of the catchment (Figure 4.1).

2.7.3 Lacustrine sedimentary unit

Lacustrine sediments are exposed along the shoreline of the lake. Some stromatolites are also mapped as patches around the lake and standing at different heights. Diatomite and shelly layers are also exposed by gully cuts and distributed at different heights. In the gullies located in the Ashange plain, peaty layers have also been seen (figure 4.6).

2.7.4 Basalt-pyroclastic intercalation unit

This unit has the second most aerial coverage (approximately 24.31 km^2) next to the alluvial and colluvial sedimentary unit; pyroxene basalt is the most common rock found both within the unweathered black rock and the deeply weathered gray to reddish rock, having a sign of spheroidal weathering that is characterized by basaltic boulders of pyroxene composition (plate 2C). The unit is also composed of aphanitic basalt and amygdaloidal basalt that overlies and underlies the pyroxene basalt. In this unit dykes are present in the south east and northern parts of the catchment (Plate 2B), but it is less extensive than the pyroclastic rock unit (Figure 2.8).

Plate 2B Road cut exposure of a set of dykes in the basalt –pyroclastic intercalation unit (south eastern part of the catchment).

2.7. 5 Pyroclastic rock unit

This unit is exposed in the north-western part of the catchment where the highest mountain, Tikur Imba ridge, is located. Fresh and highly weathered rocks are present with different colors varying between black to grayish and reddish. The dikes are oriented generally E-W, NNE-SSW and NE-SW. Most of the faults show NE-SW strike and are dipping to SW direction at an angle between 50° and 65°.

Plate 2C Spheroidal weathering on pyroxene basalt at 556805E, 138784N

2.7.6 Ultramafic rock unit

This unit is exposed near to the South-Eastern water divide of the catchment. It has the second smaller aerial coverage next to the lake sediments. The rocks are black colored with coarse grained phenocrysts of olivine, pyroxene and some plagioclase (Plate 2D). They form cliffs similar to the pyroclastic rocks in the NW part of the catchment but they are relatively less affected by geological structures.

Plate 2D Weathered Plagioclase in feldspar rich basalt

Figure2.8 Geologic map of the Ashange Catchment

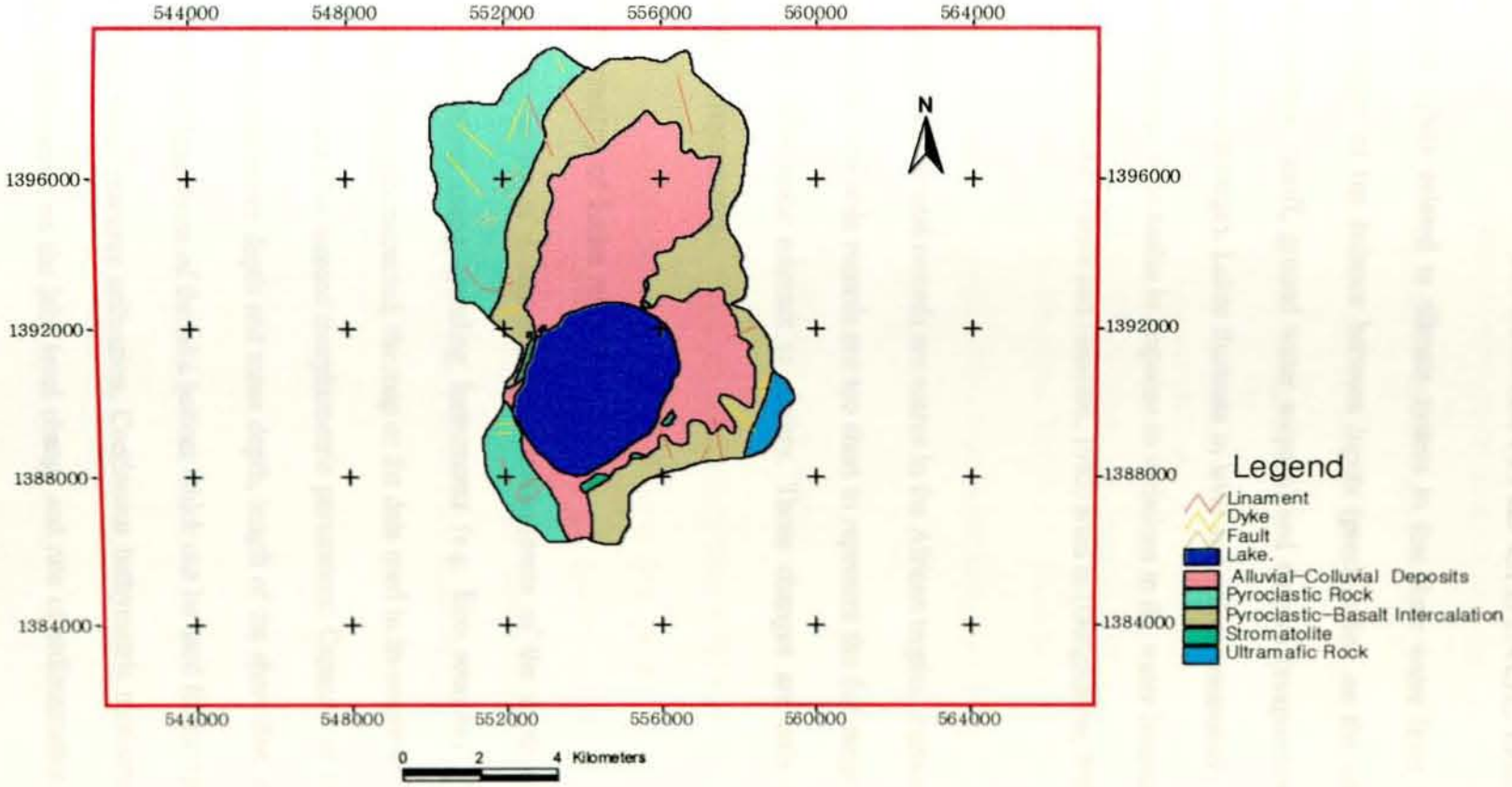

CHAPTER THREE

RECENT ENVIRONMENTAL CHANGE DETECTION

Lakes are tightly related to climate system in that their water level and chemistry are manifestations of the balance between inputs (precipitation on the lake surface, stream inflow, surface runoff, ground water seepage) and outputs (evaporation, stream outflow, ground water discharge). Lakes fluctuate in level and volume seasonally and inter-annually and at millennial time scales in response to variations in the water balance over the lake and its catchment (Street-Perrot and Harrison, 1985) sited in (Dangachew, 2002).

Continuous instrumental records are scarce in the African tropics. Furthermore, in Africa as elsewhere, the available records are too short to represent the full range of natural climate changes at time scale relevant to society. Those changes are only known from high resolution proxy records.

3.1 Bathymetry of Lake Ashange

Bathymetric survey of a lake refers to measurements of the depth of a water body at different locations using sounding instruments (e.g. Eco sounder). From the survey a bathymetric map is constructed, the map or the data used in its construction provides certain quantities that may be termed morphometric parameters: Capacity of the lake, free water surface area, maximum depth and mean depth, length of the shore line, development of the shore line, configurations of the lake bottom which can be used for navigation purposes and for a sound water resource utilization. Continuous bathymetric measurement of lakes also provides information on the lake level change and rate of sedimentation by computing the elevation capacity curve of the lake.

The bathymetric map of Lake Ashange has been constructed from readings taken by Eco sounder in 2001. 98 points on two crossing traverses have been taken, in order to draw the contours. To prepare the map of the lake area surfer 7.0 was used (Figure 3.1). The constructed map for the year 2001 is compared with the bathymetric map prepared by the Ministry of Water Resources in the year 2002.

The gauge levels measured between 1975 and 2001 from Lake Ashange show that the lake level dropped from 1975 to 1982 by about 1 m. Between 1983 and August 1991 there were no records due to the war in the region (Figure 3.2). A continuous increase of the lake level since 1992, from 0.5 m to about 4.14 m over the last nine years, is also evident from the data (Annex D).

3.2 Topographic maps and Lake Area change

From the field observation the recent lake datum is taken as 2440 m a.m.s.l.. The lake datum, from the 1996 topographic map, is situated lower than the present. Comparing the 1996 topographic map and the present lake level it has been found out that the shore line at present is located 350 meters further north and 250 meters further east of the lake. In the Southern part, the level is not much affected but a small change has been observed in the western part (Figure 3.7).

3.3 Seasonal Lake level change

A change in the lake level is also observed at different times of the year. The lake generally rises from July to November, and attains its maximum level in October or November. On the contrary the lake level decreases from December to June, the minimum level is attained in June. From the two plates taken in different season (i.e. in October and January 2003), the

lake decreased its volume in January as compared to October (Chapter IV- Plate 4B and 4C; Figure 3.3).

Due to the relatively fast increase in the lake level since 1996, the bathymetry that has been constructed using the data taken in 2001, could not fit well on the lake area of the 1996 topographic map (Figure 3.1). The 3D model of the lake is constructed using Surfer 7.0 software which simulates the bottom topography of the lake and shows that the deepest part is found in the western part of the lake (Figure 3.4).

Information from local people and the Raya Valley project report (RVDP/Feasibility report-Hydrology, December 1997) shows that in the last 50 years the lake water level is decreasing fast. They also say that the water is retreating to the southern central side, where the lake might have the maximum depth. The coverage of the lake water was about 17.5 Km^2 in 1965 and reduced to13.8 Km^2 in 1986 as observed from aerial photographs taken on June 15, 1965 and on June 13, 1986 respectively. From the topographic map of 1996 the lake covered an area of 13.2 Km^2 and from field measurements in the present, 2003, study the lake area coverage is 15.35 Km^2 (Table 3.1; Figure 3.5).

In the same way the shorelines mapped in figures 3.6A-3.6G show that the lake level decreased from 1965 to 1980 and also from 1980 to 1986. Shorelines are more exposed in the 1986 aerial photographs than in the 1980 and even more in the 1965 photo. Shorelines are well exposed only on the northern part of the lake and the number and the continuity is different in the various photos taken for the analysis. In 1965 photographs (figure 3.6A, C and G) the three Shorelines traced from the northwestern part are localized and discontinuous. However, the 1980 shorelines (figure 5.6B) are very well developed and at least three shorelines have been mapped in the North and Northwestern parts of the lake.

Shorelines are mapped all around the lake from the 1986 aerial photographs figure 3.6F and D) and they are continuous and numerous (i.e. five sets of shorelines). As there is no date, available at this stage, it is difficult to tell the time of formation of the shorelines. Figure 3.6F gives a complete picture of the generalized lake level changes in the past.

In Plate A an Italian house is shown at a former shoreline. The house was constructed in the 1930's during the Ethio-Italian war. Now the house is standing 12 m above the present lake level at an altitude of 2452 m. Sediments found surrounding the house might have been deposited at that time.

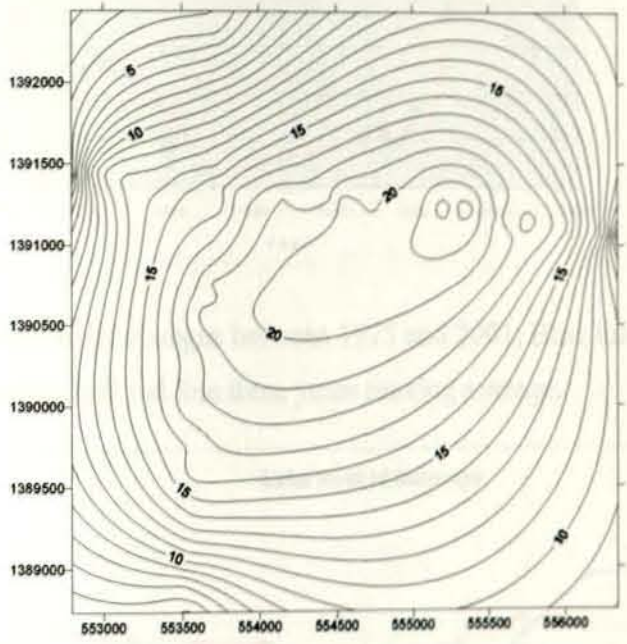

Figure 3.1 Bathymetry of Lake Ashange

Lake level data from the Ministry of water resources (Figure 3.2) shows a general agreement in the trend of a five years moving average with the rainfall data from the Maychew metrological station over the last 19 years (lake level data is missing from 1983-1991). An opposite trend of precipitation and lake level change over the last 6 years might be due to a change in the runoff coefficient as a result of changing land use land cover and/or reduced evaporation.

Elsewhere there are also present day lake level variations, which cannot be explained by a variation in the annual precipitation. The Lake Awassa rise between 1954 and 1972 was not accompanied by a reduction in evaporation: the number of wet days increased, and land was cleared for cultivation perhaps increasing runoff (Makin et al., 1974; Grove et al., 1975; Lamb 2001).

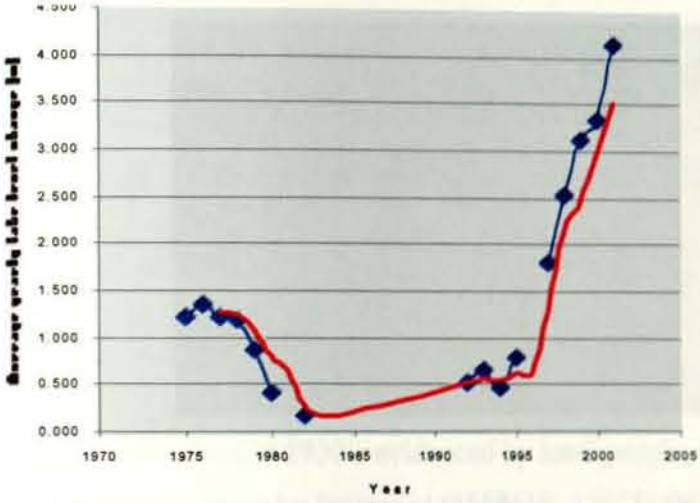

Figure 3.2 Lake level changes between 1975 and 2001; Blue line is observed yearly lake level change and red line three years moving average.

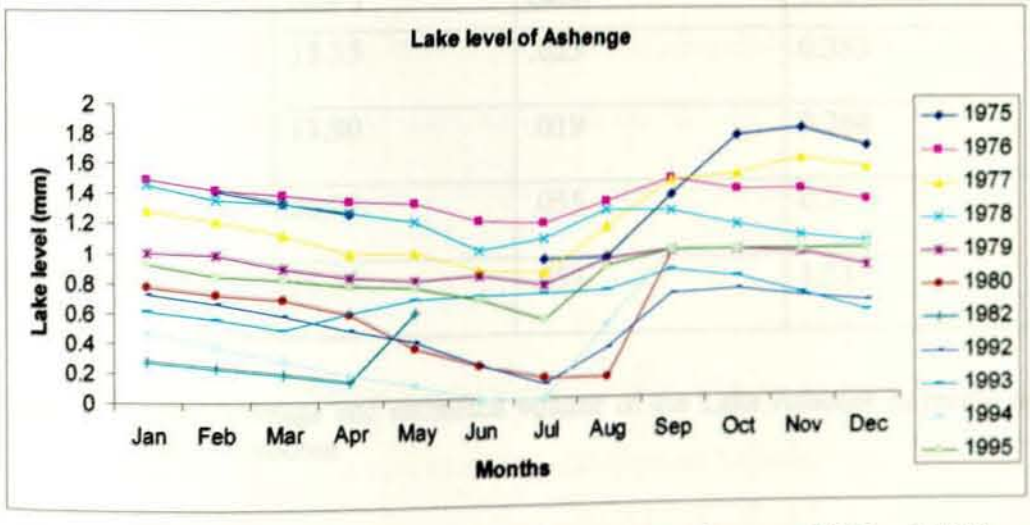

Figure 3.3 Monthly lake level change of Lake Ashenge between 1975 and 1995

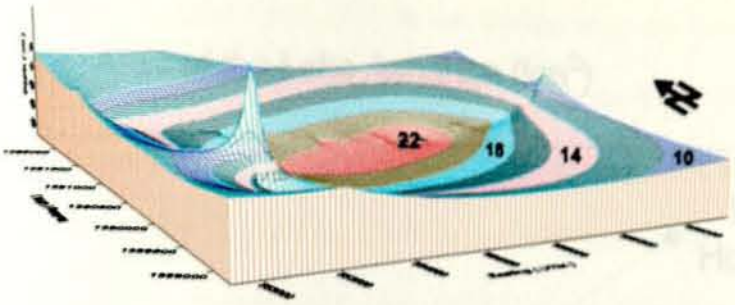

Figure 3.4 3D model of Lake Ashenge bottom

Plate 3A. the lake level in 1930's evidenced by local people, the house were reconstructed just at the shore by Italians at (555861E, 1292715N) at an altitude of 2452 m a.m.l

Year	Area of the lake (km^2)	Estimated depth (km)	Estimated volume of the lake (km^3)
2003	15.35	.023	0.353
1996	13.90	.019	0.264
1930	20.02	.035	0.7
Early Holocene	28.84	.053	1.53

Table 3.1 Area coverage and estimated volume of the Lake Ashenge in recent times and Early Holocene

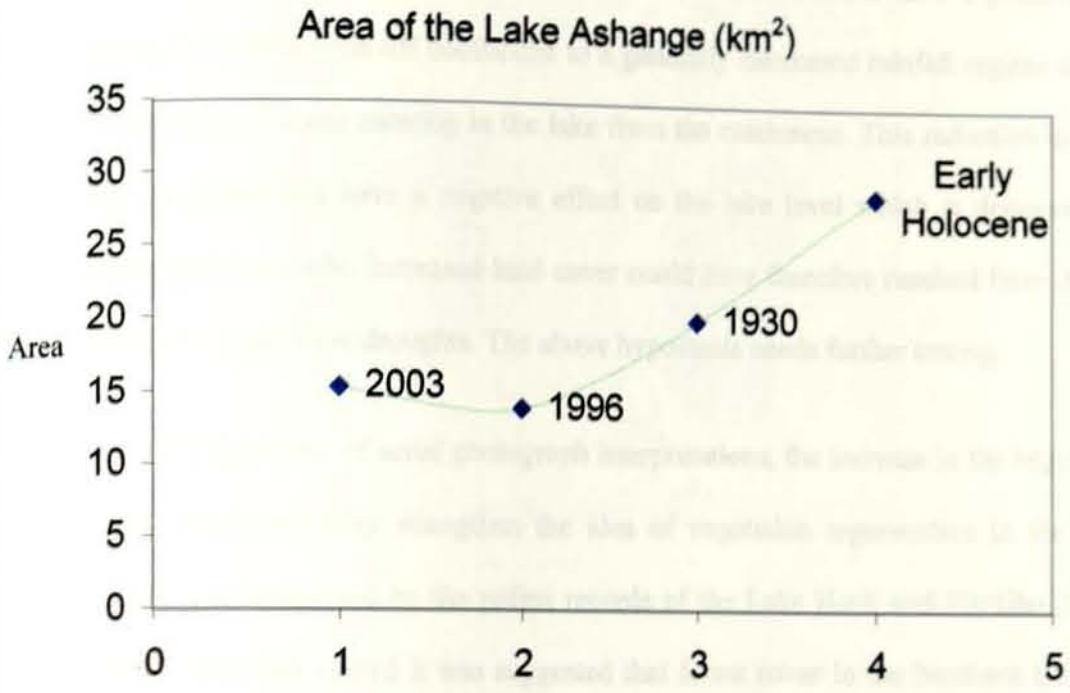

Figure 3.5 Lake Ashange lake levels reconstructed from recent and geomorphic evidence

A vegetation map of the catchment has been prepared from three aerial photographs (1965, 1980 and 1986). Comparison of the three maps has indicated that vegetation in the catchment has shown a general increase since 1965. In the western half part of the catchment, in the photo of the 1965 (Figure 3.6A) as compared to the 1980 (Figure3.6B) we can see that the vegetation was restricted close to the lake and was sparse further north. The 1980 photo (figure 3.6B) shows the vegetation were denser and could be traced along the streams up on the mountains.

Similarly, the vegetation cover increased from 1965 to 1986. In the Southeastern part of the catchment, where Bahiri Hatsera Aba Kiros and Menkere Giyorgis churches are located, the vegetation cover in 1965 (Figure 3.6G) was sparser and covers less area than the 1986 (Figure 3.6F). The vegetation cover traced far from the lake shore in the 1986 photo appears to be due to the relative lake level decreases in 1986 as compared to the 1965.

The increase in land cover since 1965 in the catchment could have a positive feed back through a reduced run off coefficient to a generally decreased rainfall regime and hence to the amount of water entering in the lake from the catchment. This reduction in water from the catchment can have a negative effect on the lake level which is documented by the instrumental records. Increased land cover could have therefore resulted from depopulation caused by successive droughts. The above hypothesis needs further testing.

From the three sets of aerial photograph interpretations, the increase in the vegetation cover in the catchment may strengthen the idea of vegetation regeneration in the absence of pressure, as evidenced by the pollen records of the Lake Hayk and Hardibo (Darbyshire., 2003). From this record it was suggested that forest cover in the Northern Ethiopia could again increase in the future, under appropriate land management, providing integrated benefits of forest-based industry, and soil and water conservation. Land use is a primary indication of the extent and degree to which man has made impression on the earth's landscape.

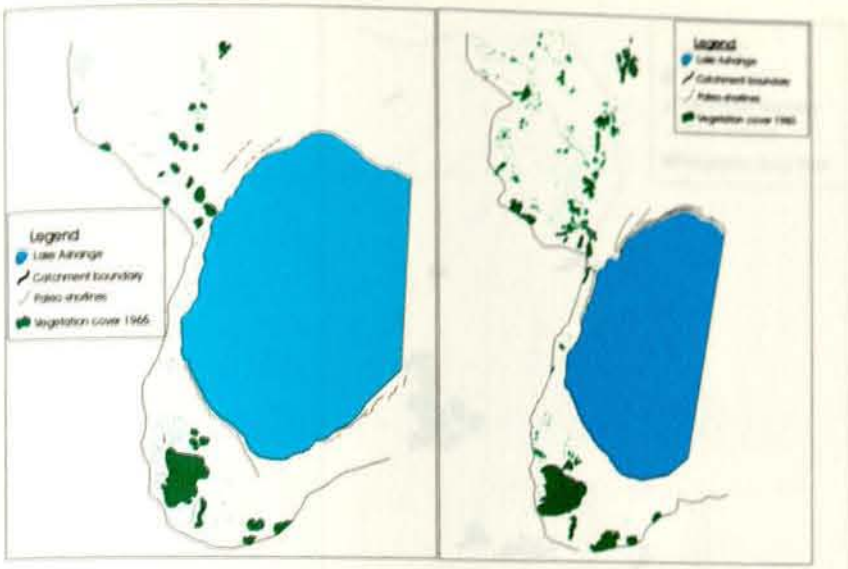

Figure 3.6A the western half of the catchment mapped from the 1965 aerial photograph

Figure 3.6B the western half of the catchment mapped from the 1980 aerial photograph

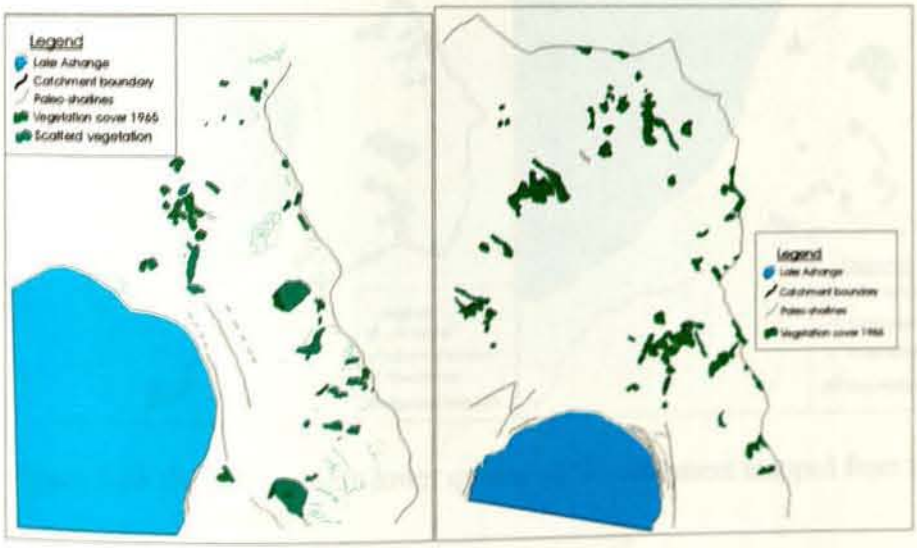

Figure 3.6C the northeastern quarter of the catchment mapped from the 1965 aerial photograph

Figure 3.6D the northern upper half of the catchment mapped from the 1965 aerial photograph

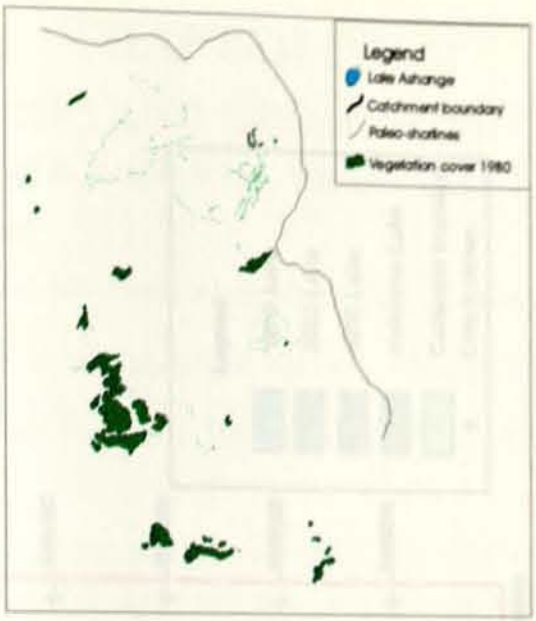

Figure 3.6E the northeastern lower quarter of the catchment mapped from the 1980 aerial photograph

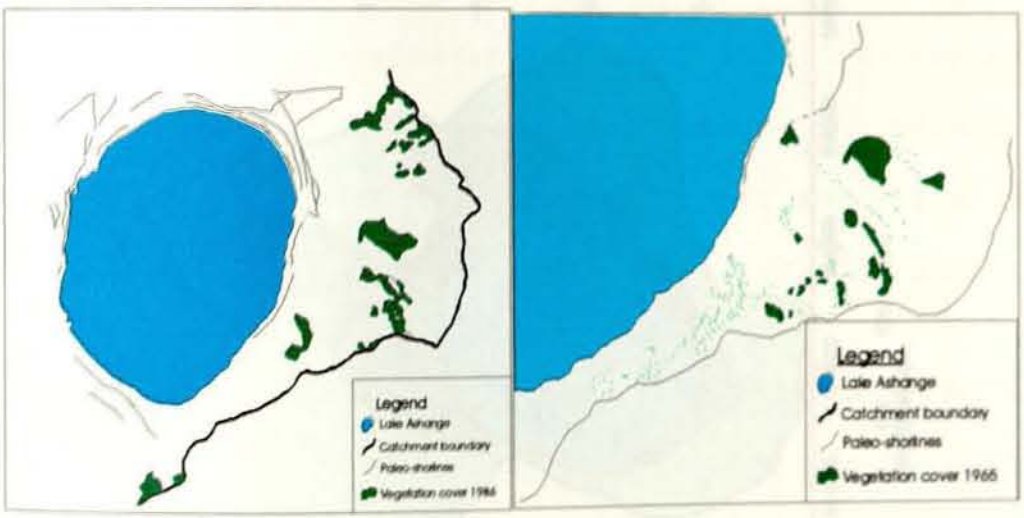

Figure 3.6F the southeastern lower quarter of the catchment mapped from the 1986 aerial photograph

Figure 3.6G the southeastern lower quarter of the catchment mapped from the 1965 aerial photograph

Figure 3.7 Lake Ashange Leke Level change

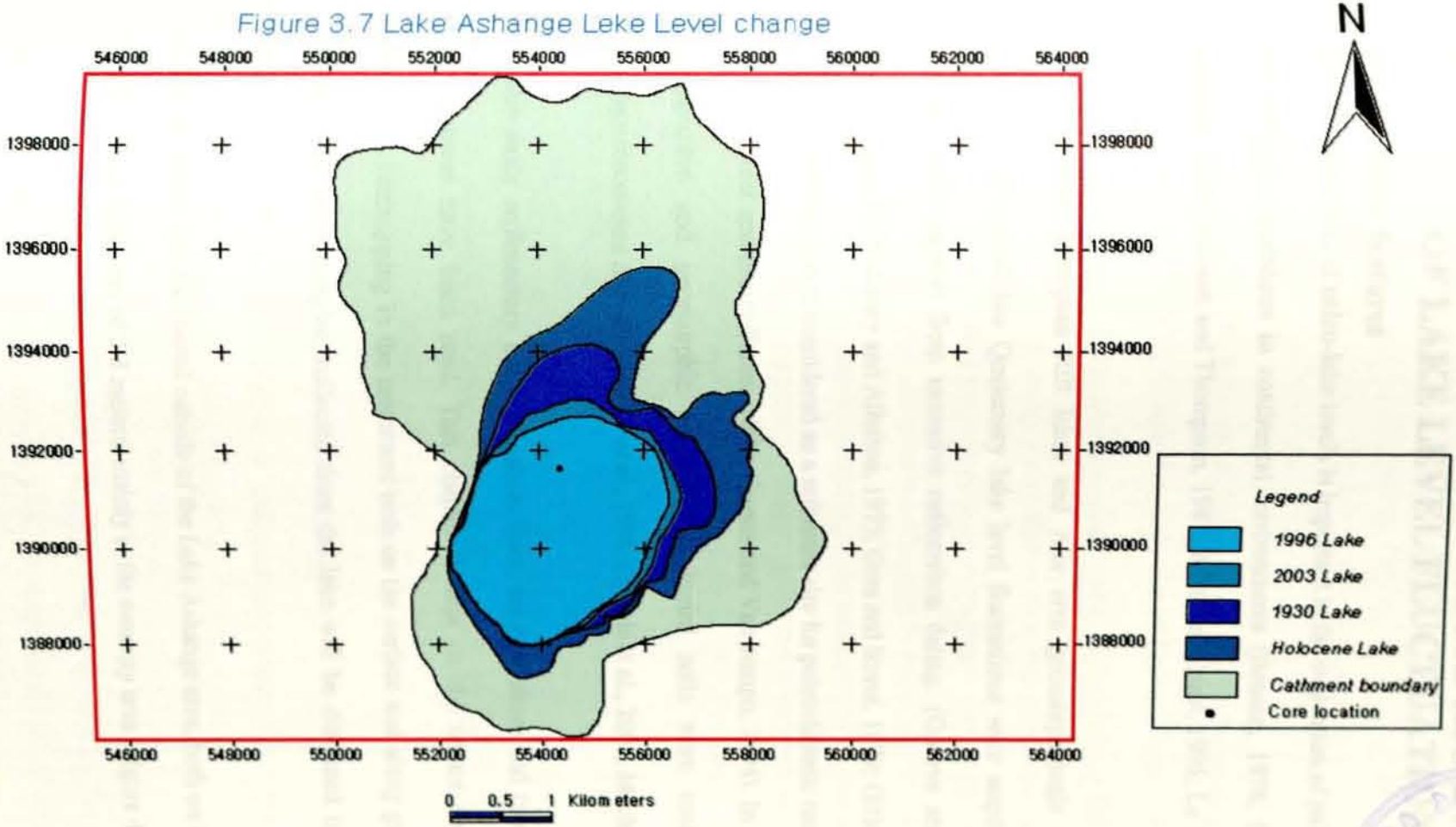

CHAPTER FOUR
STRATIGRAPHIC AND GEOMORPHIC EVIDENCES OF LAKE LEVEL FLUCTUATION

4.1 Shoreline features

The reconstruction of paleo-lake levels is important in the evaluation of paleohydrologic and paleoclimatic conditions in continental environments (Benson, 1978; Street-Perrott and Harrison, 1985; Benson and Thompson, 1987; Wohl and Enzel, 1995; Le Turdu et al., 1999 and others).

In the Central Ethiopian Rift lakes and Afar area geomorphologic and stratigraphic evidences of several late Quaternary lake level fluctuations were acquired over the last decades, with support from extensive radiocarbon dating. (Groove and Goudie, 1971; Groove et al., 1975; Laury and Albriton, 1975; Gass and Street, 1979; Gillespie et al., 1983). As a result the region is considered as a reference site for paleoclimatic reconstruction in the tropics (Street and Street-Perrot, 1990; Gasses and Van campo, 1994). In northern Ethiopia stratigraphic and geomorphic evidences of buried soils were used to reconstruct paleoenvironmenal changes (Baraki et al., 1998; Dramis et al., 2003; Machado et al., 1998).

In this study sedimentary data from shore lines, the near shore and from the deep water environment have been used. This chapter focuses on the nature and distribution of sediments outcropping in the catchment both on the surface and along gully sections. The results from core samples, collected from the lake will be discussed in the consecutive chapters.

Lake sediments are distributed outside of the Lake Ashange area, both on the surface and in gullies with a thickness of 2-5 meters, mainly in the swampy area (Figure 4.6).

Lake sediments are also distributed outside of the Lake catchment at two locations: a thin layer of diatomite exposed in a gully at (554303E, 1385904N, 2457 m) south of the catchment and along the main road north of the town of Korem at (555408E, 1384734N, 2434 m).

4.2 Gully formation

In Tigray, the change in the hydrological behavior has been attributed to an overall lowering of the infiltration capacity of the soils due to the removal of the natural vegetation (Hunting, 1974; Virgo and Munro, 1978; Machado et al., 1998). By comparing both the topographic maps at different times and during field observation it was found out that the size of the gullies was increasing with time, especially in the northern part of the catchment. On the Ashange plain active gullies are observed (Chapter II- Plate 2A). On the contrary in the southern and southwestern part of the catchment the local people are constructing terraces in the gullies and outside the gullies to decelerate the rate of soil erosion and hence gully formation.

Gullies are mainly developing in the south and north of the lake. At locations (554591E, 1388379N, 2458m), (555461E, 1393600N, 245 m) and (553139E, 1392515N. 2457m), the gullies are developing fast: some of the gullies were not present on the 1996 topographic map, and some others were then very small.

4.3 The stratigraphic record of Holocene deposits

Most sections have been studied in gully cut exposures. Six sedimentary sections have been taken from such sites (Table 4.1).

Section 1 is taken at N 12°34'683'', E 39°31'446'' (Figure 4.1). The thickness of the section is 4.8 meters. At the base, gravels are embedded within sand and occasional

beds of rounded gravel, originating from different varieties of basalt are found (i.e. olivine, pyroxene and amygdaloidal basalts are found). Very fine brown colored mud is overlaying the basal part having a gradational contact of few centimeters is further overlain by a fine grained sand layer of 26 cm thickness. The overlying unit is similar to the basal unit except for the absence of the gravel beds. The top 12 cm of this section is a brown soil in which rootlets are found.

Section 2 is taken in a gully running from N 12°34'011'', E 9°31'591'' to the lake at N 12°34'152'', E 39°31'582'' (Figure 4.2). The thickness of the section is 3.92 m. At the base, a 69 cm of fine sand is overlain by a 30 cm thick layer of sand with rounded pebbles which in turn is overlain by thick beds of alternating fine and coarse sand with sub rounded gravels in it. The thickness of the unit is 213 cm.

At the top of the lower units a thin layer of diatomite with a thickness of 2-3cm is locally exposed in the gully and dies out in either direction. The top 72 cm is a light brown soil with grass rootlets.

Figure 4.1 Section 1 taken from the Southwestern part of the catchment N 12°34'683'', E39°31'447'', (4.8 meters thick).

Figure 4.2 Section 2 taken from the Southwestern part of the catchment N 12°34'152'', E 39°31'582'' (2.18 meters thick).

Section 3 is located at N 12°33'851'', E 39°30'360'' at an altitude of 2470 m, with a total thickness of 5.22 m (Figure 4.3). The basal unit has a thickness of 90 cm and is composed of carbonate with brown silty clays. This pinches out towards the upper part of the gully. It is overlain by a 33 cm thick soil with a significant number of rootlets, this unit has a uniform horizontal thickness. On the top of the soil, sand with pebbles and cobbles is exposed and has a thickness of 29 cm. The top most unit is a thick soil with rootlets and a thickness of 370 cm.

Section 4 is located at N 12°33'896'', E 39°39'730', at an altitude of 2475 m. It has a total thickness of 2.3 m (Figure 4.4). The basal unit has a thickness of 72 cm and is composed of light brown clay. Laterally it is not extensive and pinches up the gully. A 32 cm thick diatomite layer abruptly overlies the clay. A second clay layer of 104 cm thick overlies the diatomite layer below. The top part of the section is covered by a 21 cm soil.

Section 5 is located at N 12°33'569'', E 39°29'366'' at an altitude of 2463 m in the southern part of the catchment (Figure 4.5). Here the local people have constructed

some terraces to prevent the gully from further erosion. The basal unit in this section consists of a 126 cm thick brown silty to sandy clay, a 23 cm thick layer of sand and coarse pebble, and a 35 cm thick layer of shells (most likely Ostracodes).On top of the shelly layer a 100 cm thick layer of sand and coarse pebble is found. The top most unit is a brown soil with a thickness of 56 cm.

Section 6 is located north of the lake at 555461E, 1393600N at an altitude of 2451 m, in the swampy area, through which the lake gets most of its water from the surrounding mountains and springs (Figure 4.6). As shown in figure 4.11 this part of the catchment consists actively forming gullies and exposes sediments. The gully from which the section is taken does not appear on the topographic map of the year 1996. A 130 cm thick diatomite layer is the basal unit. It is overlain by a15 cm dark peaty material with degraded plant remains and a 15 cm thick diatomite layer above it. A second dark peaty material of 125 cm thickness is found on top of the second diatomite layer which is cupped by a 60 cm alternating dark and white layers (figure 4.7).

Figure 4.3 Section 3 taken from the Southwestern part of the catchment N 12°33'851'', E 39°30'360'' (5.22 m thick).

Figure 4.4 Section 4 taken from the Southwestern part of the catchment N 12°33'896'', E 39°39'730' (2.3 m thick).

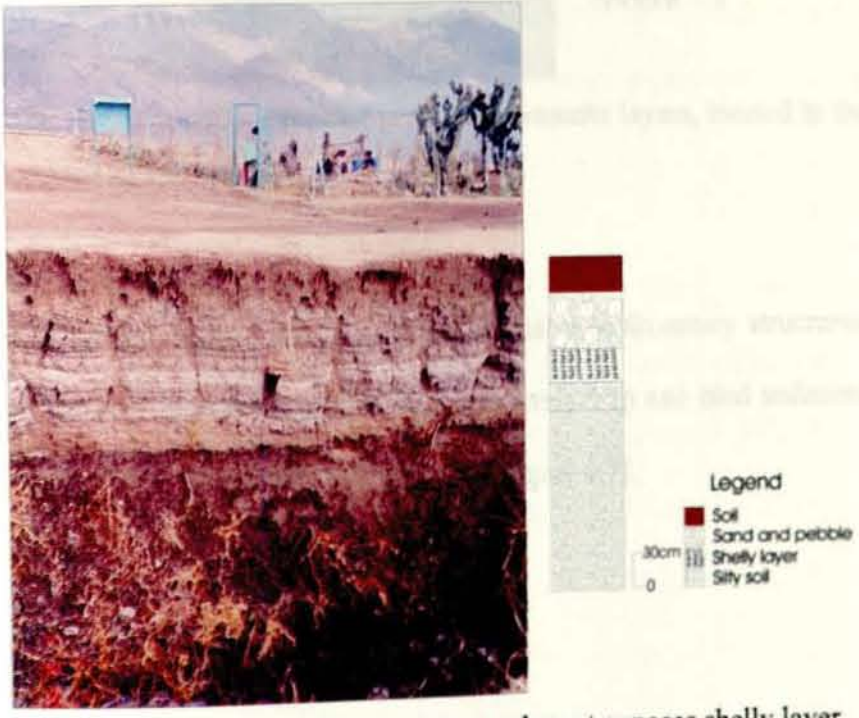

Figure 4.5 Section 5 from the southern part of the catchment exposes shelly layer, N 12°33'569'', E 39°29'366'' (2.4m thick)

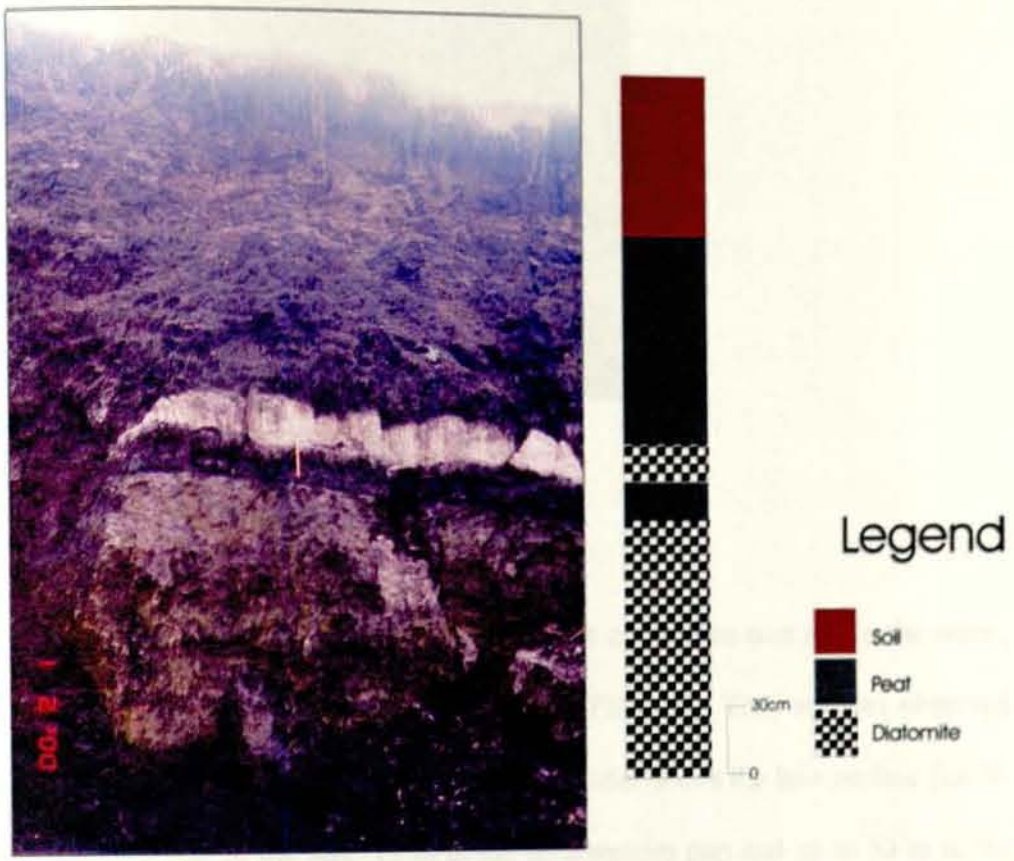

Figure 4.6 Section 6 in a gully, exposing peaty and diatomite layers, located in the swampy area 555461E, 1393600N, (3.45 m thick).

4.4 Stromatolites

Stromatolites (algal biolithites) are defined as "laminated sedimentary structures, built by dense mats of primary blue green algae which selectively trap and bind sediment particles along their mucilaginous filaments" [(Garret, 1970) Figure 4.7].

Plate 4A. Stromatolite

In the study area, stromatolites are observed both outside of the lake area and in the water, standing more than 1 m above the surface of the lake (Plate 4C). They are also observed outside of the present lake area standing at different altitudes above the lake surface [i.e. 9-14 m in the northern part of the lake, 12 m in the northwestern part and up to 30 m in the southern part of the lake (Figure 2.11)].

In lakes, stromatolites are essentially littoral or supra-littoral facies. They require warm, well-aerated water with low turbidity. If properly dated they indicate the water level at a particular time. A lake area can be reconstructed from the analysis of strandlines and section evidences (e.g. Gillespie et al., 1983). The area of a lake during a low stand may be difficult to determine if the evidence is currently submerged. Similarly, if the lake overflows during a humid phase, there is little information on the amount of excess water. Because of the fragmentary nature of the evidence it may be difficult to ascertain the chronological relationships between deposits, vital for palaeoclimatic reconstruction. However, hiatuses in section evidences can usually be easily identified

Modern examples of stromatolites are known from rocky shores of Lake Hayk, Awassa and Kivu (Grove et al., 1975; Beadle, 1974). The surface water of these lakes ranges in pH from 8.2 to 9.5 and in carbonate alkalinity from 6 to 16 mg/l. Although algal limestones are found in other parts of the world, notably in the Greate Salt Lakes and Lisan Formation of Israel (Neev and Emery, 1967), they often were formed in sodium chloride dominated waters in which much higher Ca^{2+} levels are possible.

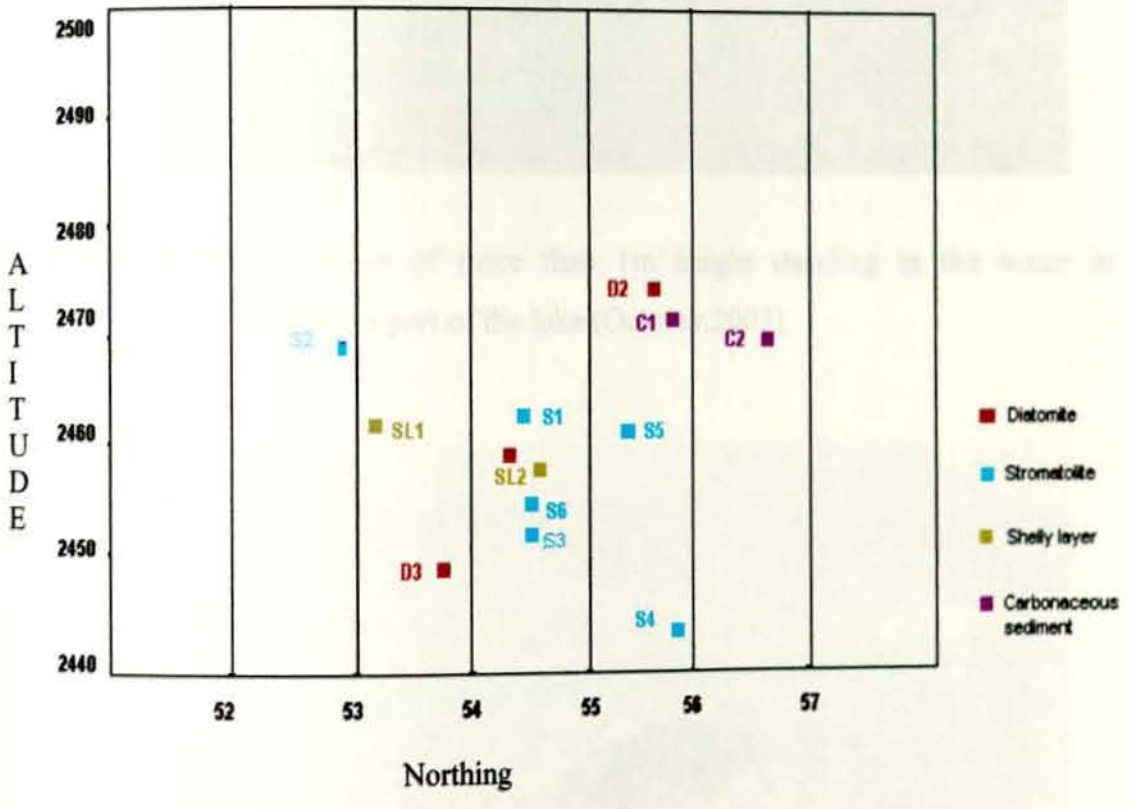

Figure 4.7 Altitudinal distributions of Sediments in the Ashange catchment.

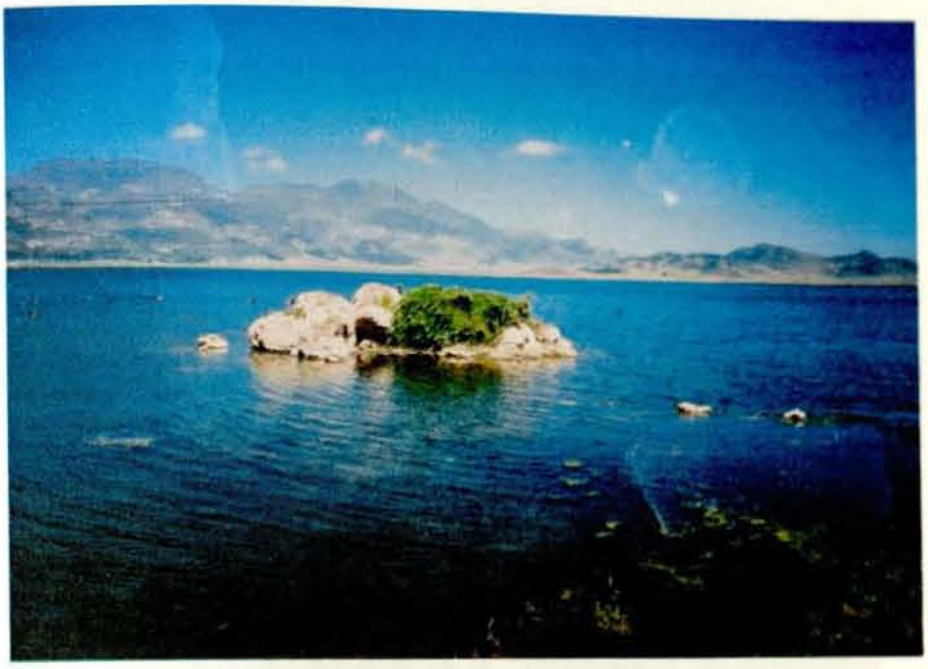

Plate 4B. Stromatolites of more than 1m height standing in the water in the southwestern part of the lake (October.2003)

Plate 4C. Stromatolites of more than 1m height standing on the lake shore in the southwestern part of the lake (January.2003)

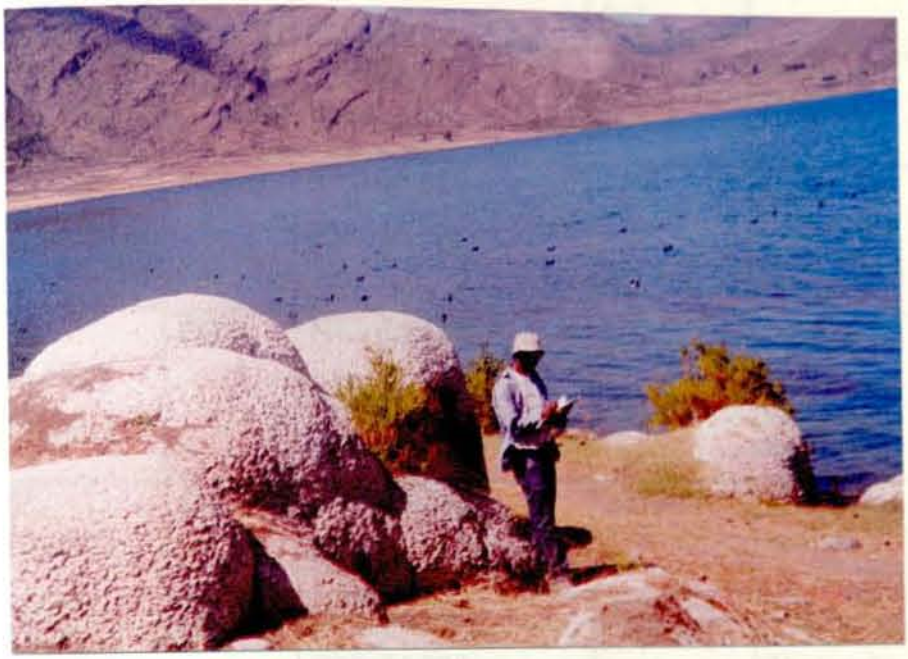

Plate 4D. Stromatolites outside of the present lake area in the southeastern part of the catchment

Plate 4E. Actively degrading land forming gullies in the Ashange plane

Samples	Gullies	Location	Altitude (m)	Remark
-	G1	N12o34.683 E39o31.446	-	Fluvial sediments
S1-03AS05	-	N12o35.816 E39o30.991	-	Carbonate sediments
S2-03AS06 03AS07	G2	N12o34.152 E39o31.582	2497	Diatomite, sand
S3-03AS08	G3	N12o33.851 E39o30.748	2470	Carbonate sediment
S4-03AS09 03AS10	G3	N12o33.896 E39o30.730	2475	Diatomite
S5-03AS011	G4	N12o33.416 E39o29.707	2462	Fluvial sediments
S6-03AS012	G5	N12o33.569 E39o29.356	2463	Shelly layer
S7-04AS01	-	(UTM) 553739E 1388050N	2448	Dark material??
-	G6	(UTM) 553139E 1392515N	2457	-
04AS02	G5	(UTM) 554303E 1385904N	2457	Shelly layer
S7-04AS03	G7	(UTM) 555461E 1393600N	2451	Peat layer

Table 4.1 Gully location and sampling points

To sum up, the understanding of paleoclimates in the region can contribute much to our understanding of global climate variability (Nicholson 1996). Paleo–lake level studies are also important for reconstructing past continental climatic records because they provide a sensitive means to evaluate water balance (Street-Perrott and Harrison, 1985). They can be used for monitoring the magnitude of hydrological changes. In combination with high-resolution lake-level chronologies, the relationship between the timing of global events and regional hydrological records can be established. Such coupling is potentially a powerful means for understanding and elucidating their imprint on continental climates.

Lake Ashange has experienced lake level fluctuations through out the Holocene. It shrunk and expanded seasonally and shows changes with rainfall amounts annually, therefore instrumental, observational and historical evidences have indicated that at decadal, annual and seasonal time scales the lake has been sensitive to rainfall variability.

As shown from stratigraphic sections, geomorphic evidences as well as the distribution of lake sediments in and outside of the catchment (figure 4.7) the lake had high-stands of about 30-(57?) meters and at least reached to 2470 m, when it spilled out of its current catchment, most probably during the early Holocene.

In the following part the results from the analysis of core samples from the Lake Ashange will be discussed and the result will be compared with those in chapter 3 and 4.

CHAPTER FIVE

RECORDS OF LAKE SEDIMENT CORES

Lakes are one of the few sites of continual continental deposition; as such they can yield a palaeoclimatic reconstruction less prone to hiatuses than other depositional environments. Closed-basin lakes can record response to changes in the balance between precipitation and evaporation through evidences from sediment, hydrochemistry and isotopic composition (Gasse et al., 1995).

Lake sediment cores contain a number of biological, physical and geochemical indicators of lake depth and chemistry. Cores can potentially yield proxy climatic data up to an annual scale of resolution.

5.1 Radiocarbon age and Lithologic description

A core of 8.1m long (the top 1.1 m taken from Kullumberg, 03AL1 and 7.0 m of Livingston core, 03AL2) was collected from 8.9 m depth of water at N12°35'694'', 39°30'501'' in October 2003 under the Lake Tana project. (Figure 3.7)

The core is sub-divided into five major lithological units (Figure 5.1) based on color, sedimentary structures and proportion of the different organic and inorganic components using the method described by Tröels-Smith (1955).

The basal radiocarbon date at 740 cm is 11,920 $\pm$ 40 14^C yrs BP. The age has been interpolated along the core assuming that the rate of sedimentation is the same for the whole length of the core and the top is modern. This brings the age at the base to13,047 14^C yrs BP.

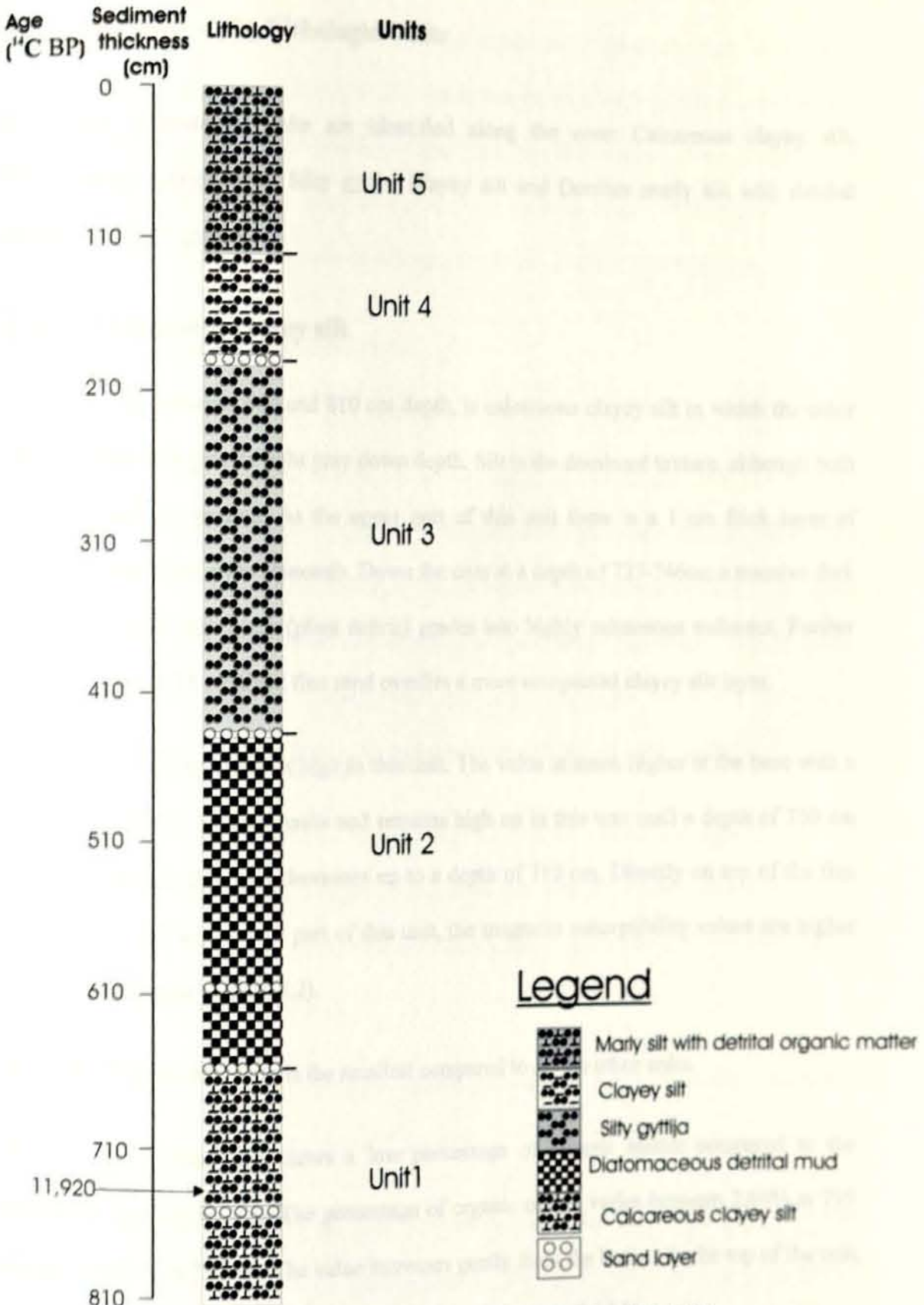

Figure 5.1 Ashange core section from 8.9m water depth (03AL1 and 03AL2).

5.2 Description of the Lithologic Units

Five major Lithological units are identified along the core: Calcareous clayey silt, Diatomaceous detrital mud, Silty gyttja, Clayey silt and Detritus marly silt with detrital organic matter (Figure 5.1).

Unit 1: Calcareous clayey silt

The basal unit, between 660 and 810 cm depth, is calcareous clayey silt in which the color changes from dark gray to light gray down depth. Silt is the dominant texture, although both clay and sand are present. At the upper part of this unit there is a 1 cm thick layer of gastropod shells and grass charcoals. Down the core at a depth of 727-746cm a massive dark gray shelly layer with herbs (plant debris) grades into highly calcareous sediment. Further down the core an 11 cm thick fine sand overlies a more compacted clayey silt layer.

The magnetic susceptibility is high in this unit. The value is much higher at the base with a value of about 400 arbitrary units and remains high up in this unit until a depth of 750 cm from the base but gradually decreases up to a depth of 710 cm. Directly on top of the fine sand layer, at the upper most part of this unit, the magnetic susceptibility values are higher than the middle part (Figure 5.2).

The water content in the unit is the smallest compared to all the other units.

The loss on ignition data shows a low percentage of organic matter compared to the remaining units of the core. The percentage of organic matter varies between 2.66% at 795 cm and 16.48 % at 730 cm. The value increases gently from the bottom to the top of the unit, but the average value for the whole length of the unit is about 8.18 %.

Unlike organic matter, the amount of carbonates in this unit is relatively high, with values ranging between 2.42 % and 23.83 %. The maximum values are attained at around 700 cm (23.8 %) and 750 cm (22.4 %) depth. Generally the values increase and are higher at the upper 110 cm of the unit with minor fluctuations and sharp decrease at 770 cm, 740 cm and 725 cm. The average value for the whole length of the unit is about 11.8 % (Figure 5.2).

Unit 2: Diatomaceous detrital mud

The diatomaceous detrital mud unit overlies the basal unit and is separated from it by a sharp contact. The unit lies between layers of fine sand at 660 cm in the lower part and 440 cm in the upper part. The color in this unit ranges between dark to very dark gray down the core and changes to light gray at the base. Detrital organic components and diatom mud are present in the whole length of the unit except at a depth of 503 cm where a bed of coarse sand of 7 cm thick is found. Charcoal from grass are found at the lower part of the unit. Very tiny equal sized bivalve fossils are found between 644 cm and 647 cm (Figure 5.1).

The magnetic susceptibility values for the whole unit are very small, but higher values are observed at the bottom 60 cm and top 20 cm of the unit with the highest value (of 48.1) at 624 cm. The highest peaks coincide with the sandy layers at the bottom, in the lower middle and top part of the unit (Figure 5.2).

The water content of this unit is higher than the lower unit (Calcareous clayey silt) and remains constant throughout the length of the unit.

The organic matter content in this unit is much higher than in the underlying unit. The content is more or less the same from bottom to the top. With an exception of minor

fluctuations, the unit has an average value of 29.08 % organic matter with a maximum value of 41.13 % at 440 cm and a minimum value of 12.08 % at 515 cm.

The carbonate content shows an opposite trend compared to the organic matter content. The carbonate content in this unit is smaller than both the underlying and the overlying units. The amount increases from bottom up to a depth of 610 cm and decreases upwards until a depth of 535 cm. The amount increases again up to the top of the unit. The value in the unit ranges between 0.0 % at a depth of 535 cm to 14.55 % at a depth of 445 cm, with an average value of 5.27 % (Figure 5.2).

Unit 3: Silty gyttja

The silty gyttja unit is found between 181 cm and 430 cm and overlies the diatomaceous detrital mud unit separated by a 1 cm of fine sand. The color ranges between gray and dark gray except at the upper part which is brown. Although herbaceous detrital organic component, diatom mud and detrital mud are present, the inorganic component is dominant. Unlike the underlying units there are no shelly and sandy layers except at the lower and upper boundaries (Figure 5.1).

The magnetic susceptibility value for this unit at its base is the same as for the underlying unit, but between 300 cm and 290 cm the value suddenly increases from 32.7 to 95.6 arbitrary units. The value remains higher with the exception of a decrease at about 200 cm.

The water content of this unit is somewhat higher than in the lower units and shows fluctuation at about 0.75 %.

The organic matter content of the unit is higher than in the calcareous clayey silt unit and smaller than in the silty gyttija. Values of 16.45% and 31.16% are the minimum and maximum organic matter contents in the unit and the average value is 21.89 (Figure 5.2).

The carbonate content in this unit is higher than in the diatomaceous mud unit but it is more or less the same as compared to the basal unit. The amount fluctuates between 3.01 % and 24.5 %. It attains a maximum value at the top of the unit and a minimum at a depth of 425 cm. The average value for the unit is 12.75 %.

Unit 4: Clayey silt

The clayey silt unit is found between 110 cm and 177.5 cm. It overlies the silty gyttja unit and is separated by a 3.5 cm thick fine sand. The color ranges between light gray to dark gray. Silt is dominant in the whole length of the unit. In the lower part, detrital organic matter and detrital mud are present in addition to the dominating silt. In the upper 55 cm, the lower components grade into a thin layer with an equal proportion of clay and mud. The unit is massive (Figure 5.1).

The water content value in this unit is in the range of the lower unit but shows much more fluctuations.

The magnetic susceptibility shows a sharp increase from 35.1 to 109.7 arbitrary units at depths of 186 cm and 174 cm respectively.

The organic matter content in this unit is higher than in the basal unit but it is lower than in the other underlying units. The amount is similar throughout with a small degree of fluctuation. The average value is 15 % and ranges between 27.6 % and 13.79 % at a depth of 115 and 165 cm respectively.

The carbonate content is smaller than in the underlying unit but it is comparable with the diatomaceous detrital mud unit. It ranges between 0.21% at 140 cm and 8.87 % at 145 cm and has an average value of 10.13 %.

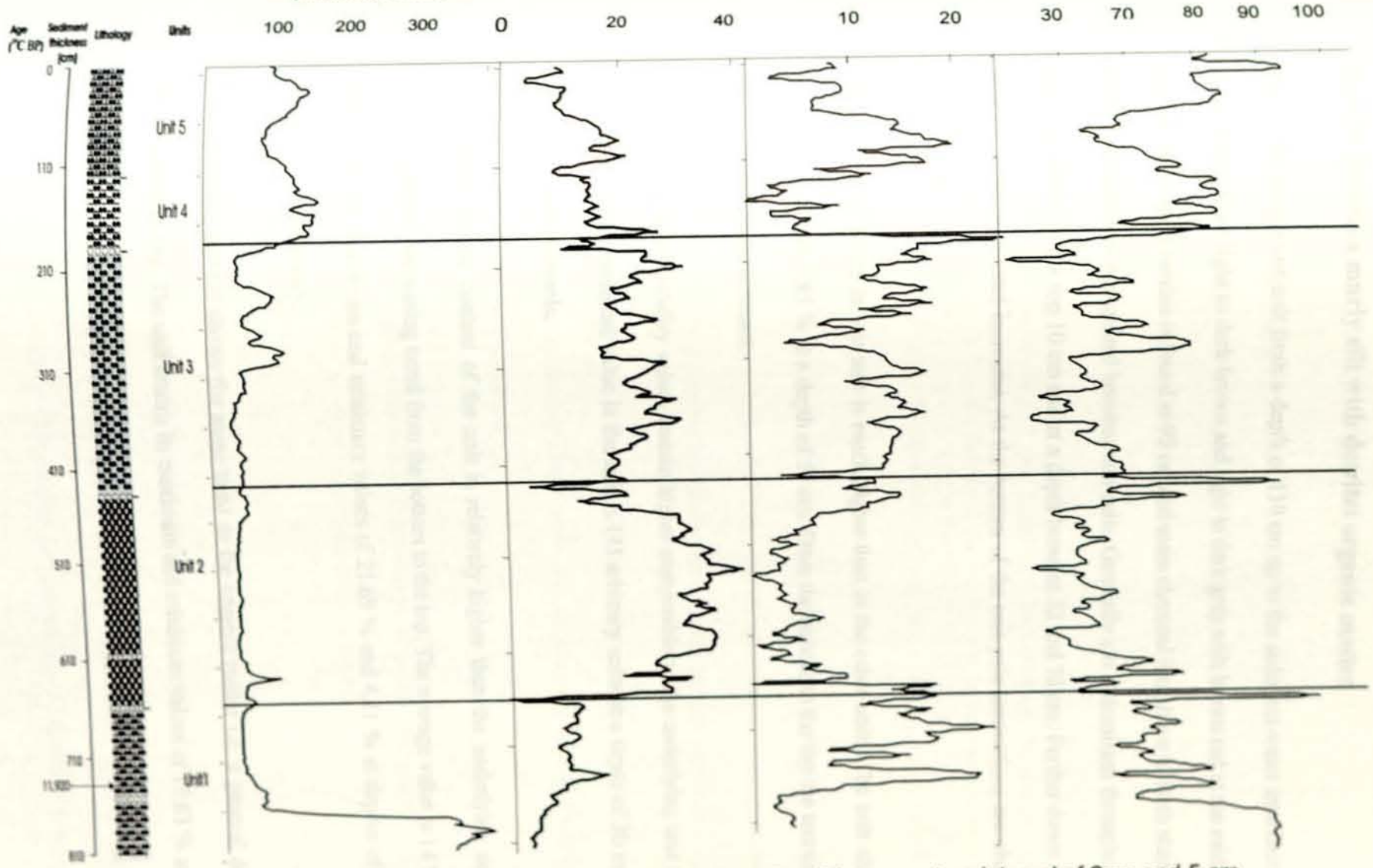

Figure 5.2 magnetic susceptibility and Los On Ignition results of the core at an interval of 2cm and 5 cm

Unit 5: Detritus marly silt with detrital organic matter

This is the uppermost unit from a depth of 110 cm up to the sediment-water interface. The color ranges from light to dark brown and light to dark gray with brown red at the middle of the unit and a pale lamina is found at 95 cm and some charcoal just above it. Both sharp and diffuse contacts are recognized between sub units. Generally silt is dominant throughout the unit, especially in the top 10 cm and at a depth between 52 and 78 cm. Further down in this unit the amount of marl increases. At the bottom of the unit pale laminations are observed (Figure 5.1).

The amount of water in this unit is much higher than in the other units. The unit attains a maximum value of 0.85 % at a depth of 50 cm. From the bottom to the top the amount first decreases and then increases.

The magnetic susceptibility values remain higher comparable to the underlying unit except at the base. The maximum value in the unit is 145 arbitrary units at a depth of 30 cm. The value decreases upwards.

The organic matter content of the unit is relatively higher than the underlying unit and shows a general decreasing trend from the bottom to the top. The average value is 14 %. The unit attains its maximum and minimum values of 21.69 % and 4.21 % at depths of 90 cm and 15 cm respectively.

The carbonate content shows the same trend as the organic matter i.e. a general decrease from bottom to top. The unit attains its maximum and minimum values of 19.63 % and 2.40 % at 85 cm and 15 cm depths respectively.

5.3 Core sediment mineralogy

5.3.1 X-ray differactometry

The identification of minerals in the core is done through the use of X-ray analysis on the 51 sub samples sampled at an interval of 16 cm from the core. (Table 5.2), using a Philips PW 1710 X-ray diffractometer.

The XRD method works on the fact that X-rays are diffracted by the atomic layers in crystals. In mineralogical studies, the diffracted X-rays are used to measure the dimensions of atomic layers in the crystals. Because each mineral has a distinct set of atomic layer spacings (d spacing), the suite of measurements can be used to identify minerals. All crystalline minerals in a sample can be identified from one XRD scan, provided that they are present in sufficient abundance; however, XRD will not detect non-crystalline components (e.g. the allophane clays) in a sample because they have no regular atomic planes.

The relationship between the wavelengths of the X-rays used, the angel between the incident and the diffracted X-rays and the distance between the atomic layers causing the diffraction is given by the Bragg's law equation:

$$n\lambda=2d\sin\theta$$

Where n= an integer (n=1 first order diffraction peak, 2 for second order peak, etc)

λ= the wavelength of the radiation used, for cu $k\alpha$ radiation

λ= 1.5418 Å

d = the atomic layer spacing (in angstrom unit) between the diffracting plate

θ = half the angle between the incident X-rays and the diffracted X-rays

The Interpretation of modern X-ray diffractograms requires several steps during which nameless electronic peaks of the diffractogram are converted into significant geologic data. The important steps are:

A. Measurement of molecular plane repeat distances (*d*-spacings)

B. Identification of mineral species.

C. Quantitative or semi-quantitative interpretation of mineral abundance.

D. Measurement of average crystallite size of selected minerals.

The XRD result of the sediment powder analysis disclosed 14 minerals. The most common minerals are quartz, calcite, aragonite, albite, montmorilonit and pyrite, while anorthite, orthoclase, dolomite, chlorite, kaolinite, illite, vermiculite and muscovite occur rarely. Individual minerals are identified by the search match method and the respective percentages are calculated from the prominent peak height measurements using a computer program and then multiplying the peak height with intensity factors given in table 5.1.

Minerals	Window (2Θ)	Intensity factor after Cook (1984)	Intensity factor (modified)
Aragonte	45.65-46.00	9.30	11.10
Calcite	29.25-29.60	1.56	1.38
Dolomite	30.80-31.15	1.53	1.81
Kaolinite	12.20-12.60	2.25	X
K-feldspar	27.35-27.79	4.30	7.82
Mica	8.70-9.10	6.00	2.56
Montmoril.	4.70-5.20	3.00	X
Plageoclase feldspar	27.80-28.15	2.80	2.08
Pyrite	56.20-56.45	2.30	5.12
Quartz	26.45-26.95	1.00	1.00

Table 5.1 Characteristic angle (2θ) and intensity factors used to calculate the minerals identified in x-ray diffraction analysis semi-quantitatively.

The intensity factors are determined in 1:1 mixture with quartz by obtaining the ratio of the diagnostic peak to which is assigned a value of 1.00.

A) Non clay minerals

As indicated in the previous chapter, lacustrine sediments can be used in the study of the paleoenvironmental evolution of a particular catchment basically because they reflect developments in the Lake Ecosystem and changes in the rate and type of processes such as weathering (Rendeberg et al., 1993). Moreover, they are often deposited in undisturbed sedimentary environments and give time integrated information on sedimentary environments of the basin and its surrounding.

Comparative studies show that a limited number of elements comprise the vast majority of lake sediments, reflecting the typical compositional variability of the continental crust, and the relative reactivity of crustal materials as they enter lake water (Choen, 2003).

At the top of the core quartz-albite-calcite and aragonite-Montmorilonite show similar trends. The first group has lower values unlike the second. In the middle part of the core quartz and albite remain present with small values while calcite increases. In the lower part of the core quartz, albite, montmorilonit and pyrite have higher values than the middle and the upper part of the core (Figure 5.3).

Quartz

Although the major fraction of silicon in lake sediments is derived from the external contribution of silicate minerals, by far the most important contribution is from the sedimentation of SiO_2 incorporated in diatom frustules. Although diatom frustules can be preserved for long periods, there are cases where dissolution and diagenetic processes make the existence of diatom silica rare even though the deposition rate is high. Silicate minerals are considered to be exclusively allogenic/detrital.

The amount of quartz in the core is generally higher at the base and smaller at the top of the core. At the bottom part of the core the amount of quartz at first decreases from the base to a depth of 698 cm where it has an amount of 2.51 % and it increases up to a depth of 493 cm where the core attains the maximum value of 69.04 %. The upper 430 cm of the core has a smaller amount of quartz with an average value of 9.05 %. In this part the smallest value is 3.7 % at a depth of 112 cm and a highest value of 20.22 is attained at a depth of 206 cm.

Like quartz feldspars are considered as allogenic/detrital and hence reflect the bed rock composition of the catchment area. Their stability towards structural changes makes them useful for evaluation of the physical processes involved in the transport and deposition of particles in lakes.

Feldspars

The dominant feldspar in the core is plagioclase feldspar i.e. albite. Albite shows a similar trend like quartz throughout the length of the core. The amount of albite in the core doesn't show much variation except at a depth of 602 cm where it attains a maximum value of 40.02 %. At depths of 770 cm, 730 cm, 675 cm, 635cm and between 586-570 cm, 413-390 cm, 190-174cm and 63-126 cm no albite has been identified while quartz is low. From the top to a depth of 477.6 cm the values are smaller and with more fluctuations than in quartz. In the interval between 477.6 and 538cm the amount of albite increased from 5.53 % to 11.49 %.

Both quartz and feldspar have the highest values between 477.6 cm and 600 cm.

Sed. Depth	Quartz	Calcite	Aragonite	Albite	Montmorilonite	Pyrite	Anorthite
0	4.4	4.4	61.7	2.7	24.3	0.00	0.00
15	10.6	0.00	63.2	4.5	21.7	0.00	0.00
31	9	0.00	53.8	0.00	30.5	0.00	0.00
47	5.8	0.00	19.2	4.9	47.4	0.00	0.00
63	12.8	0.00	73.8	0.00	11.8	0.00	0.00
112	3.7	0.00	84.80	0.00	5.91	0.00	0.00
126	6.38	0.00	20.08	0.00	46.49	0.00	0.00
142	4.47	0.00	60.84	9.14	25.56	0.00	0.00
158	2.80	0.00	74.70	2.30	20.20	0.00	0.00
174	6.69	0.00	38.96	0.00	48.86	0.00	0.00
190	7.3	0.00	0.00	0.00	0.00	0.00	0.00
206	20.22	0.00	0.00	10.34	0.00	0.00	0.00
222	14.29	0.00	8.56	0.00	0.00	0.00	0.00
238	7.32	44.77	23.85	5.01	19.04	0.00	0.00
254	11.12	83.52	0.00	5.36	0.00	0.00	0.00
270	9.80	66.09	0.00	4.89	19.22	0.00	0.00
286	11.97	48.38	0.00	10.59	29.06	0.00	0.00
302	9.39	74.32	0.00	3.63	12.67	0.00	0.00
318	9.36	75.11	0.00	3.60	11.92	0.00	0.00
334	8.9	91.1	0.00	0.00	0.00	0.00	0.00
350	6.31	93.69	0.00	0.00	0.00	0.00	0.00
366	9.29	84.13	0.00	4.02	0.00	2.56	0.00
382	11.63	61.41	0.00	5.69	13.73	7.53	0.00
398	13.25	74.30	0.00	0.00	12.46	0.00	0.00
413	9.52	74.86	0.00	0.00	15.63	0.00	0.00
429	9.03	83.19	0.00	7.78	0.00	0.00	0.00
445	11.10	85.94	0.00	2.96	0.00	0.00	0.00
461	13.99	61.65	0.00	3.60	20.77	0.00	0.00
477.6	19.64	44.82	0.00	5.53	25.61	0.00	0.00
493	69.04	0.00	0.00	18.77	12.19	0.00	0.00
538	36.86	0.00	0.00	11.49	41.96	9.68	0.00
554	37.77	0.00	0.00	13.27	40.62	8.34	0.00
570	43.60	0.00	0.00	0.00	45.72	10.68	0.00
586	34.33	0.00	0.00	0.00	40.39	13.04	0.00
602	24.41	0.00	0.00	40.06	35.53	0.00	0.00
618	23.29	0.00	0.00	14.13	42.83	8.98	0.00
634	28.26	0.00	0.00	0.00	34.26	9.89	27.59
650	29.79	4.13	0.00	0.00	47.64	12.89	0.00
675	11.56	4.52	78.18	0.00	4.39	0.00	0.00
682	11.54	3.71	81.72	0.00	0.00	0.00	0.00
698	2.51	3.25	78.72	0.00	3.51	0.00	0.00
714	11.07	6.31	79.31	0.00	0.00	0.00	0.00
730	11.64	35.46	0.00	0.00	0.00	7.08	23.75
749.6	5.73	64.51	21.95	0.00	0.00	5.48	0.00
770	17.92	4.10	0.00	0.00	0.00	8.62	30.78
784	41.39	0.00	0.00	0.00	29.91	7.07	0.00
800	31.39	6.11	0.00	0.00	15.98	4.64	0.00

Table 5.2 Proportions of minerals in the core samples analyzed at 16 cm interval

Carbonates

Carbonates in lake sediments are of detrital, endogenic or autigenic. Both calcite and aragonite can have the same origin but dolomite is commonly found as detrital. Carbonate precipitation can occur relatively rapidly over large ranges of salinity, alkalinity and temperature (Hong- Chung Li et al., 1997).

Carbonates are present in the whole length of the core in one form or the other: calcite, aragonite and dolomite. In the upper part of the core, from the surface to a depth of 190 cm aragonite dominates over the other carbonates. The average value is 54.04% in this range it and attains a maximum of 84.8 % at a depth of 112cm and a minimum of 19.2% and 20.8 % at 47cm and 126cm depths. Parallely calcite shows a relatively higher amount and it compensates aragonite at a depth of 47cm. No dolomite is detected in this interval.

Calcite dominates over the other carbonates between depths of 174cm and 493cm. The average value of calcite in this interval is 72.44 % and attains a maximum value of 93.69 % at a depth of 350cm and minimum values of 47.77 % and 48.38 % at depths of 238cm and 286cm respectively. A very small percent of aragonite is identified between 206cm and 270cm but no dolomite is present. Further down the core between 493cm and 634cm no calcite and no dolomite has been documented

At the bottom, calcite and aragonite reappear at a depths of 634 cm and 650 cm respectively. Calcite has a maximum value of 64.57 % at 749.6 cm and aragonite 81.72 % at a depth of 682 cm in which both decrease at the base of the core. Dolomite re-appear at a depth of 800 cm and attains a value of 27.27 %.

Pyrite

Pyrite is one of the most common minerals in the diffractograms. No pyrite is documented in the sediment between the surface and depths of 350cm, 398cm to 477.6cm and 618cm to 714cm. The average value being 7.66% it attains a maximum of 13.04 % at a depth of 586 cm.

Pyrite can occur both as allogenic/detrital and antigenic mineral in lake sediments (Jansson, 1983) and it has the same trend as quartz and albite.

Montmorilonite*

Montmorilonite can be found as allogenic/detrital and rarely as antigenic mineral (Last and Smol, 2003). From the sediment surface to a depth of 190 cm the amount is generally higher with maximum and minimum values of 48.86 % and 5.26 % at 174 cm and 112cm respectively. The amount decreases further down the core until 538 cm but raises again up to 682cm and attains a maximum value of 47.64 % at 650 cm. Further down the core no montmorilonite has been traced up to 770 cm where the amount starts increasing to a maximum of 29.91 % at a depth of 784 cm.

Montmorilonite shows a similar trend with aragonite and has an opposite trend with calcite.

Minerals such as anorthite, orthoclase, chlorite, kaolinite, illite, vermiculite and muscovite occur very rarely and only at a certain depth of the core.

---

* Montimorilonit: Despite it is a clay mineral, it is discussed in this section since it is identified in the whole powder XRD analysis, so it is the clay fraction in the samples

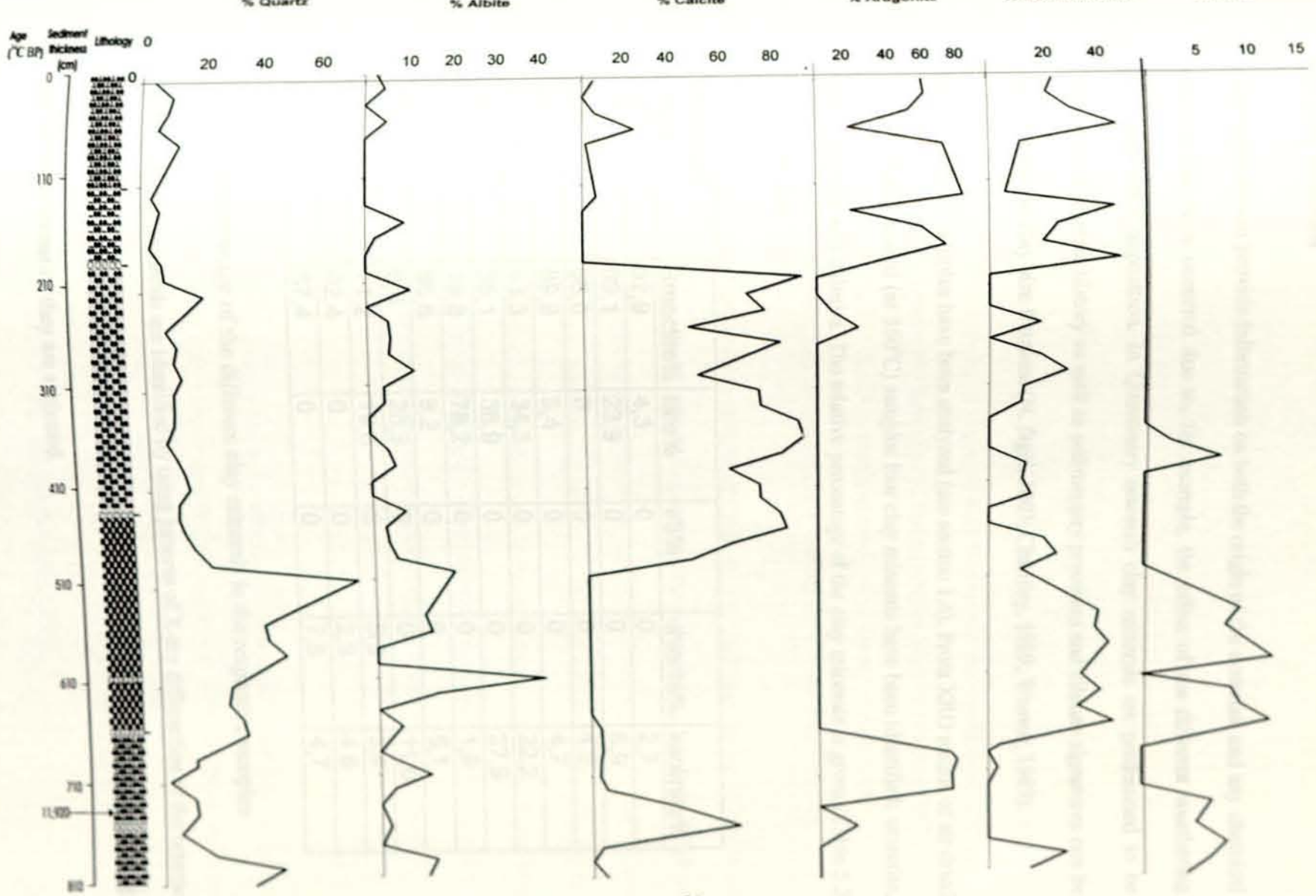

Figure 5.3 Mineralogy of the core analyzed at 16 cm interval

B) Clay minerals

Clay minerals can provide information on both the origin of the materials and any chemical changes that have occurred due to, for example, the effect of the different weathering processes since deposition. In Quaternary research clay minerals are predestined to be indicators of climate history as well as sedimentary processes and climate signatures can be recorded by the clay size fractions (N. fagel, 2003; Chamley, 1989; Weaver, 1989).

In this study 12 samples have been analyzed (see section 1.4). From XRD results of air dried glycolated and heated (at 550°C) samples four clay minerals have been identified: smectite, illite, kaolinite and chlorite. The relative percentage of the clay minerals is given (Table 5.3 and Figure 5.4)

sediment depth	Smectite%	illite%	I/S%	chlorite%	kaolinite%
142	92,9	4,3	0	0	2,7
174	69,1	23,9	0	0	6,9
238	95,0	0	0	0	4,9
286	89,8	5,4	0	0	4,7
477.5	43,3	34,3	0	0	22,2
493.5	35,1	36,9	0	0	27,9
618	19,8	78,2	0	0	1,9
634	86,6	8,2	0	0	5,1
650	6,6	26,3	0	0	11,0
730	71,2	19,6	0	5,6	3,4
770	92,4	0	0	2,9	4,6
784	87,4	0	0	7,8	4,7

Table 5.3 Percentage of the different clay minerals in the respective samples

Individual clay minerals are identified by using patterns of X-ray differaction of the oriented aggregates that enhance the basal, or 001 reflection. Each clay mineral behaves differently for the three scenarios they are subjected.

Smectite

Smectite is a clay mineral in which the octahedral sheet is sandwiched between two tetrahedral sheets. Montmorilonite is the commonest type of smectite, which is readily identified in the whole powder XRD. Smectite is easily identified by comparing diffraction pattern of air dried and ethylene glycol solvated preparations. The glycol-preparation gives a very strong 001 reflection at about 5.2° 2Θ (16.9 Å), which, in the air dried condition, shifts to about 6° 2Θ (15 Å) if the clay is saturated with divalent ion and equilibrated with air at room temperature and moderate humidity. A further confirmation is accomplished by K-saturation and drying at 300 °C. This treatment breaks smectite at 10 Å and shifts it to the right, producing a diffractogram pattern similar to that of illite (Moore and Reynolds, 1997).

Smectite is the most common clay mineral through the core. Although the top 100cm is not represented by the clay, a relatively higher amount is observed at 142cm, 238cm and 286 cm samples. In samples down core, the amounts are small (477.5 cm, 493.5 cm. 618 cm and 650 cm). Further down the value increases in the samples analyzed at 730 cm, 770 cm and 784 cm. Although it is difficult to generalize, with the small number of samples treated here, it seems that higher amounts of smectite are observed in the upper and bottom parts of the core. This seems similar to the montmorilonite values from whole powder XRD result.

Illite

Illite is clay with smectite structure and an abundance of interlayer K^+. It can be described as a mechanical mixture of fine grained smectite and muscovite. Illite is found in higher amounts in the samples treated for clay minerals and it is identified by a series of weak broad peaks at 2Θ 8.7 (10.1Å) and 17.7 (5.0 Å) that is not appreciably affected by glycolation and heating to 550°C (Moore and Reynolds, 1997).

Generally the upper part of the core is characterized by a relatively small amount of illite. The samples at a depth of 142 cm, 174cm and 238 cm have illite contents of 4%, 23 % and 0 % respectively. The value of illite increases down in the core with individual values of 34 % and 36 % at depths of 477 cm and 493.5 cm respectively and it attains a maximum value of 78 % at a depth of 618 cm. The illite continent decrease to zero further down the bottom of the core. So generally the upper and lower parts of the core have smaller values than the middle part.

Kaolinite/Chlorite

Kaolinite and chlorite have the simplest combination of octahedral and tetrahedral sheets in which an octahedral sheet is linked to the tetrahedral sheet by sharing some of the oxygen ions. For the sake of simplicity kaolinite and chlorite are discussed together despite their different structure and geological occurrences. Chlorite has a basal series of diffraction peaks superimposed on the number of kaolinite 001 series. Most kaolinites have the 002 peak at 24.9^0 2Θ. And common chlorites have their 004 reflection at about 25.1^0 2Θ. If large concentrations of both phases are present, the best method of identification is to look for the kaolinite 003 and chlorite 003 peaks. Generally the characteristic peaks for the two minerals are given in the Table 5.4.

Glycolation and heating is also very important to identify the two minerals i.e. both are unaffected with glycolation but the kaolinite peak completely breaks up on heating to 550°C while the chlorite peaks break and shift to the left with a pronounced peak of 14.2 Å at 6.3 2Θ.

Clay mineral	2Θ degrees of Cu Kα	d-spacing(Å)	Remark
Kaolinite	12.6	7.16	collapses at 550°C
	25.0	3.58	collapses at 550°C
Chlorite	12.6	7.10	collapses at 550°C
	18.9	4.74	collapses at 550°C
	25.0	3.55	collapses at 550°C
	6.3	14.4	After heating 550°C

Table 5.4 Characteristic angle and d-spacing of kaolinite and chlorite.

Kaolinite is found in all the samples. The value is smaller in the upper first four samples of the core: at 142cm, 174 cm, 238 cm and 286 cm with a maximum value of 6%. At depths of 477cm and 493.5 cm a value of 22% and 27% are recorded and these values are the highest in the whole length of the core. In the lower part of the core except at a depth of 650cm (with 11%) the amount is smaller.

Unlike Kaolinite, chlorite is represented by only three sampling points from the base of the core with an average value of 5.45%.

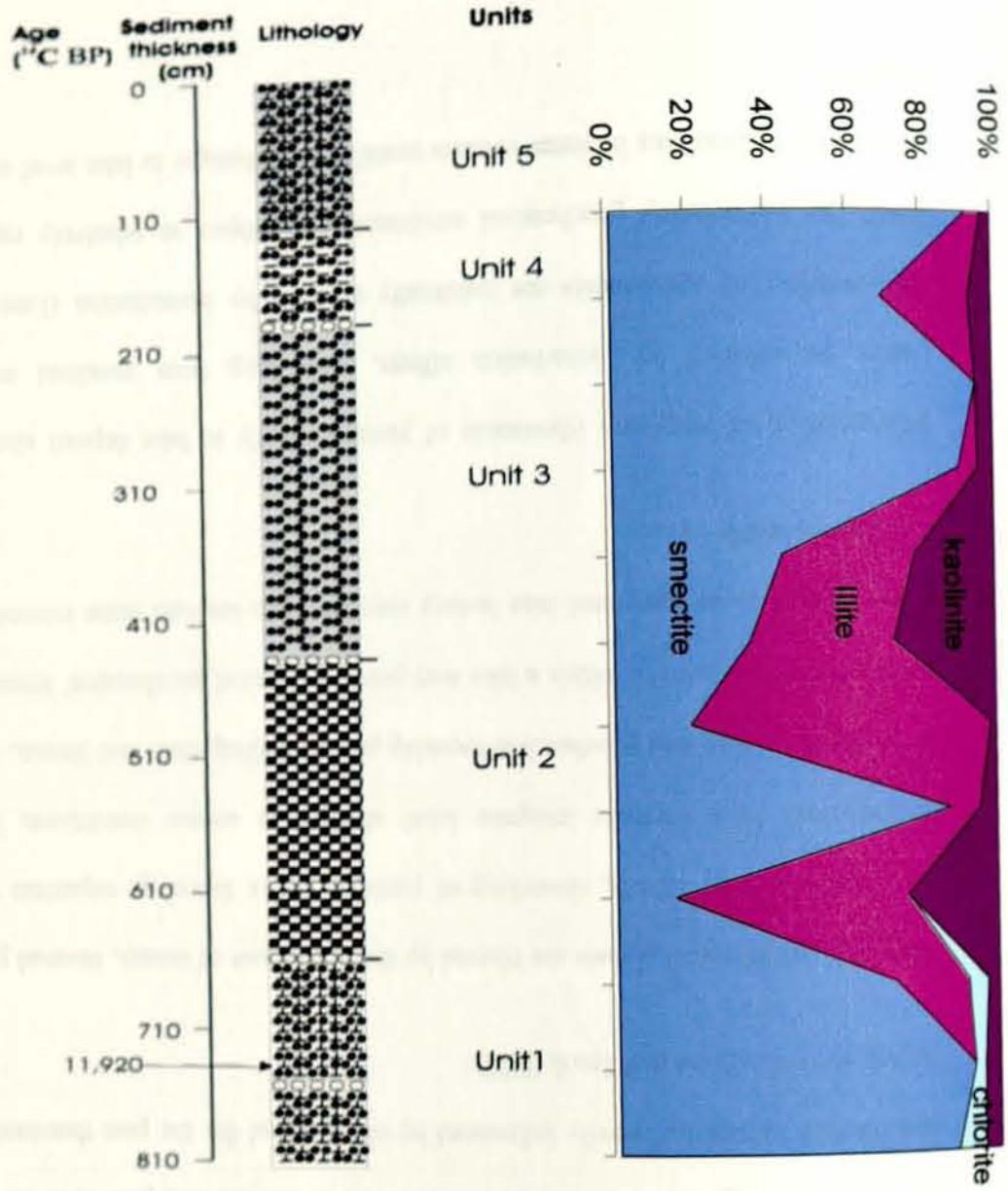

Figure 5.4 clay minerals proportion of the Lake Ashange core

CHAPTER SIX
GEOCHEMISTRY OF THE SEDIMENT

Lake sediment geochemistry is the product of external inputs from water shade geology, ground water, vegetation, and the air-shed, as well as internal lake processes. Both external and internal inputs are heavily influenced by climate, and for the past thousand years, by human activities (Last and Smol, 2003).

Although geochemical signals are blurred by the whole host of messy, internal process (lag and residence time effects, reworking of particles, redox focusing, organism uptake and bioturbation) lake deposits integrate local changes in source conditions, background sedimentation rates and geochemical focusing processes (Engstrom and Swain, 1986). As a result, different locations within a lake may provide different geochemical histories, and an interpretation of an integrated lake history may take into account these internal variations and their probable causes.

Interpretation of long-term (thousands of years) cyclicity in lake deposit chemistry may hardly be affected by bioturbation effects, since long term maximal and minimal concentration of components are minimally affected by bioturbation (Last and Smol, 2003).The sedimentary geochemical environment is subject to relatively rapid changes induced by fluctuations in water column stratification, changes in lake level and influx of particles.

Marine and lake sediment cores provide good records for paleoenvironmental reconstruction, and within the framework of a multi-disciplinary approach mineralogy and geochemistry can play an important role. Mineralogical and geochemical features of sediments reflect the evolution of the basin area, in most cases controlled by climate variations, recording

1540	650	19.373	20.325	19.529	0.796	19.529	19.529	0.156	0	0	0	0	100
1545	655	17.206	18.222	17.512	0.71	17.477	17.423	0.306	0.035	0.054	11.4379085	17.6470588	70.9150327
1550	660	18.039	18.975	18.293	0.682	18.262	18.227	0.254	0.031	0.035	12.2047244	13.7795276	74.015748
1555	665	16.448	17.542	16.785	0.757	16.749	16.687	0.337	0.036	0.062	10.6824926	18.3976261	70.9198813
1560	670	19.022	19.979	19.28	0.699	19.251	19.212	0.258	0.029	0.039	11.2403101	15.1162791	73.6434109
1565	675	18.235	19.14	18.453	0.687	18.429	18.406	0.218	0.024	0.023	11.0091743	10.5504587	78.440367
1570	680	16.208	17.238	16.532	0.706	16.504	16.447	0.324	0.028	0.057	8.64197531	17.5925926	73.7654321
1575	685	18.776	19.62	19.008	0.612	18.983	18.95	0.232	0.025	0.033	10.7758621	14.2241379	75
1580	690	19.085	19.82	19.27	0.55	19.249	19.219	0.185	0.021	0.03	11.3513514	16.2162162	72.4324324
1585	695	18.472	19.411	18.743	0.668	18.716	18.669	0.271	0.027	0.047	9.96309963	17.3431734	72.6937269
1590	700	18.373	19.448	18.759	0.689	18.728	18.636	0.386	0.031	0.092	8.03108808	23.8341969	68.134715
1595	705	17.196	18.191	17.493	0.698	17.467	17.416	0.297	0.026	0.051	8.75420875	17.1717172	74.0740741
1600	710	16.082	17.114	16.422	0.692	16.389	16.327	0.34	0.033	0.062	9.70588235	18.2352941	72.0588235
1605	715	17.748	18.781	18.086	0.695	18.054	17.995	0.338	0.032	0.059	9.46745562	17.4556213	73.0769231
1610	720	17.432	18.46	17.73	0.73	17.7	17.666	0.298	0.03	0.034	10.0671141	11.409396	78.5234899
1615	725	19.167	20.162	19.466	0.696	19.437	19.415	0.299	0.029	0.022	9.69899666	7.35785953	82.9431438
1620	730	19.201	20.13	19.389	0.741	19.358	19.329	0.188	0.031	0.029	16.4893617	15.4255319	68.0851064
1625	735	16.423	17.322	16.688	0.634	16.658	16.636	0.265	0.03	0.022	11.3207547	8.30188679	80.3773585
1630	740	16.365	17.359	16.7	0.659	16.67	16.645	0.335	0.03	0.025	8.95522388	7.46268657	83.5820896
1635	745	16.59	17.513	16.943	0.57	16.911	16.857	0.353	0.032	0.054	9.06515581	15.2974504	75.6373938
1640	750	17.11	18.074	17.583	0.491	17.554	17.448	0.473	0.029	0.106	6.13107822	22.410148	71.4587738
1645	755	17.233	18.381	17.769	0.612	17.731	17.616	0.536	0.038	0.115	7.08955224	21.4552239	71.4552239
1650	760	18.056	19.214	18.547	0.667	18.514	18.468	0.491	0.033	0.046	6.7209776	9.36863544	83.910387
1655	765	17.934	19.267	18.66	0.607	18.624	18.568	0.726	0.036	0.056	4.95867769	7.71349862	87.3278237
1660	770	16.735	18.195	17.694	0.501	17.647	17.625	0.959	0.047	0.022	4.90093848	2.29405631	92.8050052
1665	775	16.77	18.276	17.733	0.543	17.691	17.666	0.963	0.042	0.025	4.36137072	2.596054	93.0425753
1670	780	16.8	18.232	17.749	0.483	17.709	17.686	0.949	0.04	0.023	4.21496312	2.42360379	93.3614331
1675	785	22.63	24.219	23.684	0.535	23.64	23.621	1.054	0.044	0.019	4.17457306	1.80265655	94.0227704
1680	790	19.43	21.04	20.525	0.515	20.483	20.45	1.095	0.042	0.033	3.83561644	3.01369863	93.1506849
1685	795	19.51	21.092	20.6	0.492	20.571	20.529	1.09	0.029	0.042	2.66055046	3.85321101	93.4862385
1690	800	19.64	21.182	20.741	0.441	20.707	20.67	1.101	0.034	0.037	3.08810173	3.36058129	93.551317
1695	805	18.9	19.974	19.672	0.302	19.651	19.621	0.772	0.021	0.03	2.72020725	3.88601036	93.3937824

changes in erosion and transportation processes, in weathering rates, in biological productivity and in early digenetic reactions (Calanchi et al., 1996).

Productivity periods are indicated by rich inorganic matter and biogenic silica, with low magnetic susceptibility values and low terrigenous chemical element concentrations (Al_2O_3, TiO_2).

Long-term climate trends have been shown to correlate with variation in sediment biogenic silica in Lake Baikal, while climatic change has been inferred from variations in Aeolian supply of mineral matter to lakes in the USA (Dean, 1974)

Together with diatom and pollen data, sediment chemical data provide a comprehensive long-term record of environmental change, or of recent human impact (Last and Smol, 2001).

6.1 Weathering in the Catchment

The geochemical investigations of 41 samples throughout the length of the core on bulk sediment were used to calculate the respective percentages of oxides: SiO_2, Al_2O_3, Fe_2O_3, MnO, MgO, CaO, Na_2O, K_2O, TiO_2, P_2O_5, SO_3 and major and trace elements: As, Ba, Bi, Ce, Co, Cr, Cu, Ga, Hf, La, Mo, Nb, Nd, Ni, Pb, Pr, Rb, Sc, Sm, Sr, Th, U, V, Y, Zn, Zr.

To characterize weathering conditions in the catchment the following ratios were calculated: Na_2O/Al_2O_3, Na_2O/TiO_2, K_2O/Al_2O_3, K_2O/TiO_2, $(Na_2O+K_2O)/Al_2O_3$, $(Na_2O+K_2O)/TiO_2$. To evaluate the amount of allocthonous sediments Al_2O_3/CaO, TiO_2/CaO are calculated (Table 6.1 and Figure 6.1).

Chemical weathering results from the adjustment of thermodynamically unstable minerals to the surface environment of abundant water and atmospheric gases.

Based on the behavior of elements or ions in water solutions they are classified in to three categories: (I) soluble cations, (II) hydrolysates and (III) soluble anion- complexes. The mode of solubility is controlled by the ionic potential (= ion charge/ ion radius): Cations with an ionic potential of <3 belong to the soluble ions (all alkalis, alkali-earth metals and Fe^{2+}). During chemical weathering of primary minerals, the alkalis are resolute to being soluble and are carried away in solution or leached. With increasing radius, however, the mobility of ions decreases and the tendency towards a high degree of adsorption to fine grained sediments or soil particles increases. In this way larger cations such as K^+, Rb^+ are increasingly taken out of water solution through adsorption, unlike Na^+. In other words due to the partial adsorption of K^+ to clay minerals and organic substances the K^+ is not removed as strongly from the partly weathered horizons as Na^+. Elements with ionic potential above 10 are soluble anion complexes ($SO4^{2-}$,CO_3^{2-},BO_3^{3-}...). Ions with potentials between 3 and 10 precipitate quickly from watery solutions as hydroxides (hydrolysates: Al^{3+}, Fe^{3+}, Ti^{4+}). Although the mode of solubility of single ion is influenced by further parameters (presence of particular anion, activities of solubility companions, pH value, Eh and temperature), fairly reliable patterns of behavior emerges for the 'simple' ions (alkalis, earth alkalis, Al^{3+}, Ti^{4+}) (Berner, 1971; Lindsay, 1979; Drever, 1982; Brookins, 1988; Krauskopf and Bird 1995; Smykatz-Kloss et al. 1998).

The alkalis are normalized by TiO_2 and Al_2O_3 which are proven to be almost constant in all the sediment profiles (Gallet et al., 1998, Smyktz-kloss et al., 1999/2000) and Na_2O/Al_2O_3 and Na_2O/TiO_2 are used as "Chemical Indexes of Alteration"

6.2 Paleoproductivity

From total mineralogy, paleo-productivity is deduced from the biogenic silica content, determined by normative calculation based on bulk XRF analyses and organic matter content.

Normative biogenic silica values (Si bio nor = SiO_2-2.8* Al_2O_3; Robinson et al., 1993) were calculated to evaluate the diatom productivity. (Table 6.2 and Figure 6.3).

The geochemical profiles of the analyzed samples from the core for specific ratios, enables to differentiate the core into four major zones (i.e. I-IV) Figure 6.1- 6.3.

The four zones are: zone I (614 cm to the base of the core), zone II (350- to 614 cm), zone III (126 to 350 cm) and zone IV (0 to 126 cm) show generally different trends with minor fluctuations in a single zone.

Zone I

Zone I is the lower part of the profile up to 614 cm depth and it is characterized by relatively high value of Na_2O/Al_2O_3, Na_2O/TiO_2, K_2O/Al_2O_3, K_2O/TiO_2, $(Na_2O+K_2O)/Al_2O_3$, $(Na_2O+K_2O)/TiO_2$ ratio as compared to all the other zones except the upper most zone. A generally increasing trend in the amount of the ratio in the profile is observed up to 666 cm. from the bottom of the core. Then it decreases up to the top of this zone.

In this zone almost all of the above ratios attain their maximum and minimum values at depths of 666 cm and 714 cm respectively.

The Al_2O_3/CaO, TiO_2/CaO ratios have high values between 614 cm and 666 cm. Unlike the other ratios the values show a decreasing trend from the bottom of the core to 714 cm. Then the values increase to the top of the zone (Table 6.3 and Figure 6.2)

Zone II

Zone II is the zone between 350 cm and 614 cm. It is characterized by a relatively constant amount. Na_2O/Al_2O_3, Na_2O/TiO_2 and $(Na_2O+K_2O)/Al_2O_3$ have lowest values between 461 cm and 614 cm in the zone. The ratios are relatively higher between 350 cm and 461 cm. On the contrary K_2O/Al_2O_3, K_2O/TiO_2 and $(Na_2O+K_2O)/TiO_2$ attain higher values at the bottom of the zone between 461cm and 614 cm and gradually decrease towards the top.

Al_2O_3/CaO and TiO_2/CaO show highest values between 461 cm and 614 cm and attain maximum values of 3.93 and 0.43 respectively at a depth of 570 cm. In the upper part both ratios have a constant value and have average values of 0.25 and 0.05 respectively.

Zone III

Zone III comprises the interval between 146 cm and 350 cm. In this zone, the values show a wide rang and large fluctuations which is expressed by the zigzag shape of the curve in the profile. Na_2O/Al_2O_3, Na_2O/TiO_2, K_2O/Al_2O_3, $(Na_2O+K_2O)/Al_2O_3$ and $(Na_2O+K_2O)/TiO_2$ show a strong 'Z' shape implying a large range of values. K_2O/TiO_2 shows a narrow range of values and is manifested by a weak 'Z' shape. $K2O/Al_2O_3$ shows the weaker 'Z' shape.

Both Al_2O_3/CaO and TiO_2/CaO generally have the same trend. Except between 206 cm and 350 cm (i.e. Zone II-A) and 206 cm to 142 cm (Zone III-B). In sub-zone III-A the amount attains a peak at 286 cm. Sub zone III-B has higher values than sub-zone III-A.

Zone IV

Zone four is the upper most zone that extends up to a depth of 142 cm. This zone is characterized by fluctuating values as zone III but with a rather narrow range. Na_2O/Al_2O_3, K_2O/Al_2O_3, $(Na_2O+K_2O)/Al_2O_3$ and $(Na_2O+K_2O)/TiO_2$ have higher values as compared to zone III but are comparable to zone I. Na_2O/TiO_2 and K_2O/TiO_2 show similar trends as in zone II but have peaks at 126 cm and 15 cm (Table 6.1).

In this zone, both Al_2O_3/CaO and TiO_2/CaO have the same trend throughout the zone. The values are higher than in zone III; lower than in zone II and comparable with the values of zone I. Higher and lower values are recorded at depths of 126 cm and 95 cm respectively. Generally the values decrease from the bottom to the top of the zone.

Generally, the same trend for values of Na_2O/Al_2O_3, Na_2O/TiO_2, K_2O/Al_2O_3, K_2O/TiO_2, $(Na_2O+K_2O)/Al_2O_3$ and $(Na_2O+K_2O)/TiO_2$ are observed. These are important parameters to interpret the weathering conditions. In the same way, Al_2O_3/CaO and TiO_2/CaO have the same trend throughout the length of the core. These parameters are important to indicate the amount of allochtonus sediment input from the catchment into the lake.

Depth	$\frac{Na_2O}{Al_2O_3}$	$\frac{Na_2O}{TiO_2}$	$\frac{K_2O}{Al_2O_3}$	K2O TiO_2	$\frac{K_2O+Na_2O}{Al_2O_3}$	$\frac{K_2O+Na_2O}{Ti_2O}$
0	0.08	0.45	0.08	0.46	0.17	0.92
15	0.17	1.05	0.14	0.90	0.32	1.95
31	0.10	0.62	0.10	0.6	0.20	1.22
47	0.09	0.59	0.09	0.59	0.19	1.18
63	0.12	0.72	0.09	0.57	0.22	1.29
79	0.09	0.51	0.08	0.5	0.18	1.01
95	0.13	0.78	0.09	0.56	0.22	1.35
112	0.10	0.52	0.09	0.50	0.19	1.03
126	0.10	1.00	0.14	1.46	0.24	2.46
142	0.08	0.42	0.09	0.48	0.17	0.91
158	0.07	0.33	0.09	0.42	0.16	0.76
190	0.10	0.69	0.09	0.65	0.2	1.35
206	0.13	0.91	0.10	0.72	0.23	1.63
222	0.10	0.53	0.10	0.55	0.20	1.09
238	0.10	0.48	0.09	0.46	0.20	0.95
270	0.07	0.56	0.09	0.66	0.17	1.23
286	0.06	0.42	0.08	0.60	0.14	1.02
302	0.10	0.61	0.10	0.61	0.20	1.23
318	0.09	0.59	0.09	0.58	0.18	1.18
334	0.10	0.64	0.10	0.67	0.20	1.31
350	0.14	0.95	0.09	0.66	0.24	1.61
382	0.09	0.64	0.10	0.70	0.19	1.35
398	0.10	0.55	0.09	0.51	0.20	1.07
413	0.10	0.54	0.10	0.56	0.20	1.1
429.5	0.1	0.52	0.10	0.56	0.20	1.09
445	0.09	0.51	0.10	0.59	0.20	1.11
461	0.08	0.59	0.10	0.72	0.18	1.31
477	0.08	0.68	0.10	0.83	0.19	1.51
570	0.08	0.75	0.11	1.01	0.19	1.77
614	0.10	0.74	0.10	0.76	0.20	1.51
618	0.11	0.91	0.12	1.03	0.24	1.94
634	0.11	0.93	0.12	1.05	0.24	1.99
650	0.09	0.73	0.11	0.91	0.21	1.65
666	0.15	1.67	0.11	1.20	0.26	2.88
682	0.11	1.19	0.10	1.02	0.21	2.21
698	0.10	1.13	0.10	1.13	0.21	2.27
714	0.06	0.39	0.08	0.54	0.15	0.94
730	0.08	0.73	0.10	1	0.19	1.73
749	0.10	1.23	0.10	1.18	0.21	2.41
770	0.11	0.91	0.14	1.16	0.25	2.07
784	0.08	0.43	0.09	0.49	0.17	0.92
800	0.11	1.13	0.14	1.53	0.26	2.67

Table 6.1 Values of ratios indicating the chemical index of alteration.

depth	Bio Si
0	12.46
15	11.78
31	8.87
47	11.43
63	12.86
79	10.13
95	14.51
112	11.51
126	14.14
142	9.79
158	9.27
190	9.76
206	10.21
222	12.72
238	10.84
270	7.74
286	5.15
302	10.24
318	10.00
334	7.74
350	10.66

depth	Bio Si
382	12.76
398	25.68
413	31.54
429.5	33.47
445	19.52
461	20.54
477	21.50
570	34.46
614	8.55
618	33.92
634	35.33
650	33.75
666	12.4
682	12.3
698	8.08
714	9.13
730	9.35
749	3.54
770	14.2
784	10.95
800	13.72

Table 6.2 Normative biogenic silica values (Si bio nor=Sio_2-2.8*Ai_2O_3; Robinson et al., 1993)

depth	$\frac{Al_2O_3}{CaO}$	$\frac{TiO2}{Cao}$
0	0.89	0.16
15	0.56	0.09
31	0.80	0.13
47	1.22	0.20
63	0.26	0.04
79	0.41	0.07
95	0.18	0.03
112	0.46	0.08
126	2.08	0.20
142	0.61	0.12
158	1.60	0.33
190	0.29	0.04
206	0.16	0.02
222	0.43	0.08
238	0.28	0.06
270	0.39	0.05
286	0.83	0.11
302	0.24	0.04
318	0.23	0.03
334	0.21	0.03
350	0.17	0.02

depth	$\frac{Al_2O_3}{CaO}$	$\frac{TiO_2}{Cao}$
382	0.41	0.06
398	0.24	0.04
413	0.28	0.05
429.5	0.29	0.05
445	0.31	0.05
461	0.58	0.08
477	0.93	0.11
570	3.93	0.43
614	0.24	0.03
618	3.98	0.49
634	3.51	0.42
650	3.77	0.48
666	0.11	0.01
682	0.13	0.01
698	0.13	0.01
714	1.29	0.20
730	0.59	0.06
749	0.13	0.01
770	1.74	0.21
784	1.27	0.24
800	2.46	0.24

Table 6.3 Values of Al_2O_3/CaO and TiO_2/Cao

depth	K_2O/Na_2O_3
0	1.02
15	0.85
31	0.95
47	0.99
63	0.79
79	0.97
95	0.71
112	0.96
126	1.45
142	1.12
158	1.26
190	0.94
206	0.79
222	1.03
238	0.94
270	1.16
286	1.40
302	1
318	0.98
334	1.03
350	0.69

depth	K_2O/Na_2O_3
382	1.09
398	0.90
413	1.03
429.5	1.07
445	1.15
461	1.21
477	1.22
570	1.34
614	1.02
618	1.13
634	1.12
650	1.23
666	0.71
682	0.85
698	1
714	1.37
730	1.35
749	0.96
770	1.26
784	1.11
800	1.34

Table 6.4 Values of K_2O/Na_2O indicating the degree of chemical weathering in the catchment

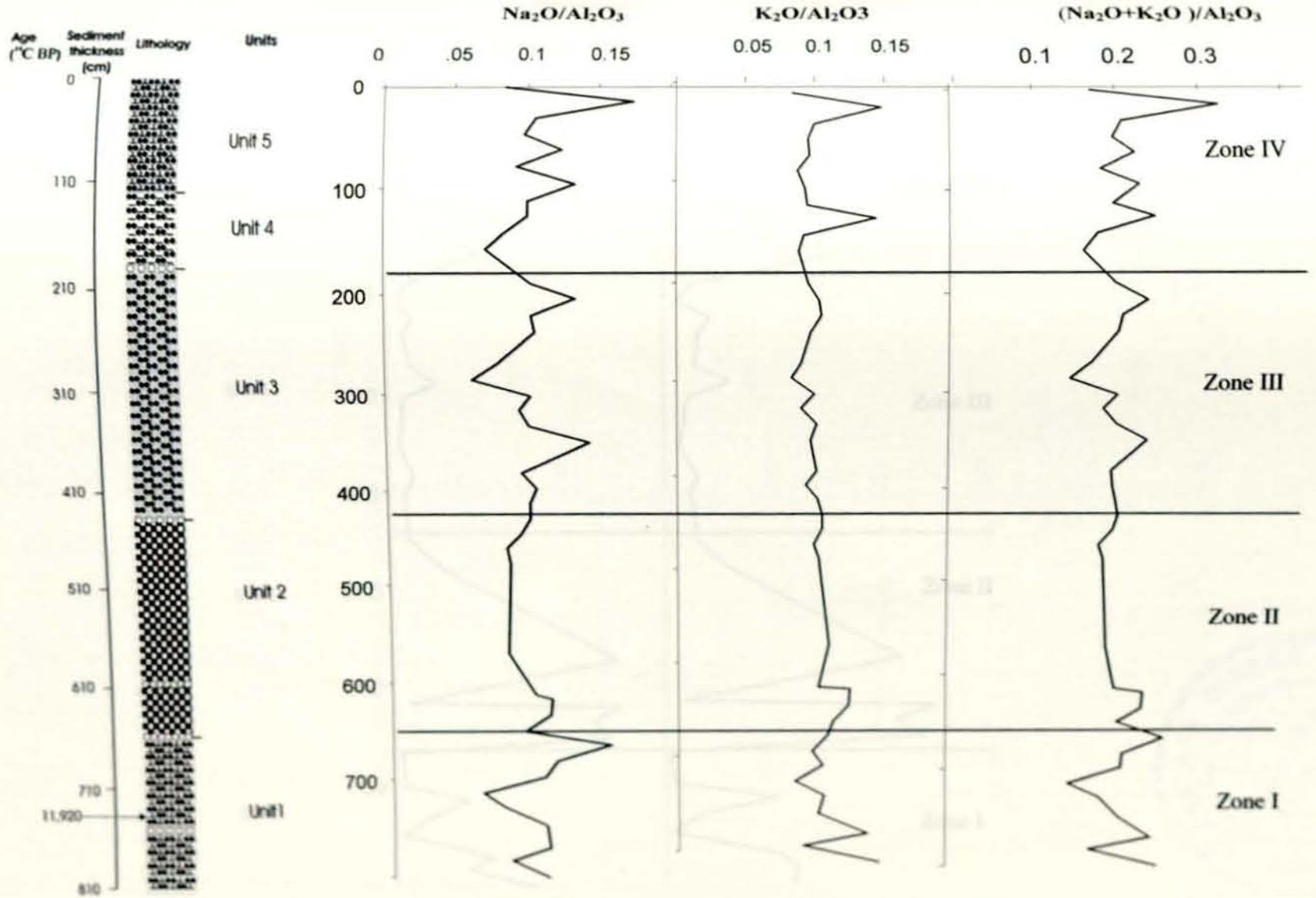

Figure 6.1 geochemical ratios indicating weathering in the catchment

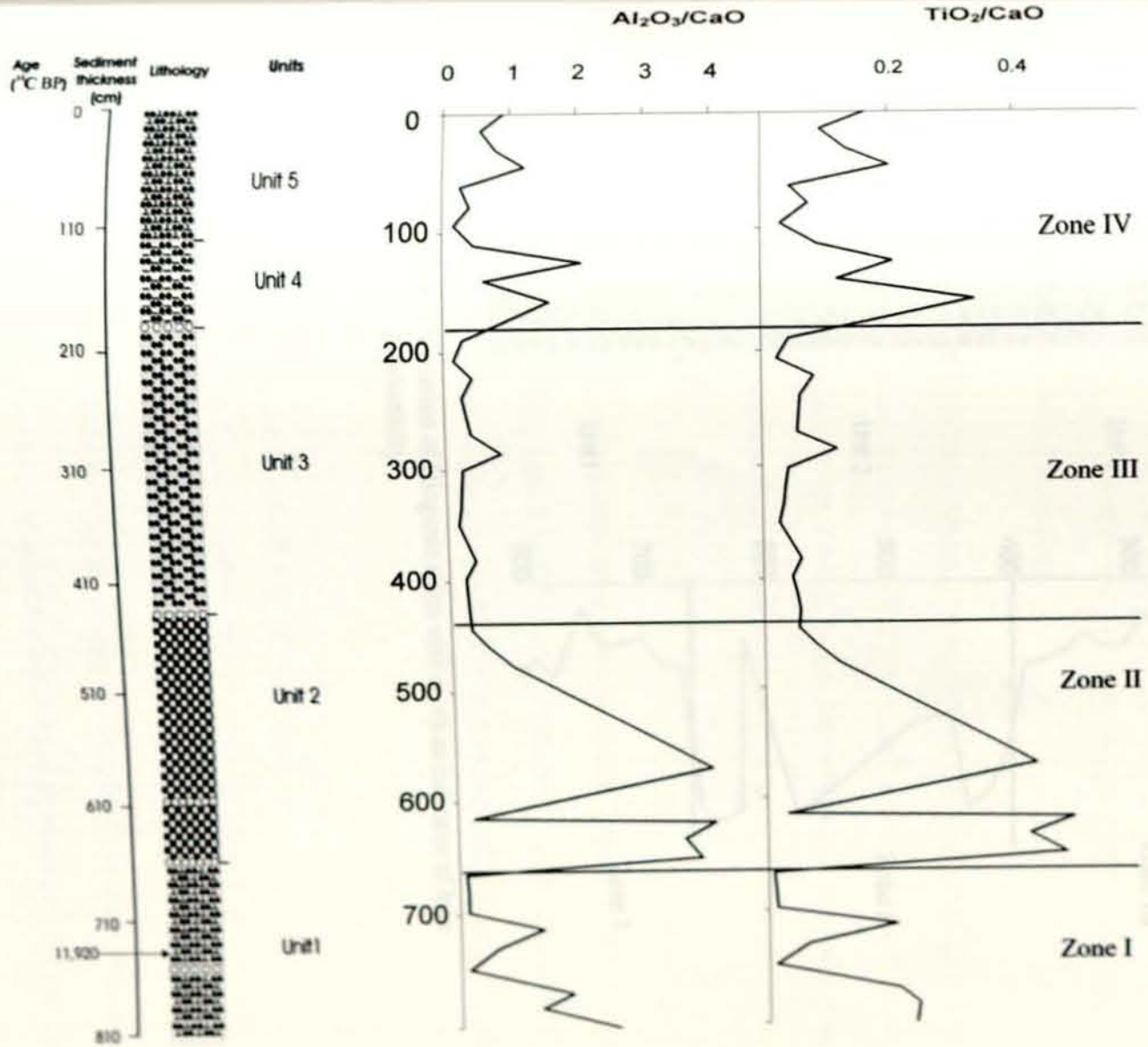

Figure 6.2 geochemical ratios to indicate allochtonus sediment supply to the lake

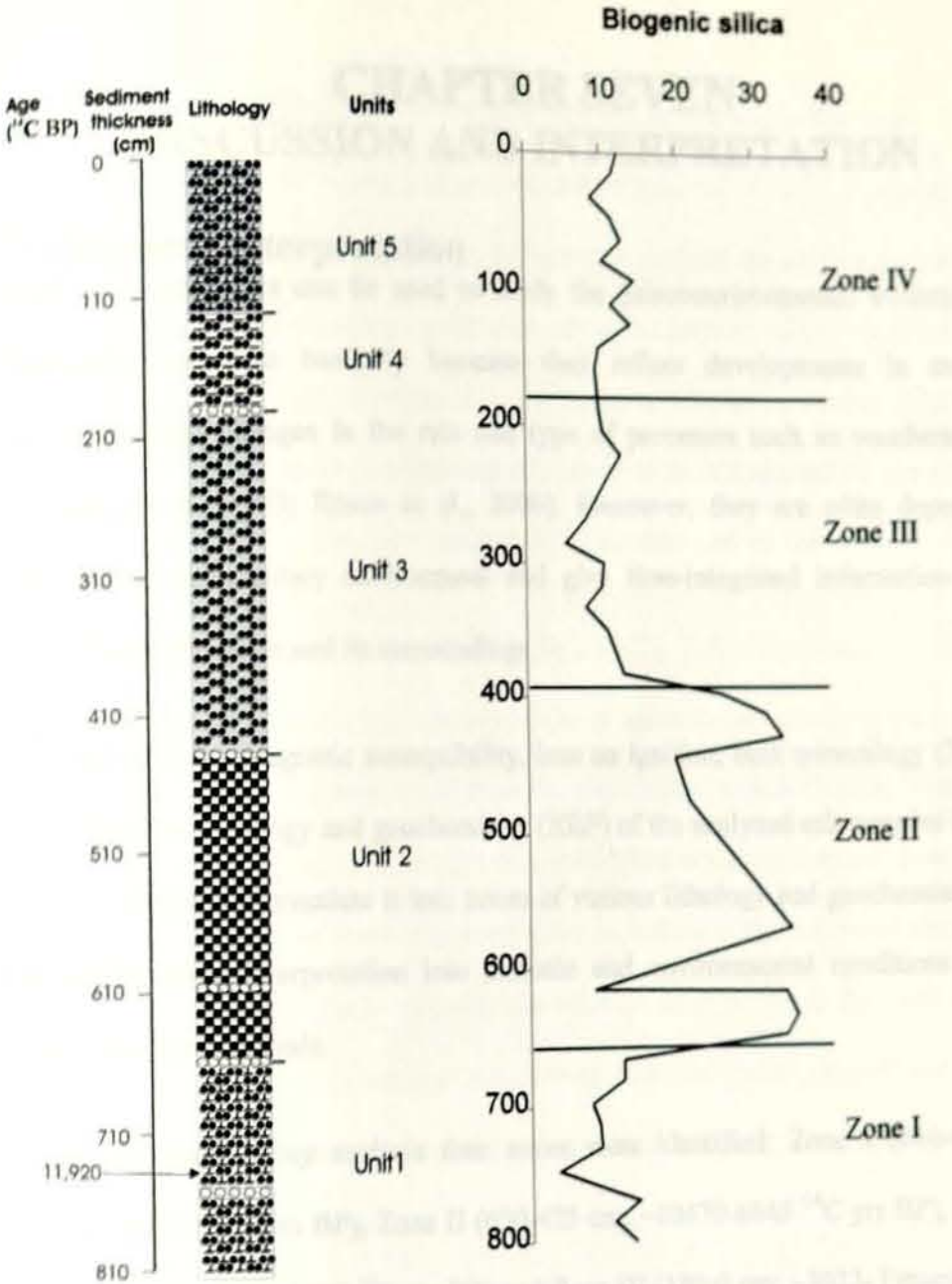

Figure 6.3 Variation of Biogenic silica with depth as indicator of lake productivity

CHAPTER SEVEN
DISCUSSION AND INTERPRETATION

7.1 General Interpretation

Lacustrine sediments can be used to study the palaeoenvironmental evolution of a particular catchment basically because they reflect developments in the Lake Ecosystem and changes in the rate and type of processes such as weathering (e.g. Renberg et al., 1993; Rosen et al., 2000). Moreover, they are often deposited in undisturbed sedimentary environment and give time-integrated information on the evolution of the basin and its surroundings.

Profiles from the magnetic susceptibility, loss on ignition, bulk mineralogy (XRD) as well as clay mineralogy and geochemistry (XRF) of the analyzed sub-samples from the core allowed to differentiate it into zones of various lithology and geochemistry. This helped to make interpretation into climatic and environmental conditions for the respective time intervals.

From the multi-proxy analysis four zones were identified: Zone I (810-650 cm; ~13047-10470 ^{14}C yrs BP), Zone II (650-425 cm; ~10470-6845 ^{14}C yrs BP), Zone III (425-180 cm; ~6845-2899 ^{14}C yrs BP) and Zone IV (180-0 cm; ~3022- Present ^{14}C yrs BP).

Zone I (810-650 cm; ~13,047-10,470 ^{14}C yrs BP)

Zone I is the basal zone. It is characterized by high values of magnetic susceptibility. The magnetic susceptibility attains a maximum value of ~ 411 (Arb. Units) at a depth of 788 cm and value decrease from the bottom to the top of the zone. The high magnetic susceptibility values could indicate a high amount of sediment yield into the lake from the catchment through erosion.

The organic matter content of this zone is also the lowest of all the zones. It has an average value of ~ 8.18 % and attains a maximum value of 16.48 % at a depth of 730 cm. A negative correlation is observed in the trends between the organic matter and the carbonate content. In this zone carbonates attain the highest values compared to the other zones. The average carbonate is 11.46 % with a maximum value of 23.83 % at a depth of 700 cm. In general low amount of organic mater content and the opposite trend of carbonate clearly indicate low productivity of the lake and low lake level.

High ratios of Na_2O/Al_2O_3, Na_2O/TiO_2, K_2O/Al_2O_3, K_2O/TiO_2, $(Na_2O+K_2O)/Al_2O_3$, $(Na_2O+K_2O)/TiO_2$ also exist in this zone. Most of the ratios attain maximum values at a depth of 666 cm and fluctuate throughout the zone. Alkali metals (Na and K) are easily soluble in water and they simply go into solution and are easily leached from the soil column. As a result, the above ratios are good indicators of the degree of alteration or chemical weathering in the catchment. The relatively high values in this zone therefore indicate a less intense chemical weathering and the predominance of physical weathering in the catchment. The limited water activities in the catchment indicate rather dry climatic condition.

Biogenic silica is calculated from the geochemical data (section 1.4.2). The amount of biogenic silica in this zone is the smallest of all the other zones. The biogenic silica in this zone attains an average value of 12.75 % and a minimum value of 3.55 % at a depth of 749 cm. The small content of biogenic silica indicates a low productivity of the lake in the period covering this zone.

Generally zone one is characterized by a high sediment supply from the catchment area, a low organic matter, a high carbonate content and a relatively higher ratios of alkalis

with hydrolysates and a low amount of biogenic silica indicating relatively cold and dry climatic condition, and a low productivity of the lake a low lake level (Figure 7.3).

The dynamics of landscape in East Africa during the Late Glacial (LG)-Holocene suggests that the amount of sediment moved to the lacustrine basins (sediment yield) reached its maximum at the beginning of the climatic optimum, in the same period in fact the vegetation cover were depleted in response to the LGM aridity. Lake Abhé and the neighboring basins filled up rapidly the late glacial and at the onset of the Holocene period (Gasse and Street, 1978a).

Based on ^{14}C dated peat deposits, the beginning of deglaciation in the Bale Mountain was estimated at 14,000-13,000 ^{14}C years BP (Mohammed and Bonnefille, 1998). A low lake level in the Ziway-Shala basin is documented for the Last Glacial Maximum (LGM) – late OIS 3 (22,000-12,000 ^{14}C years BP) (Gasse and Fontes 1989). During the LGM, Lake Abhé was dry (Gasse, 1974, 1990). An increase in Chenopodiceae pollen around 11,500 ^{14}C years BP in a peat deposit in Arsi (3800 m.a.s.l.), is an evidence for late Pleistocene aridity (Bonnifille and Hamilton (1986) sited in Nyssen (2003).

The late Pleistocene-Holocene hydrological fluctuations appear to have been characterized by a series of abrupt events that reflect complex interactions between orbital forcing, atmosphere, ocean and land surface conditions (Gasse, 2000).

Zone II (650-425 cm; ~10470 - 6845 ^{14}C yrs BP)

This zone is bounded by sand layers both at the bottom and the top. It attains the lowest magnetic susceptibility values of all zones with an average value of ~ 15.2 (Arbitrary Units). The magnetic susceptibility values are relatively higher between 610- 626 cm and 642-650 cm corresponding to the sandy layers in the diatomaceous detrital mud

unit. The rather low magnetic susceptibility values indicate a low amount of detrital sediment transport from the catchment to the lake (i.e. deposition from the lake is greater than sediment transported in to the lake).

The organic matter content of this zone is the highest of all zones. It has an average value of ~ 28.9 % and attains a maximum value of 41.13 % at a depth of 515 cm. Similar to zone I, a negative correlation is observed in the values and trends of organic matter and carbonate content. The carbonates attain lower values than in zone I and are comparable to contents in the bottom part of Zone IV. Carbonate has an average value of 5.06 % and a minimum value of 23.83 % at a depth of 535 cm. The high amount of organic mater and the corresponding low amount of carbonates indicate a high productivity of the lake and a high lake level. The zone is rich in diatoms.

Generally small values in the ratios of Na_2O/Al_2O_3, Na_2O/TiO_2, K_2O/Al_2O_3, K_2O/TiO_2, $(Na_2O+K_2O)/Al_2O_3$, $(Na_2O+K_2O)/TiO_2$ are observed in the profiles (Figure 6.1). Despite the general small values of the ratios, Na_2O/Al_2O_3, Na_2O/TiO_2 attain the smallest value of all the zones and K_2O/Al_2O_3 and K_2O/TiO_2 attain relatively high values. The high amount of the latter ratios could be due to the partial adsorption of K^+ to clay minerals and organic substances (Smykatz-kloss et al., 2000). As a result K^+ is not removed as strongly from the partly weathered horizons as Na^+, so the resulting increase in K_2O/ Na_2O ratios could indicate rather intense chemical weathering as well. From all the profiles and especially from the K_2O/Al_2O_3 and K_2O/TiO_2 profiles we can clearly see that the zone in the respective time interval is characterized by the presence of a relatively high intensity chemical weathering. The results indicate that the intensity of chemical weathering in the zone increased from the base to the top. The interpreted

higher water activity coupled with the favorable condition for chemical weathering leads to conclude that the period was warm and wet.

The amount of biogenic silica in this zone is the highest of all zones. The average value is 26.79 % and it has a wide range (i.e. 8.56 %- 35.34 %). It attains the lowest and highest values at 614 cm and 650 cm respectively. The highest value of biogenic silica in the whole length of this zone indicates highest productivity for periods covering this zone.

Zone II as a whole is characterized by a low sediment supply from the catchment, high organic matter and low carbonate content and lower ratios of alkalis with hydrolysates and high biogenic silica value indicating a warm and wet climatic condition with high lake level and high productivity in the lake (Figure 7.3).

Although a generally warm and wet climatic condition has been interpreted for this zone, however at a depth 461 cm (~ 7425 ^{14}C years BP) there are signals of lower productivity, higher sediment yield and higher carbonate content. Therefore at this point probably an abrupt arid climate could have interrupted the generally warm and wet Early Holocene.

The Early Holocene in East Africa was considerably more humid than the present (Lamb et al., 2000). Geomorphic evidence of the Ziway-Shala lakes have shown high levels, during which period the presently separated four lakes of the basin were merged together and the water surface rose to about 112 m above the present level of Lake Shala (Table 7.1). Street (1979) estimated that the Early Holocene rainfall was 48 % greater than modern precipitation in the region. In the Lake Abhé, at the beginning of the Holocene from 10000 to 8000^{14}C years BP, sedimentary facies reflect very low

turbidity, indicating that precipitation was abundant and evenly distributed throughout the year (Gasse, 1977). The lake level reconstruction of both the Lake Ziway-Shall and Abhé (Street 1979a, Gasse and Street 1978; Gasse et al. 1980; Gillespie et al. 1983; Gasse 2000) show a large but short-term water-level lowering culminating at 7.8-7.2 ^{14}C Kyr BP.

Extensive dark clays from the Ethiopian highlands were deposited in Sudan during the Early Holocene (11,200-6000 ^{14}C years BP), when there were high temperatures and increased rains (Williams and Adamson, 1980; Butzer, 1980).

Aggradation of travertine dams, with related swampy-lacustrine basins which should occur with warm air temperature, cold ground temperature and wet climate began in the Early Holocene (Dramis et al., 2003).

Area	Time Period (yr BP)	Rainfall		Source
		mm/yr	%	
Ziway-Shala Basin, Ethiopia (7° to 8° 30'N)	9,400 to 8,000		+25	Street, 1979; Gillespie *et al.*, 1983
Turkana basin	10,000 to 7,000	+80 to +140	+10 to +19	Hastenrath and Kutzbach, 1983
Lake Turkana, Kenya	10,000 to 4,000	+200	+27	Vincens, 1989
Nakuru-Elmenteita basin	10,000 to 8,000	+260 to +300	+29 to +33	Hastenrath and Kutzbach, 1983
Naivasha basin	9,200 to 5,650	+90 to +155	+10 to +17	Hastenrath and Kutzbach, 1983
Victoria basin	1880 AD	+170 to +220	+14 to +18	Hastenrath and Kutzbach, 1983
Lake Naivasha	1890s AD	+150		Vincent *et al.*, 1989

Table 7.1 Tropical precipitation during the Holocene relative to the present

Zone III (425-180cm; ~6845 - 2899 ^{14}C yrs BP)

This zone, similar to zone II is bounded by sand layers. It is characterized by silty gyttija. The magnetic susceptibility value is not uniform. At the bottom, between 425 cm and 300 cm the value is lower with an average of 22.93 (Arb. Unit). The amount sharply increases to an average value of 56.21 (Arb. Unit) at the top of the zone,

between 300 and 180 cm. In the upper part, the values are small especially between 214 and 196 cm and evidently the sediment supply from the catchment to the lake was minimal both between 425-300 cm and 214-196 cm. Generally the sediment supply increases from the bottom to the top of the zone.

The organic matter content of Zone III is higher than in Zone I but lower than in Zone II, the average value being 21.71 %. It attains a maximum value of 31.16 % and a minimum value of 17.02 % at depths of 200 cm and 290 cm respectively. Although the amount of carbonate is higher than in Zone II and lower than in Zone IV, the trend is still opposite to the organic matter content. It shows a wide range of variation. The carbonate content has an average value of 13.0% and it ranges from 3.51 % to 17.77 % at 285 cm and 245 cm respectively. The moderately higher amount of organic matter in this zone compared to zone II could show that the lake was moderately productive and the water was stagnant to allow the formation of gyttija. The organic matter produced in the lake however seems to have been diluted by detrital input from the catchment, which is indicated by the relatively high magnetic susceptibility values especially at the top of the zone.

All elemental ratios show similar trends, (Na_2O/Al_2O_3, Na_2O/TiO_2, K_2O/Al_2O_3, K_2O/TiO_2, $(Na_2O+K_2O)/Al_2O_3$, $(Na_2O+K_2O)/TiO_2$) but the range of variation of the values is different. Na_2O/Al_2O_3, Na_2O/TiO_2, $(Na_2O+K_2O)/Al_2O_3$, $(Na_2O+K_2O)/TiO_2$ varies in a wide range, while K_2O/Al_2O_3 and K_2O/TiO_2 shows a uniform trend all through the zone. This probably indicates similar chemical weathering rates in the catchment. Na_2O/Al_2O_3, Na_2O/TiO_2, K_2O/Al_2O_3, K_2O/TiO_2, $(Na_2O+K_2O)/Al_2O_3$, $(Na_2O+K_2O)/TiO_2$) attain high values at a depth of 350 cm and 206 cm but between these depths the lowest value is observed at 286 cm. In this zone both physical and

chemical weathering processes should be evident. From the ratio K_2O/Na_2O it is clearly seen that the lower part of the zone is dominated by chemical weathering as compared to the rest of the zone which is dominated by physical weathering. So it indicates that warm and wet conditions in zone III slowly diminished from bottom to top to be replaced by a drier condition.

The amount of biogenic silica in this zone is lower than zone II. It shows a general decrease from the bottom to a depth of 286 cm where it attains the lowest value. The amount again increases to the top where it shows an average value of 14.18 %. This indicates that the biological productivity of the lake dropped towards the middle of the zone. This may indicate that the lower and upper parts of the zone could be wetter than the middle part.

As compared to the lower Zones (Zone I and Zone II), Zone III experiences intermediate climatic conditions (i.e. Relatively less wet than Zone II and wetter than Zone I) indicating fluctuations in the wet-dry condition.

The bottom of zone III is generally characterized by a low sediment supply from the catchment as compared to the top. The top and bottoms of the zone contain moderately high organic matter, relatively moderate amount of carbonates, high ratios of alkalis with hydrolysates and biogenic sedimentation of silica at the top and the bottom. However low amounts are found in the middle of the zone. These indicate that the top and bottom parts are moderately warm and wet unlike the middle part which is drier and or colder, especially at a depth between 268 cm and 297 cm (between ~4,317 ^{14}C years BP and ~4,784 ^{14}C years BP) (Figure 7.3).

Although not as evident as the above sub zone, at the depth of 335 cm and 350 cm (~5396 - 5,638 ^{14}C years BP), a low productivity/weak chemical weathering signal seems to represent a short aridity interval.

Lake Ziway-Shala fell drastically after ca.5-4.5 ^{14}C Kyr BP and Lake Abhé after 4.5-4.1 ^{14}C Kyr BP. The 6.5 ^{14}C Kyr BP $\delta^{18}O$ record from carbonates in Lake Awassa does, however, show broad regional climate changes (Lamb A.L. et al. 2002). Co-varying and increasing $\delta^{18}O$ and $\delta^{13}C$ values from ~ 4.8 ^{14}C Kyr BP suggests an aridification of climate after the early Holocene insolation maximum. After 4.0 ^{14}C Kyr BP, humid condition return until after ~2.8 ^{14}C Kyr BP when $\delta^{18}O$ increases again, reflecting drier condition.

Increased detrital deposits (silt, clay) in lake Abhé during the middle Holocene indicate more irregular and intense rains (Gasse, 1977). The climate in the Mid Holocene was less humid than the previous period (Lamb et al, 2000). In northern Ethiopia since ca. 4700 ^{14}C years BP a period of alternating phases of tuffa dam incision and aggradation occurred. Growing aridity, from 5000 to 4000 ^{14}C years BP provoked soil erosion and deposition which covered the existing soils, as witnessed by palaeosols (Messerlie and Frei, 1985; Ogbaghebriel et al., 1997; Sagri et al., 1999). The buried soils range in age between 5160 ± 80 (May Meakden, Tigray) and 300 ± 60 ^{14}C years BP (Adi Kole, Tigray) (Messerlie and Frei, 1985; Ogbaghebriel et al., 1997; Sagri et al., 1999).

Zone IV (180-0 cm; ~2899 - Present ^{14}C yrs BP)

Zone IV covers the top 180 cm of the core. At the base, the zone is marked by a sand layer. The zone is characterized by clayey silt at the bottom and grades to calcareous clayey silt at the top. The magnetic susceptibility value reaches one of the highest, with

an average value of 116.34 (Arb. Unit). The magnetic susceptibility value increases from the base to a depth of 138 cm, where it attains a maximum value for the zone (i.e 160.4 (Arb. Unit)). It then decreases until a depth of 78 cm (i.e. 73.9 (Arb. Unit)) and then increases up wards. The sediment supply from the catchment to the lake was maximized during this period except at about a depth of 100 cm -56 cm. Probably this interval represents a warmer period than the other parts of the zone.

The organic matter content in this zone is lower than in zone III and zone II but it is higher than in Zone I. It contains an average organic matter value of 13.9 %. High values are situated between depths of 95 cm and 60 cm as well as at 105 cm and above 60 cm to the top. The carbonate content in this zone shows extreme values at different depths and shows big fluctuations. The average value of organic matter for the zone is 9.1 %. The bottom part of the zone has the lowest value and increases towards the top and attains similar values as in zone III but lower than in Zone I. Further to the top of the zone the amount decreases again.

The generally smaller amount of organic matter in the zone shows that the period was the productivity in the lake was lower due to perhaps drier and colder conditions than during depositions in zone II and III. This situation however was intercepted by ra elatively warm and wet phase indicated by higher values at the middle of the zone.

The ratios of Na_2O/Al_2O_3, Na_2O/TiO_2, K_2O/Al_2O_3, K_2O/TiO_2, $Na_2O+K_2O)/Al_2O_3$ and $(Na_2O+K_2O)/TiO_2$ first decrease from the bottom of the zone to a depth of 158 cm where it attains a minimum value. They then increase until 142 cm depth and become constant upwards except at a depth of 15 cm where the values become much higher. At a depth of 126 cm K_2O/Al_2O_3 and K_2O/TiO_2 show high values.

From the signals of weathering it seems that, at the bottom of the zone chemical weathering was weak. Upwards to 126 cm the intensity seems to increase. Above 126 cm the influence of physical weathering dominates over chemical weathering. The same trend is observed in the K_2O/ Na_2O ratio (i.e. the rate of chemical weathering increases from the bottom of the zone up to 126 cm and decreases all the way up to the top). The zone is generally characterized by dry climatic conditions, that are interrupted by periods of wet and warm conditions.

The amount of biogenic silica in this zone is lower at the bottom than at the top with a little decrease at the very top of the zone. The bottom part up to a depth of 142 cm has an average biogenic silica content of 9.52 %, the average value increases to 11.75 % in the remaining portions of the zone. The biological productivity of the lake was minimal except at the middle of the zone indicating a warm and wet period in this part. middle.

Generally the zone experiences, a high sediment supply at the base and top with a minimum in the middle, a maximum organic matter content in the middle as compared to the top and the bottom parts, a high chemical weathering index and biogenic silica content in the middle. All these indicating cold and/or dry conditions in the whole length of the zone which is interrupted by wet and warm phase with better productivity (Figure 7.3).

Right at the lower part of the zone the climate changed from a warm and wet condition to a dry condition. At a depth between 82 cm and 102 cm (~ 1324 ^{14}C yr BP = 680 AD and 1643 ^{14}C yr BP = 361 AD) very low magnetic susceptibility and high productivity signals have been recorded. This sub-Zone could be related to the "Medieval warm Period" represented in the region. Further up in the core at about 25-35 cm depth (~ 404 ^{14}C yr BP = 1602 AD – 564 ^{14}C yr BP = 1440 AD) a very high sediment yield and

low biologic productivity led to conclude the period could correspond to the "Little Ice Age". The above events have been identified and discussed in the region (Bonnefille and Mohammed; 1994, Darbyshire et al. 2003. (Figure 7.2).

In the late Holocene, there is enrichment in clay and silt, corresponding to more arid conditions (Gasse, 1977). Stable isotope analyses of inorganic calcite in Lake Turkana, which drains southern Ethiopia by the Omo River, shows an increase in heavier ^{18}O isotopes between 4000 to 2000 ^{14}C years BP. This is explained by a change in climatic conditions on the Ethiopian plateau (Ricketts and Johnson, 1996). The study of the infilled valley deposits in Tigray has enabled the identification of several soil degradation and soil formation periods spanning the past 4000 yr. From ca. 4000 to 960 yrs BP five major events were identified, i.e. three wet periods between 4000-3500 yrs BP, 2500-1500 yrs BP and two degradational episodes between 3500-2500 yrs BP and 1500-1000 yrs BP (Machado et al., 1997). Starting from ca. 3500 ^{14}C years BP, a general shift of the climate towards drier conditions with minor wet phases around 2400 and 1000 ^{14}C years BP is recognized (Dramis et al., 2003).

7.2 Interpretation of clay minerals

Clay minerals in sediments can be useful indicators of pleoclimatic conditions. Although they do not produce direct indications of climate parameters, they provide integrated records of overall climatic impacts. Occasionally, they may be superior to the more conventional methods, such as pollen or oxygen isotope analysis (Singer, 1984).

Levels relatively rich in chlorite, illite , palygoriskite and quartz are interpreted as corresponding to relatively dry periods, while a more humid period leads to a more intensive weathering and consequently to the dominance of clay minerals which are

more advanced in the relative stability scale, such as kaolinite. Smectite is taken to indicate a climate with contrasting seasons and a pronounced dry season.

The proportion of smectites in clay fraction decreases with increasing rainfall. A series of paleosols developed on a sequence of basalt flows from the early plestocene contain clay mineral assemblages with a smectite/kaolinite ratios considerably higher than that determine in the clay fraction of a modern soil developed at the same site, indicating the basalt derived paleosols developed under the climate that was significantly drier than at the present day (Singer, 1984).

A mineral assemblage containing chlorite in the clay fraction and micas, quartz and amphibolites in the silt fraction has frequently been observed in soils and in sediments produced by high-altitude or cold-climate weathering (Campbell and clardige, 1982). Thus, chlorite and illite are indicative of weak weathering intensities (Singer, 1984). In tropics on the other hand, where leaching and chemical weathering are intense, there is a conspicuous abundance of kaolin group and gebbsite groups near continental masses. The distribution of chlorite is observed to be nearly reciprocal to that of kaolinite (Biscaye, 1965; Zimmerman, 1977).

Although it is difficult to generalize and make a boundary between the changes recognized in the clay minerals obtained from only 12 samples for the whole length of the core, an attempt has been made to group them and give analysis on the sampling points. Based on the general trend of the individual samples, the core is divided into three zones.

Zone I

Zone I is the bottom zone of the core between 650 cm and the base of the core. In this zone all the clay minerals are present except illite at the base of the zone. Chlorite is present only in this zone and varies between 3 % and 8 %. Smectite is the dominant clay mineral in the zone and it varies between 71 % and 88 %. As a result, the ratio of smectite to kaolinite is high. The small amount of kaolinite and the presence of chlorite coupled with the high value of the ratio between smectite and chlorite indicates that the period which the zone covers is dry except for the upper part where the amount of kaolinite gets higher but the ratio between smectite and kaolinite is smaller. This could indicate a transition to a more humid trend.

Zone II

Zone II is the middle zone covering the longest part of the core between 174 cm and 650 cm. The zone is characterized by a generally low amount of smectite and absence of chlorite. With the exception of the top and the bottom parts of the zone kaolinite and illite have high values. Similarly the ratio of smectite to kaolinite is relatively low except at depths of 238 cm, 286 cm and 634 cm Table 7.2 and Figure 7.1). The zone attains the lowest value of smectite to kaolinite ratio of 1.2 at a depth of 493.5 cm while the highest value is 19.3 at a depth of 238 cm. Therefore, the low value of smectite/kaolinite ratio indicates that the period was wet. On the contrary the upper and lower parts of the zone indicate a dry period.

Zone III

Zone III is the upper part of the core between 174 cm and 142 cm. The top 142 cm of the core was not analyzed for clay minerals since the clay fraction were not enough to separate for the analysis. The zone is characterized by higher amounts of smectite,

lower amounts of illite and kaolinite as compared to zone II. The ratio of smectite to kaolinite has the highest value of 34 in this zone at a depth of 142 cm. In addition to the higher value of kaolinite the higher amounts of Smectite/kaolinite ratio indicates the period covering this zone was dry. The higher amount of smectite also signifies the period characterizing a climate with contrasting seasons and having a pronounced dry season.

Generally the lower part of the core experiences higher values of smectite/kaolinite indicating a cold and dry period. Between 650 cm and 286 cm the ratio is generally small except at the two sampling locations 634 cm and 618 cm indicating a humid condition. The general increase of the value between 286 cm and 142 cm with the exception of the interruption at a depth of 174 cm indicates the onset of a generally pronounced dry season and climate with contrasting seasons (Singer, 1984).

Sediment depth(cm)	Smectite/Kaolinite
142	33.95
174	9.94
238	19.26
286	19.10
478	1.94
494	1.25
618	10.44
634	16.88
650	0.60
730	20.62
770	20.06
784	18.41

Table 7.2 Smectite/kaolinite value with depth

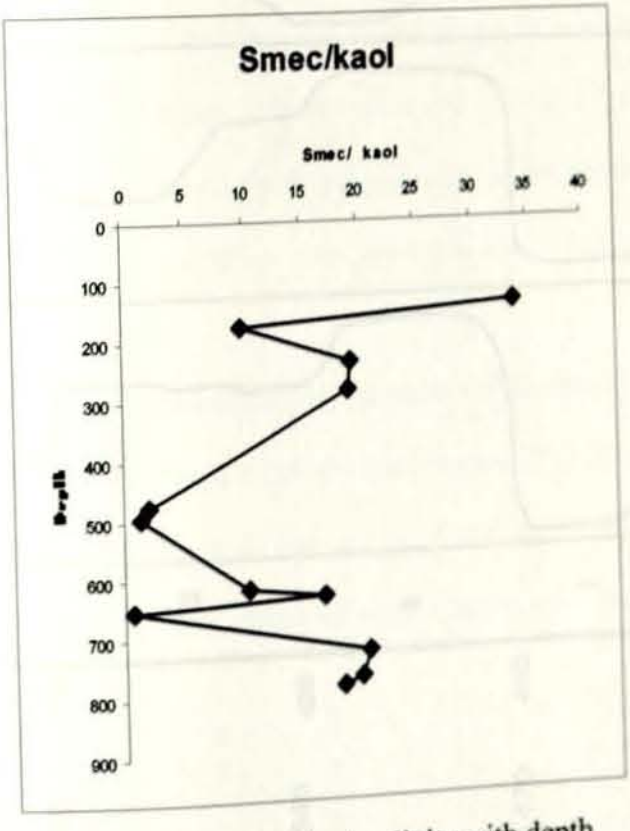

Figure 7.1 variation of Smectite/kaolinite with depth

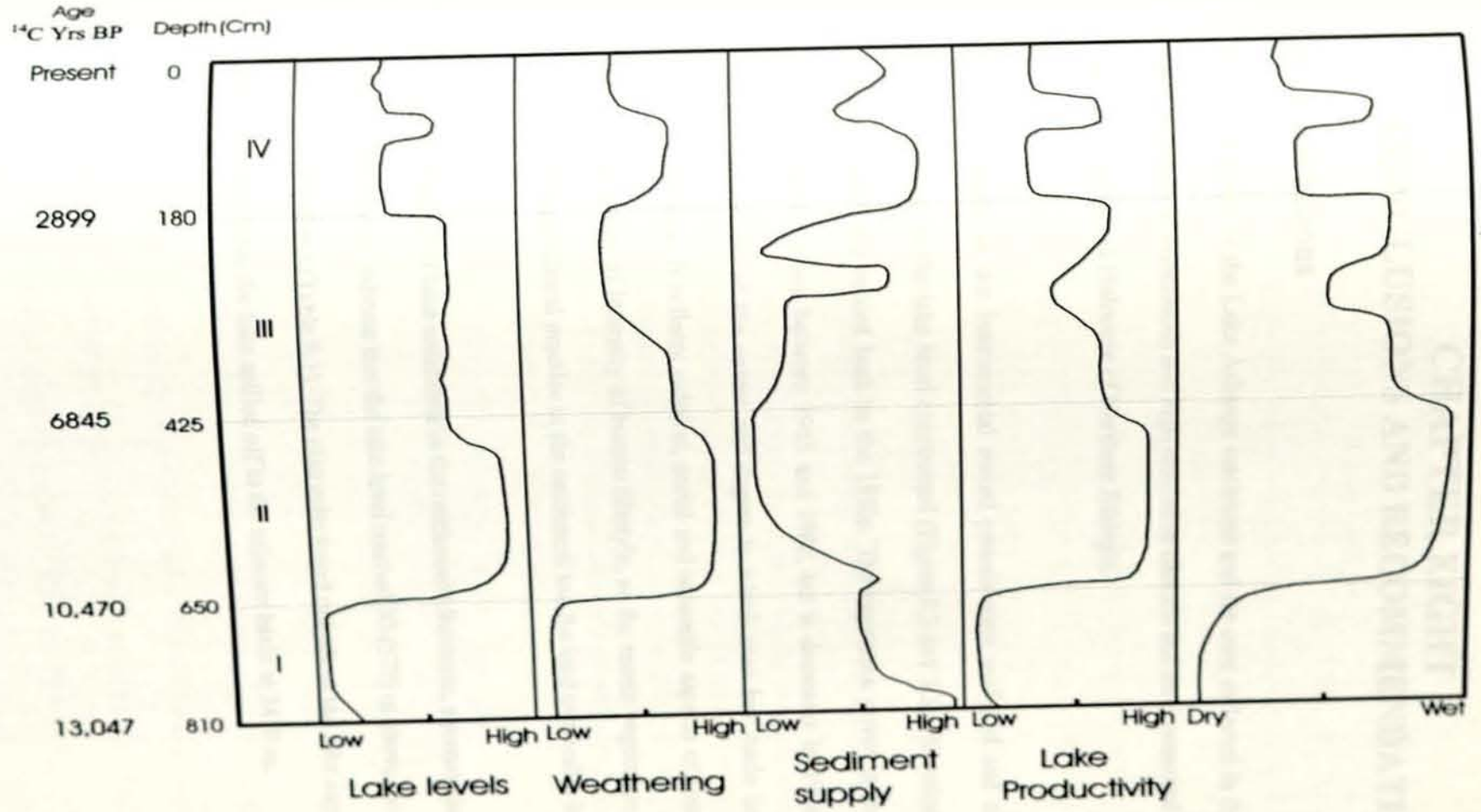

Figure 7.2 Summery of the Climatic condition of Lake Ashange and the catchment since Late Pleistocene.

CHAPTER EIGHT
CONCLUSIONS AND RECOMMENDATIONS

8.1 Conclusions

Integrated study of the Lake Ashange catchment and the core collected in the lake gave the first evidences of continuous and high resolution climatic and environmental changes for the late Pleistocene and Holocene of Northern Ethiopia.

Recent changes in the instrumental record periods were analyzed and the seasonal and annual changes in the lake level constructed (Figure 3.2 and 3.3). Historical data were also used to extend the record back to the 1930s. The vegetation cover in the catchment has increased in the years between 1965 and 1980, but it decreases in 1986. Land use is a primary indication of the extent and degree to which man has made impression on the earth's landscape. It reflects political, social and economic aspects of human cultures, and provides an index of intensity of human lifestyle, so the recent vegetation change could be the result of agricultural practice in the catchment and the land ownership in the country.

The distribution of lake sediments in the catchment (diatomite, stromatolites, etc.) and section evidences indicate that the lake level reached 30-(57?) m above the present lake level (i.e. 2440 m) (Table 8.1). The diatomite found outside of the lake supports the high lake level at a time the lake spilled off to the adjacent basin at 2470 m.

Lakes	High lake-level stands above the present limit (m)
Asal	112
Afrera	40
Ashange	30-(57)?
Awassa	10-40
Beseka	10
Ziway-Shala	112

Table 8.1 High lake-level stands of some of the lakes (Source: Gasse, 1977; Gasse and Street, 1978; Gasse et al., 1980; Present work)

The studied core is dominantly organic and measures 8.1m and is recovered under 9m of water depth. The basal radiocarbon age shows a date of 11,920 ± 40 years BP. Other radiocarbon dates from samples corresponding to important shifts in the studied proxies are under analysis. Because of this, linear extrapolation of age versus sediment depth has been applied by considering the top of the core as modern.

Zone I is the basal zone between 810 cm-650 cm and with an estimated age 13,047-10,470 ^{14}C yr BP interval is characterized by high sediment yield, low chemical weathering and low lake level. The climate in this zone is interpreted as cold and dry.

Zone II is between 650 cm-425 cm and with an estimated age of 10,470-6,845 ^{14}C yr BP. The interval is characterized by low sediment yield, high chemical weathering and high lake level. The climate is interpreted as a more stable wet and warm. At ~ 7425 ^{14}C yr BP an arid interval is documented in a generally wet and warm Early Holocene.

Zone III is between 425 cm -180 cm with an estimated age of 6,848- 2,899 ^{14}C yr BP. The interval is characterized by low sediment yield at the base and high at the top, low productivity at the base and the top of the zone interrupted. This was interrupted by a high productivity at the middle indicating a moderate lake level. The climate in the zone is then interpreted as dry except at an estimated age of 4,317 ^{14}C yr BP.

Zone IV is the upper most zone of 180 cm with an estimated age of 2,899 ^{14}C yr BP. The zone is characterized by a high sediment yield from the catchment low chemical weathering and low productivity. It is more generally interpreted as a dry interval with wet pulses. Some important events are also traced in the upper part of the core: at a depth between 82 cm and 102 cm (~ 1324 ^{14}C yr BP = 680 AD and 1643 ^{14}C yr BP = 361 AD) corresponding to the "Medieval warm Period" and at about 25-35 cm depth (~ 404 ^{14}C yr BP = 1602 AD – 564 ^{14}C yr BP = 1440 AD) to the "Little Ice Age".

Dramatic changes in water resources have enormous consequences on human populations, generating famines, migration, civilization foundation and collapses. The advanced urban civilizations in Egypt (Hassans, 1981), Mesopotamia and India mysteriously collapsed at around 4000 yrs ago . This collapse of old World societies is likely to be related to 4.2-4 ka dry events that affected the monsoon domain and eastern Mediterranean. There is no doubt that Holocene drought and flood episodes have been more dramatic and more persistent than those of the instrumental record of the last century, which does not represent the full range of natural climatic variability of the current interglacial period. There is no guarantee that similar shifts with serious social impacts cannot happen again. We need to estimate its amplitude, to better constrain the timings and to obtain high resolution Holocene records from the surrounding oceans, before concluding their relations with short-term events known elsewhere and to analyze potential mechanisms. Understandings of natural

fluctuations in water resources that occur at the time scale of human lives should be a first propriety in future research (Gasse, 2000).

The impact of human activity on natural vegetation has been particularly effective in the area since the second millennium B.C. (Butzer, 1981; Fattovich, 1990). Although it difficult to differentiate the degree of human impact on the environment, it is likely that human beings were intensifying the environmental change in the region at least in the last estimated 3,000 years BP.

8.2 Recommendations

- Knowledge of the short-term vegetation response to climate and land-use variation in the past may help to provide a basis for land use management and conservation policy for anticipated future changes. Lamb et al., 2002.
- Additional dates on the core especially at sediment depths of 450 cm, 300cm and 180 cm will be helpful to calculate the rate of sedimentation for different time intervals and to know the major changes in the core so that to compare some important events with other works in the Ethiopian rift and the Afar and also elsewhere in East Africa.
- Catchment samples should be dated to tell the time when Lake Ashange experienced fluctuations and the highest lake stand and also the exact time of spill off of the lake.
- The Hydrology and Hydrogeology of the catchment should be studied; to check if there is an interaction between the lake and ground water.
- Seismic survey would be good on the northern part of the lake to check the extent of lake sediment buried by the time the lake covered it.
- As evident in the south western part of the catchment, if the land is properly managed, the degraded land could be rehabilitated.
- To exploit the good landscape of the basin and the beauty of the lake, it will be good to establish recreational after appropriate environmental impact studies and later monitoring activities centers. This might help to benefit the regional government as a whole and the surrounding in particular.

REFERENCES

Azzaroli, A., 1968. On the evolution of Gulf of Aden. XXIII International Geololgical Congress 1, 125-134.

Barakhi O., Brancaccio L ., Calderoni G., Coltorti M., Dramis F. and Mohammed M.U. 1998. The Mai Mekdan sedimentary sequence - A reference point for the environmental evolution of the highlands of Northern Ethiopia. Geomorphology. 23: 127-128.

Bard. K., Coltorti, M.., DiBlasi, M., Dramis, F.,Fattovich, R., 2000. The environmental history of Tigray (Northern Ethiopia)in the middle and latr Holocene: a preliminary outline. African Archaeological Review 17 (2), 65-86.

Beadle, L.C., 1974. The inland waters of Tropical Africa. Longman, London

Benson, L.V., 1978. Fluctuations in the level of pluvial Lake 40,000 years.Quaternary Research 9, 300-318

Benson, L., Thompson, R., 1987. The physical records of lakesin the Great Basin. In: Ruddiman, W.F., Wright. H.E.J.(Eds.). North Atlantic and Adjacent Oceans Duringthe Last Deglaciation. The Geology of North America, Geological Society of America, Boulder,CO.

Berner, R.A. (1971) : Principles of Chemical Sedimentology.- Mc Graw Hill, New York

Beydoun, Z.R., 1970. Southern Arabia and northern Somalia: comparative geology, PHIL. Trans. Roy. Soc. 267, 267-292.

Billi P. 1998. Climatic change. In Land Resources Inventory and Environmental Changes analysis and their application to Agriculture in the Lake region (Ethiopia). In: Sagri M Co-ordinator. Report submitted to EC. Project STD 3 contract no Ts 3-CT 92-76 (1993-1998). 108-122 p

Bonnefille R. and Mohammed U. 1994. Pollen inferred climatic fluctuations in Ethiopia during the last 3000 yrs. Palaeogeography, Palaeoclimatology, Palaeoecology. 109: 331-343

.

Brancaccio, L., Calderoni, G., Coltorti. M., Dramis, F., 1997. Phases of soil erosion during the Holocene in the highlands of Western Tigray. (Northern Ethiopia): a preliminary report. In: Bard, K. (Ed.), The environmental and human ecology of the Northern Ethiopia in the late Holocene . Instituto Universtario Oreintalea, Napoli, pp. 30-48.

Brookins, D.G. (1988): Eh-pH Diagram for Geochemistry.-Springer-Verlag, Berlin-Heidelberg- New York

Butzer K. W., Isaac G. L., Richardson J. L. and Washbourn-Kamau C. 1972. Radiocarbon dating of East African lake levels. Science. 175: 1069-1076.

Butzer, K., 1980. Pleistocenehistory of the Nile valley in Egypt and lower Nubia. In: Williams, M., Faure, H., (Eds.), The Sahara and the Nile . Balkema, Rotterdam. pp.238-252.

Calanchi, N., Danelli & Lucchini. 1966a. Inorganic Geochemistry of two cores fromfrom the Meso-Adreatic Depression (MAD): trace elements as geochemical indices of Paleoenvironmental changes in the Late Quaternary. Journal of Abstracts. 1:94

Chalié F., and Gasse F. 2002. A 13,500 years diatom record from the Tropical East African Rift Lake Abiyata (Ethiopia). Palaeogeography, Palaeoclimatology, Palaeoecology, 187: 259-283.

Chamley, H., 1980a. Clay sedimentation and Paleoenvironmrnt in the area of Daito Ridge since the Early Eocene.

Chorowiz, J., Collet, B., Bonavia, F., Mohr, P., parrot, J.F and Korme, T., 1988. The Tana Basin, Ethiopia. Ibteraplateau uplift, rifting and subsidence. Tectonophysics 295, 351-367.

Cohen, A..L., Parkington, J.E., Brundrit, G.B. Van de Merwe, N., 1992. A Holocene marine climate record in mollusc shells from southwest African coast. Quaternary Research 38, 379-385

Cook, H.E., P.D. Johnson, J.C. Matti & I. Zemels, 1975. Methods of sample preparation and X-ray diffraction analysis, X-ray Mineralogy Laboratory, Deep See Drilling Project, University of California, Riverside. In Hayes, D.E. & L.A. Frakes (eds.) Initial Reports. DSDP 28, Washington: 999-1007

Darbyshire I., Lamb H.F. and Mohammed M.U. (2003) Forest Regrowth in Northern Ethiopia During the last 3000 years. The Holocene, 13 (in press).

Dagnachew Legesse, Gasse F., Radakovitch O., Vallet-Coulomb C., Bonnefille R., Verschuren D., Gibert E. and Barker P. 2002. Environmental changes in a tropical lake system (Ziway-Shalla basin; Main Ethiopian Rift) over the last centuries - Preliminary results from short cores from Lake Abiyata. Palaeogeography, Palaeoclimatology, Palaeoecology, 187, 233-258.

Dagnachew Legesse, Vallet-Coulomb C., and Gasse F. 2003.Hydrological response of a catchment to climate and land use changes in Tropical Africa: Case study South Central Ethiopia. J. Hydrol.,. 275: p. 67-85.

Dean, JR., Walter, E., (1974). Determination of carbonate and organic matter in calcareous sediments and sedimentary rocks by loss on ignition: comparison with other methods. Journal of Sedimentary Petrology, Vol. 44, No. 1, p. 242-248

Derver, J.I. (1982): The Geochemistry of Natural Waters. Prentice-Hall, New york

Dramis, F., Mohammed M.U.calderoni G. and Mitiku H. (2003) Holocene climate changes from buried soils in Tigray (Northern Ethiopia): comparision with lake levele fluctuations in the Main Ethiopia Rifts. Quaternary Research 60 (2003) 274-283

Engstrom, D.R., & E.B. Swaim, 1986. The chemistry of lake sediments in time and space. Hydrobiologia 143: 37-44

Fagel, N., 2003. Late Quaternary clay minerals assemblages in Lake Baikal and paleoclimate reconstruction. Geophysical Research Abs. Vol. 5, 11823, 2003.

Fattovich, R., 1990. Remarks on the pre-Axumite period in Northern Ethiopia. Journal of Ethiopian Studies, Studies 23, 1-33

Fontes J.C. and Pouchan P. 1975. Les cheminees du lac Abhe (TFAI): station hydroclimatique de l'Holocène. C.R. Acad. Sci. Paris. 280D: 383-386.

Gallet, S., Jahn, B.M., van Vliet- Lanoe, B., Dia, A. & Rosello, E. 1998. Loess geochemistry and its implications for particle origin and composition of the upper continental crust. EPSL 156, 157-172

Gasse F. 1977. Evolution of Lake Abhé (Ethiopia and T.F.A.I.) from 70,000 B.P. Nature 265: 42-45.

Gasse, F. and Street, F.A. (1978a). Late Quaternary lake level fluctuation and environments of the northern Rift valley and Afar region (Ethiopia and Djibouti). Paleogeography Paleoclimatology Paleoecology. 24, 279-325.

Gasse, F. and Street, F.A. (1978b). The main stages of the late Quaternary evolution of the northern Rift Valley and Afar Rift lakes (Ethiopia and Djibouti). Polish Archives Hydrobiology. 25, 145-150.

Gasse F. and Descourtieux C. 1979. Diatomées et évolution de trois milieux éthiopiens d'altitude différente, au cours du Quaternaire supérieur. Palaeoecology of Africa. 11: 117-134.

Gasse F. and Van Campo E. 1994. Abrupt Post–Glacial climate events in West Asia and North Afri monsoon domains. Earth and Planetary Science Letters. 126: 435-456.

Gasse F., Juggins S. and Ben Khelifa L. 1995. Diatom-based transfer functions for inferring past hydrochemical characteristics of African lakes. Palaeogeography, Palaeoclimatology, Palaeoecology. 117: 31-54.

Gasse F. 2000. Hydrological changes in the African tropics since the Last Glacial Maximum. Quaternary Science Reviews. 19: 189-211.

Gamachu, D., 1977. Aspects of climate and water budget in Ethiopia. Addis Ababa University Press.

Geze, F. (1975). New dates on Galla lake level (Ethiopian Rift Valley). Bull.geophys.Obs., Addis Ababa 10, 59-68)

Gillespie R. Street-Perrott F.A., Switzur R. 1983. Post glacial arid episodes in Ethiopia have implications for climate prediction. Nature. 306: 680-683

Gilbert E. Travi Y., Massault M., Cherenet T., Barbecot F. and Laggoun Defarge F. 1999 carbonate and organic AMS-C-14 ages in Lake Abiyata sediments (Ethiopia) Hydrochemistry and paleoenvironmental implications. Radio carbon 41: 271-286

Griffiths J.F. 1972. Ethiopian highlands.- Landsberg, H.E. (ed): World Survey of Climatology 10. Amsterdam. pp. 369-381.

Grove, A.T. and Goudine, A.S. (1971a). Late Quaternary Lake levels in the Rift Vally of southern Ethiopia and elsewhere in tropical Africa. Nature 234, 403-405.

Grove, A.T., Street, F.S. (1975). Former lake levels and climatic change in the rift valley of southern Ethiopia. Geogr. J. 141, 177-202.

Hamilton A.C. 1982. Environmental history of East Africa. A study of the Quaternary. Academic Press, London. 328 P.

Hassan F. 1981. Historical Nile Floods and their implication for climatic change. Science. 212: 1142-1145.

Ingrid A. Ukstins, Paul R. Renne, Ellen Wolfenden , Joel Baker , Dereje Ayalew , Martin Menzies (2002). Matching conjugate volcanic rifted margins: 40Ar/39Ar chrono-stratigraphy of pre- and syn-rift bimodal flood volcanism in Ethiopia and Yemen

Kebede S. Lamb H.F., Telford R.J, Leng M.J. and Umer M. U. 2002. Lake ground water relationships, oxygen isotope balance and climate sensitivity of the Bishoftu crater lakes, Ethiopia. In: Odada, E. and Olago, D. (eds) The East African Great Lakes Region: Limnology, Paleoclimatology and Biodiversity. Advances in Global Research Series, Kluwer.

Krauskops, K.B. & Bird, D.K. 1995. Introduction to Geochemistry. 3rd Ed., McGraw-Hill, New York

Kurkura Kabeto, Yoshihiro Sawada, Robert Bussert, Dirk Küster (2004). Geology and Geochemistry of Maichew Volcanics, northwestern Ethiopian Plateau

Kutzbach J.E., Guetter P.J., Behling P.J., Delin R. 1993. Simulated climatic changes: results of COHMAP climate-model experiments. In: Global climates since the last Glacial maximum. University of Minnesota press, Minneapolis. pp. 5-11.

Lamb A.L., Leng M.J., Lamb H.F. and Mohammed M.U. 2000. A 9000-yr oxygen and carbon isotope record of hydrological change in a small crater lake. The Holocene. 10: 167-177.

Lamb A.L., Leng M.J., Lamb H.F., Telford R.J. and Mohammed M.U. 2002. Climatic and non-climatic effects on the □18O and δ13C composition of Lake Awassa, Ethiopia, during the last 6.5Ka.Quaternary Science Reviews

Last, M.W. and Smol, P.J. 2003. Tracing environmental change using lake sediments. Kluver Academic Publishers.

Laury, R.L and Albrittion, C.C.Jr. (1975). Geology of Middle Stone Age archeological sites in the Main Ethiopian Rift Valley. Geol. Soc. Am. Bull. 86, 999-1011.

Le Turdu C., Tiercelin J.J., Gibert E., Travi Y., Lezzar K.E., Richert J.P., Massault M., Gasse F., Bonnefille R., Decobert M., Gensous B., Jeudy V., Tamrat E., Mohammed M.U.,

Martens K., Atnafu B., Chernet T., Williamson D., Taieb M. 1999. The Ziway Shalla basin system, Main Ethiopian Rift: Influence of volcanism, tectonics and climatic forcing on basin formation and sedimentation. Palaeogeography, Palaeoclimatology, Palaeoecology. 150: 135-177

Lezine A.M. and Bonnefille R. 1982. Diagramme pollinique Holocene d'un sondage du lac Abiyata (Ethiopie, 7°42' Nord). Pollen et Spore. 3-4: 463-480.

Li, H.C., Stott, L.D., Hammond, D.E. 1997. Temprature and salinity effects on O^{18} Fractionation for rapidly precipitated carbonates:Laboratory experiments with alkaline lake water. Department of Earth Sciences, University of southern California, Los Angeles, CA 90089-0740

Lindsay, W.L. 1979. Chemical Equlibra in Soils. Wiley & Sons, New York.

Lowe, J.J. and Walker, M.J.C 2001. Reconstructing Quaternary Environments. Prentice-Hall 2nd edition

Machado J.M.; Perez-Gonzalez A. and Benito G. 1997. Erosion processes and land degradation episodes during the last 3000 yr at the Axum Region (Tigray, Northern Ethiopia). In: Federici, P.R. (Ed.) Int. Conf. geomorphology-Abstracts. Geografia e Dinamica Quaterneria, supplement 3, vol. Tl, p.258.

Machado J.M.; Perez-Gonzalez A. and Benito G. 1998. Paleo-environmental changes during the last 4000 yrs in Tigray, Northern Ethiopia. Quaternary Research. 49: 312-321.
Marc Davies, Ian Parkinson and Nick Rogers (2003) The Origin of High-Ti Picrites from the Ethiopian Flood Basalt Province

Makin, M., Kingham, T., Waddans, A., Birchall, C.,Tamene, T., 1974. Development prospects in the Southern Rift Valley, Ethiopia. Draft land resour.stud. land resour. Div. Minist. Ocersease Dev. No PR/25/74, p.199.

Meral, G., Abate, E., Azzaroli, A., Bruni, P., Canuti, P., Fazzuoli, M., Sagri, M., Cacconi, P., 1979. A Geological Map of Ethiopia and Somalia (1973). 1:2000000 and comments, University of Florence, Italy.

Messerli B., Hurni H., Kienholz H. and Winiger M. 1977. Bale Mountains: largest Pleistocene Mountain glacier system of Ethiopia. X INQUA congress. Birmingham. Abstracts: 1.

Messerli B., Feri, E., 1985. Klimagschichte und Paläoböden in done Gebirglen Afrikas zwischen Äquator und nördlichem wendekreis. Geomthodica (Basel) 10, 31-70

Messerli B., Rognon P.H. and Winiger M. 1980. The Saharan and East African uplands during the Quaternary.- Wiliams M.A.J. (Ed): The Sahara and the Nile . Balkema, Rotterdam. PP 87-148.

Mohammed M.U. and Bonnefille R. 1998. A Late Glacial to Late Holocene pollen record from a high land peat at Tamsaa, Bale Mountains, South Ethiopia. Global and Planetary Change. 16-17: 121-129.

Mohammed, M.U., Dagnachew, L., Gasse, F., Bonnefille, R., Lamb, H., Leng, M. and Lamb A. (2004) Late Quaternary Climate Changes in The Horn of Africa.

Mohr, P., 1963. The Geology of Ethiopian University Collage of Addis Ababa press. 270 pp

Mohr P.A. 1971: The Geology of Ethiopia. University Press, Addis Ababa, 2nd edition.

Mohr, P. and Zanettin, B., 1988, The Ethiopian Flood Basalt Province Continental Flood Basalts, Kluwer academic Publisher, Dordrecht, Boston/London, 341pp, , Dordrecht, the Netherlands.

Moore, D.M. & Reynolds, R.C., 1997. X-ray Diffraction and the Identification and Analysis of Clay Minerals (2nd edition). Oxford University Press, Oxford, 378pp.

Nillson E. 1940. Ancient changes of climate in British East Africa and Abyssinia – Geografisker Annaler 22: 1-79.

Nyssen, J., Poesen, J., Vandeyenreken, H., Moeryesons, J., Deckers, J., Mitiku, H., Salles. C., 2003a. Spatial variablity of rain and its erosivity in atropical mountain catchment, Tigray, Northern Ethiopia. Proc. 2nd International conference on tropical climatology, meteorology and Hydrology, Brussels, Belgium, Dec. 12-14. Institute of Royal Meteorologique Brussels, in press.

Ogbaghebriel, B., Brancaccio, L., Calderoni, coltorti, M., Dramis, F., Belay, T., Mohammed. U., 1997. Geomorphological and sedimentary recordsof Holocene climate changes and

human impact in the highlands of Northern Ethiopia. In: Federici, P.R. (Ed). 4th Int.conf.Geomorphology-Abstracts. Geographica Fisica e Dinamica Quaterneria, Supplement 3, vol.Tl, p.77.

Ogbaghebriel, B., Brancaccio, L., Calderoni, coltorti, M., Dramis, F., Belay, T., Mohammed. U., 1998. The Mai Makden sediment sequence: a reference point for the environmental evolution of the highlands of the northern Ethiopia. Geomorphology 23, 127-138.

Owen R.B., Barthelme J.W., Renaut R.W., Vincens A. 1982. Paleolimnology and archaeology of Holocene deposits north-east of Lake Turkana. Nature. 298: 523-528

Pilger A.- Rösler A., Temporal relationships in the tectonic evolution of the Afar depression (Ethiopia) and the adjacent Afro-Arabian system, `` Afar between continental and oceanic Rifting`` Pilgar and Rosler Schweizerbart Verlag, Stuttgart 1-25 (1976).

Raya Valley Development Study Project (RVDP), 1998, Feasibility Study Report, Hydrogeology, Addis Ababa, Ethiopia.

Ricketts, R., Jonson, T., 1996. Climate change in the Turkana Basin as deduced form a 4000 yrs long delta O^{18} record. Earth and Planetary science letters 142 (1-2), 7-17.

Robinson, I., Mackay, R., Afewerki, S., Yragalem, A., 1995. A Review of the Agricultural Rehabilitations Programs of Eritrea. Center of Arid Zone Studies, Bangor . 61 pp.

Robinson C., G.B. Shimmied & K.M. Creer. 1993 Geochemistry of Lago Grande di Montichio, S. Italy. Lecture notes in Earth Sciences, 49. Springer, Berlin.

Sagri M., Atnafu B., Benvenutti M., Billi P., Carnicelli S., Dainelli N., Di Grazia S., Ferrari G.A., Iasio C., Kebede S. and Ventra D. 1999. Geomorphological Evolution of the Lake Region (Ethiopia) and Climatic Changes. In: Environmental background to Hominid evolution in Africa. Book of Abstracts. XV INQUA Congress, Durban, S. Africa. pp. 154-155.

Said R. 1993. The River Nile. Pergamon, Oxford. 320 pp.

Singer, A., 1984. The Paleoclimatic interpretation of clay minerals in sediments.Earth Science Reviews, 21 251-293

Street, F.A. (1979). The relative importance of climate and hydrological factors in influencing lake level fluctuations (abstract). In ''Symposium on 'sahara and surrounding seas- sediments and climatic changes'.'' Acadamy of Art and Sciences, Mainz, 1st-4th April 1979.

Street F. A. 1979a. Late Quaternary Lakes in the Ziway-Shalla Basin, southern Ethiopia. Cambridge University. 493 pp.

Street F.A. 1979b. Late Quaternary precipitation estimates for the Ziway-Shalla basin, Southern Ethiopia. Palaeoecology of Africa. 11: 135-143.

Street F.A. and Grove A.T. 1979. Global maps of lake-level fluctuations since 30,000 yr B.P. Quaternary Research. 12: 83-118.

Street-Perrott, F.A. and Perrott, R.A. 1990. Abrupt climate fluctuations in the tropics, the influence of Atlantic Ocean circulation. Nature. 343: 607-611

Smykatz-kloss, W.; Knabe, K.; Rögener, K.; Hüttle, C. And zöller, L. (1998): Paleoclimatic changes in central Sinia.- Paleoecology of Africa 25, 143-155.

Smykatz-kloss, W.; Roscher, B.; Knabe, K.; Rögener, K.; and zöller, L. (1998/2000): Wüsten forschung und Paläoklimatologie in zenteralen Sinia.- Chemie d. Erde 59, 245-258.

Smykatz-kloss, W.; Smykatz-kloss, B.; Naguib, N.; and zöller, L.(2000) The reconstruction of the paleoclimatological changes from mineralogical and geochemical composition of loess and alluvial loess profiles. Paleoecology of Quaternary drylands, Springer.

Suzuki, H., 1967. Some aspects of Ethiopian climates. Ethiopian Geographical Journal 5(2), 19-22.

Tegene, B., 1997. VAriablities of soil catena on degraded hill slopes of WAtiya catchment, Wolo, Ethiopia. SINET, EthiopiaJournal of Science 20, 151-175.

Tröels-Smith, J. 1955. Karakterisering of lØse jordarter Danmarks geologiske undersØgelse series IV. 3(10), 73 pp.

Telford R.J., Lamb H.F. and Mohammed M.U. 1999. Diatom derived paleoconductivity estimates for Lake Awassa, Ethiopia: evidence for pulsed inflow of saline ground water. Journal of Paleolimnology. 21: 409-421.

Tröels-Smith J. 1955karaketerisering af lØse jprdarter danmarks Geologiske UndersØgelse Service IV, 3(10), 73 pp.

Vallet-Coulomb C., Dagnachew Legesse, Gasse F., Travi Y. and Chernet T. 2001. Lake Evaporation estimates in tropical Africa from limited meteorological data. Journal of Hydrology. 245: 1-18.

Verschuren D., Laird K.R., and Cumming B.F. 2000. Rainfall and drought in equatorial East Africa during the past 1,100 years. Nature. 403: 410-414.

Virgo, K., Munro, R., 1978. Soil and erosion features of central Plateaue region of Tigrai, Ethiopia. Geoderm 20, 131-157.

Webb, P., and von Braun, J. 1994. Famine and Food security in Ethiopia: Lesson for Africa. Wiley, Chichester.

Williams, M., Bishope, P., Dakin, F., Gillispie, R., 1977. Late Quaternary lake levels in Southern Afar and the adjecent Ethiopia Rift. Nature 267, 690-693.

Williams, M., Adamson, D., 1980. Late Quaternary depositional historyof the Blue Nile and White Nile Rivers in central Sudan. In: Williams, M., Faure, H. (Eds.), The Sahara and the Nile Quaternary environments and Prehistoric Occupation in Northern Africa. Balkema, Rotterdam. Pp. 281-304.

Wright, H.E., Mann,. D.H. and Glasser, P.H. 1983: Piston corers for lakes and wetland sediments. Ecology 65, 657-659

Zewedu, E., Högber, P., 2000a. Reconstruction of forest site history in Ethiopian highlands based on ^{13}C natural abundance of sols. Ambio 29, 83-89.

Zanettin, B. and Justine-Visentin, E. 1974.The volcanic succession in central Ethiopia. 2.The volcanics of the western Afar and Ethiopian rift margins.- Mem. Ist. Geol.Miner.Univ.Padova, 33, Padova.

Zanettin, B., Justine-Visentin, E., Gregnanin, A., Mezzacasa, G., Piccirillo, E.M. 1975. New chemical analysis of the Tertiary Volcanics from the central Ethiopian Plateau.

Zanettin, B., Justine-Visentin, E., Piccirillo, E.M., 1977. Volcanic succession, tectonics and magmatology in central Ethiopia.

Zilifi, D. and Eagle, M. (2000). Nyanza Project 2000Annual Report.

Zimmer mann, H.B., 1977. Clay-mineral stratigraphy and distribution in the Southrtn Atlantic Ocean, In: P.R. Supko, K. Perch-Nielson et al., Initial Reports DSDP, 39. U.S.Gov.Print.off., Washington, DC pp. 395-405

Annex-A

				ANIONS				CATIONS			
Sample Name	Conductivity	Temperature	pH	Cl-	NO3-	PO4 3-	SO4 2-	Na+	K+	Mg2+	Ca2+
Inflows: N & NW Ashenge	(uS.cm-1)	(-C)		(meq/l)	(meq/l)	(meq/l)	(meq/l)	(meq/l)	(meq/l)	(meq/l)	(meq/l)
AW 02	614	-	7.2	0.264	0.221	0.063	0.325	0.823	0.146	7.999	12.571
AW 03: Plain (03AD6,)	657	-	8	0.071	0.232	0.008	0.370	1.009	0.000	2.405	3.323
AW 04 (03TD8,)	740	-	7.9	0.055	5.588	0.002	0.024	0.710	0.000	2.663	4.886
AW 05 (03TD9,)	577	-	8.6	0.246	0.379	0.003	0.123	0.590	0.038	3.291	2.104
AW 06 (03TD10,)	640	-	8.7	0.591	2.713	0.039	0.555	0.634	0.055	3.373	2.760
Inflows: S & SE Ashenge											
AW 08 (03TD16,)	664	-	8.3	0.355	0.825	0.016	0.283	0.965	0.039	2.690	2.570
AW 07 (g.w.)	607	-	7.3	0.141	1.704	0.002	0.067	0.767	0.010	1.866	3.428
Lake samples											
AW 01: 03AL1c (s.w.i.)	2535	-	-	2.081	1.425	0.030	6.747	14.420	0.827	44.836	23.341
AW 09 (03TD20 trawl,)	2135	-	-	2.417	2.037	0.005	1.879	13.013	0.450	11.122	0.182
AW 10 (03TD20 trawl,)	2098	-	-	2.447	5.883	0.006	1.950	13.204	0.362	11.299	0.536
AW 11 (03TD20 trawl,)	2106	-	-	2.424	0.403	0.006	1.906	13.295	0.388	11.603	0.206
AW 12 (03TD20 trawl,)	2085	-	-	2.464	0.374	0.009	1.950	13.033	0.488	11.470	0.203
AW 13 (03TD20 trawl,)	2092	-	-	2.370	2.702	0.005	1.923	13.631	0.471	11.967	0.197

Water samples	Long.	Lat.	Sampling locations
03AW01	12° 35.400' N	39° 13.415' E	Location of **03A1L**, from the sediment water interface, depth 13.5 m
03AW02	12° 35.870' N	39° 30.763' E	Walking west round lake, possibly a groundwater spring
03AW03	12° 36.060' N	39° 30.447' E	1st major inflow, Ashenge Plain
03AW04	12° 36.106' N	39° 30.113' E	Ashenge Plain, minor 'salty' inflow
03AW05	12° 35.934' N	39° 29.747' E	Ashenge Plain, 'just' flowing minor inflow
03AW06	12° 35.696' N	39° 29.478' E	Ashenge Plain, 2nd major inflow (possibly the larger)
03AW07	12° 34.084' N	39° 31.147' E	Groundwater sample from water pump
03AW08	12° 33.461' N	39° 29.966' E	Inflow 'spring?'
03AW09	12° 35.700' N	39° 30.674' E	Surface water transect into deeper area of lake
03AW10	12° 35.611' N	39° 30.505' E	Surface water transect into deeper area of lake
03AW11	12° 35.447' N	39° 30.326' E	Surface water transect into deeper area of lake
03AW12	12° 35.329' N	39° 30.220' E	Surface water transect into deeper area of lake
03AW13	12° 35.121' N	39° 30.055' E	Surface water transect into deeper area of lake

Annex-B

EASTING	NORTHING	DEPTH
1391046.0	556336.8	4.9
1391062.0	556333.1	5.6
1391064.0	556318.6	7.1
1391071.0	556300.5	8.1
1391081.0	556267.9	10.1
1391082.0	556248.0	12.0
1391092.0	556224.4	11.6
1391092.0	556208.1	12.4
1391093.0	556191.8	13.4
1391095.0	556173.7	13.7
1391095.0	556135.7	14.0
1391097.0	556099.5	14.8
1391099.0	556070.5	15.6
1391104.0	556043.4	16.0
1391117.0	555983.6	17.8
1391126.0	555913.0	18.0
1391151.0	555759.0	19.5
1391170.0	555628.6	18.1
1391184.0	555543.5	20.2
1391202.0	555462.0	20.5
1391215.0	555400.4	22.0
1391221.0	555338.9	22.7
1391219.0	555282.7	21.5
1391233.0	555203.1	22.5
1391235.0	555058.2	21.0
1391240.0	554994.8	20.0
1391251.0	554924.2	20.5
1391255.0	554786.6	20.1
1391255.0	554730.5	19.5
1391262.0	554676.2	20.0
1391267.0	554603.7	20.1
1391269.0	554542.2	20.5
1391271.0	554458.9	19.0
1391278.0	554288.7	18.5
1391283.0	554156.5	19.0
1391297.0	554042.4	18.4
1391307.0	553964.6	17.8
1391308.0	553870.4	17.5
1391345.0	553709.2	16.3
1391346.0	553640.4	15.3
1391363.0	553539.0	14.8
1391368.0	553491.9	14.8
1391388.0	553430.3	14.0
1391407.0	553368.7	13.5
1391419.0	553272.8	13.3
1391416.0	553146.0	13.1
1391427.0	553088.1	12.9
1391439.0	553006.6	12.0
1391454.0	552946.8	10.5
1391452.0	552890.7	8.9
1391450.0	552861.7	6.0

EASTING	NORTHING	DEPTH
1391448.0	552854.5	5.0
1391446.0	552827.3	6.5
1391444.0	552811.0	9.4
1391443.0	552802.0	0.0
1392443.0	553732.5	3.1
1392375.0	553729.0	3.4
1392336.0	553729.1	3.8
1392259.0	553723.8	4.5
1392198.0	553723.9	5.7
1392154.0	553718.6	6.1
1392089.0	553713.2	6.8
1391973.0	553711.7	8.6
1391883.0	553713.6	9.7
1391798.0	553719.2	10.7
1391669.0	553717.7	12.1
1391605.0	553716.0	13.1
1391540.0	553717.9	13.5
1391470.0	553718.0	14.2
1391387.0	553721.8	15.4
1391306.0	553722.0	15.4
1391225.0	553725.7	15.6
1391122.0	553720.5	16.6
1391028.0	553720.7	17.1
1390890.0	553720.9	18.1
1390755.0	553703.1	19.2
1390663.0	553676.1	18.4
1390572.0	553661.8	19.8
1390482.0	553638.4	19.0
1390353.0	553591.6	17.9
1390264.0	553562.8	17.4
1390202.0	553535.7	17.4
1390130.0	553528.6	17.3
1390060.0	553532.4	17.8
1391077.0	556282.4	9.0
1389957.0	553536.2	17.3
1389824.0	553543.7	16.4
1389750.0	553556.5	16.1
1389606.0	553567.6	16.4
1389525.0	553558.7	15.8
1389415.0	553560.8	14.7
1389310.0	553566.4	13.8
1389234.0	553553.8	12.8
1389079.0	553530.6	10.6
1389011.0	553516.2	9.3
1388915.0	553505.6	7.2
1388801.0	553536.6	5.9
1388736.0	553538.5	4.8

Annex-C

Element: **Monthly Total Rainfall**

Region: **Tigray**

Station: **Maychew**

Year	Jan	Feb	Mar	April	May	June	July	Aug	Sep	Oct	Nov	Dec	Total	Average	5 years moving avg
1953	-	-	-	-	63.9	6.8	252.3	242	89.1	7.5	5.1	62.5	729.2	91.15	
1954	0	37	56.5	9	71.4	19.6	283	336.2	136	36.8	0	14	999.5	83.29167	
1955	27.5	3.6	52.1	56.2	46	3.5	174.3	145.2	89	1.8	10	22.3	631.5	52.625	73.34167
1956	6.8	1	35.4	153.3	0	12.2	168.7	222.1	121.7	44	1.4	0	766.6	63.88333	65.415
1957	0	19.1	194.9	117.9	50.9	6.9	76.6	368.8	41.4	28.1	4.5	0	909.1	75.75833	63.72167
1958	17.1	23.4	19.3	116.5	12.3	24.7	207.6	160.5	16.1	13.1	1	6.6	618.2	51.51667	62.14
1959	0	38.3	47.8	10.4	51.5	10.2	335.3	231.7	96.2	56.9	16.2	3.4	897.9	74.825	64.08333
1960	11.1	9.7	58.4	51.7	119	-	-	-	-	-	-	18.4	268.3	44.71667	62.91167
1961	0	-	22.3	143.4	7.5	17.8	218.5	177.7	32.2	43	-	-	662.4	73.6	69.49583
1962	-	0	66.9	-	-	-	-	-	-	-	-		66.9	69.9	70.84083
1963	-	-	63	127.5	116.4	-	-	99.5	30.6	15	207.8	15.7	675.5	84.4375	76.01386
1964	0	54.8	46.4	58.7	36.7	36	336.7	170.9	92.2	52.6	38.5	55.1	978.6	81.55	67.77886
1965	0	34.1	58.3	122.1	4.9	-	60.2	232.8	109.3	98.1	41.6	15	776.4	70.58182	53.79886
1966	7.1	29.5	14	79.1	-	-	-	-	-	-	-	-	129.7	32.425	36.91136
1967															20.60136
1968															6.485
1969															6.742
1970															15.09629
1971	-	0	5	0.2	101.3	0	42.5.	83.8	-	69	8.8	69	337.1	33.71	26.18429
1972	-	-	-	-	-	34	95	71.5	28.9	25.2	33.3	4.5	292.4	41.77143	55.35229
1973	0	0	0	31.2	43	8.7	232.8	138.7	77	23	-	-	554.4	55.44	65.74229
1974	-	-	-	-	121.3	80.4	128.2	278.7	95	-	-		703.6	145.84	59.00029
1975	30.1	50.1	6.1	55.2	29.1	77.1	167.9	-	-	0	-		415.6	51.95	50.646
1976	0	-	-	-	-	-	-	-	-	-	-				58.683
1977	-	-	-	-	-	-	-	-	-	-	-				29.515
1978	-	-	-	-	28	203	149.5	2	-	-	-		382.5	95.625	33.30833
1979	-	-	-	-	-	-	-	-	-	-	-	-			38.40833
1980	0	92	-	156.5	27.5	-	71.5	-	-	78	-		425.5	70.91667	49.19583
1981	0	0	25.5	-	-	-	-	-	-	-	-	0	25.5	25.5	30.07083

1982	-	149.5	-	52.5	60.5	6	13.5	132	17	0	0	0.5	431.5	53.9375	30.07083
1983															15.8875
1984															10.7875
1985															0
1986															0
1987															0
1988															0
1989															0
1990															15.848
1991															27.12967
1992	-	-	56.2	19.9	102.8	0.9	144.2	250.9	50.2	53	48.8	65.5	792.4	79.24	42.61148
1993	41.2	35.1	75.9	135.2	125.5	3	57.5	125.6	33.7	42.9	0	1.3	676.9	56.40833	57.30648
1994	0	-	53.4	83.6	42.2	28.9	234.1	311.3	68.7	5	20	4.3	851.5	77.40909	73.22148
1995	0	59.7	26.6	122.7	72.8	21.2	252.3	195.6	54.1	15.7	0	61	881.7	73.475	71.21348
1996	8.8	1.2	123.5	146.4	141.2	66.6	117.2	246.5	42.1	4.1	57.3	0	954.9	79.575	74.70182
1997	15.8	0	51.7	59.3	38.4	83.8	166.5	64.2	63.8	206.1	80.8	0	830.4	69.2	71.34167
1998	65.1	33.3	35	39.4	116.5	-	-	214.8	223.5	10.9	0	0	738.5	73.85	71.73833
1999	45.4	0	10.8	22.3	15.9	12.7	176.7	253.5	77.8	109.9	0.4	1.9	727.3	60.60833	68.82667
2000	0	0	5.9	17.7	65.1	12	195.8	194.4	126.7	151.3	61.7	74.9	905.5	75.45833	65.815
2001	0	2	92.9	9.2	34.5	26.2	212.2	283.2	83.7	25.3	0	11	780.2	65.01667	63.57833
2002	83.7	0	34.3	67.5	40.9	21.6	67.4	188.6	92.9	19.3	0	33.5	649.7	54.14167	51.45667
2003	24.4	38.2	93	193.6	13.1	13.7							376	62.66667	36.365
Total															23.36167
Average															12.53333

Element: ***Mean Max Temperature***

Region: ***Tigray***

Station: ***Maychew***

Year	Jan	Feb	Mar	Apr	May	June	July	Aug	Sep	Oct	Nov	Dec	Annual average
1953	-	-	-	-	27.7	29.4	22.2	24.7	25.5	26.1	26.2	22.1	25.4875
1954	25.5	26.5	26.7	-	28.1	29.6	23.3	23.7	26.1	25.4	25.8	24.6	25.825
1955	23.7	26.3	26.8	27.1	29.5	29.4	27.2	25.8	25.1	27.4	28.2	26.7	27.4125
1956	24.7	27.4	28	25.2	-	29.7	25.4	24.5	26.7	25	24.9	25.7	25.98571
1957	25.4	23.8	23.8	27.2	30.3	32.6	28	25.6	27.1	27.8	26.9	26.9	28.15
1958	25.1	24.3	26.9	27.3	32.1	30.7	25.7	26.2	27.1	27.4	27.2	24.9	27.6625
1959	25.6	25.8	24.5	28.2	30.1	30	25.5	25.7	25.8	24.3	24.4	23.7	26.1875
1960	23.9	25.2	25	28.4	30.4	-	-	-	-	-	-	19.7	25.05
1961	21.7	-	21.7	22.1	25.6	25.8	21.2	20.8	23.5	22.6	-	-	23.25
1962	-	22.2	22.9	-	-	-	-	-	-	-	-	-	22.55
1963	-	-	23.1	21.6	23.3	-	-	23.6	24	23.2	19.5	18	21.93333
1964	-	20.1	23.1	22.6	25.1	24.7	21.8	22.3	22.3	20.2	20.7	18.1	21.9
1965	20	20.8	22.5	22	25.2	-	25.6	22.8	23.2	21.6	21.6	21.8	23.11429
1966	21.7		23.3	23.7	-	-	-	-	-	-	-	-	22.9
1967	-	-	-	-	-	-	-	-	-	-	-	-	-
1968	-	-	-	-	-	-	-	-	-	-	-	-	-
1969	-	-	-	-	-	-	-	-	-	-	-	-	-
1970	-	-	-	-	-	-	-	-	-	-	-	-	-
1971	-	-	-	-	-	-	-	-	-	-	-	-	-
1972	-	-	-	-	-	20	22.7	22.9	23.2	21.7	20.2	20.3	21.57143
1973	21.1	23	24.6	25	24.4	25.6	22.2	22.5	22.9	20.6	-	-	23.03333
1974	-	-	-	-	20.5	20.8	20.4	-	20.4	-	-	-	20.525
1975	-	19.6	22.5	21.4	23.7	23.3	21.9	-	-	20.1	-	-	22.25
1976	20.5	-	-	-	-	-	-	-	-	-	-	-	-
1977	-	-	-	-	-	-	-	-	-	-	-	-	-
1978	-	-	-	-	-	-	-	-	-	-	-	-	-
1979	-	-	-	-	-	-	-	-	-	-	-	-	-
1980	20	19.9	-	22.7	26.2	25.7	22.9	-	-	20.6	20.8	20.8	22.83333
1981	21	21.8	19.7	20.9	23.8	26.4	23	23.4	-	-	-	20.4	23.4

1982	-	21.7	-	21.9	23.6	27.7	28.3	26.9	24.9	25.3	25.4	25.3	25.925
1983	-	-	26	26.2	27	27.1	-	-	-	-	25.2	23.9	25.8
1984	24.1	24.5	26.1	27	25.7	25.8	25.3	24.8	25.1	18.6	15.6	13.8	21.8375
1985	-	-	-	-	-	-	-	-	-	-	-	-	-
1986	-	-	-	-	-	-	-	-	-	-	-	-	-
1987	-	-	-	-	-	-	-	-	-	-	-	-	-
1988	-	-	-	-	-	-	-	-	-	-	-	-	-
1989	-	-	-	-	-	-	-	-	-	-	-	-	-
1990	-	-	-	-	-	-	-	-	-	-	-	-	-
1991	-	-	-	-	-	-	-	-	-	-	-	-	-
1992	-	-	22	23.1	23.7	25.7	23.3	21.8	21.5	19.6	18.1	17.7	21.425
1993	16.6	17.5	20.5	19.5	21.7	25.2	22.7	23.8	23.2	20.8	20.6	20.3	22.2875
1994	20.4	-	21	23	24.2	24.7	21	20.9	20.9	21.1	20.1	19.6	21.5625
1995	20.5	20.8	21.7	21.9	23.4	26.4	23.2	22	22.5	22	21.3	19.6	22.55
1996	19	21.4	21.8	22.1	22.2	23.1	22.4	22.4	23.2	21.7	19.5	18.4	21.6125
1997	19.1	21.1	22.2	23.4	24.4	24.9	22.5	22.4	24.2	20.3	19.1	-	22.54286
1998	18.9	19.6	22.1	24.4	-	-	-	21.4	22.4	21.2	20.7	20.2	21.18
1999	19.2	22.8	22	24.3	25.8	26.9	20.8	21.4	22	20.1	20.8	19.2	22.125
2000	20.5	21.8	23	22.9	25.1	26.4	22.8	21.9	22.1	20.3	19.4	18.5	22.0625
2001	18.5	21.1	20.7	22.9	-	-	-	-	-	-	-	-	20.8
2002	-	-	24.1	23.6	25.8	25.4	25.2	23	21.8	21.8	21.1	19.3	22.925
Average	21.52917	22.45833	23.3897	23.8483	25.5889	26.292	23.627	23.3	23.648	22.3346	21.963	21.096	

SUMMARY OF HYDROMETRIC DISCHARGE DATA

STATION:- **L.Ashenge** | STATION No.:- **020001**

BASIN:-**DENAKIL** | Co-Ordinate:-

DRAINAGE AREA, Km^2:- | MEAN ELEVATION, **m.a.s.l.:2250**

YEAR	*	JAN	FEB	MAR	APR	MAY	JUN	JUL	AUG	SEP	OCT	NOV	DEC
	I							0.980	1.100	1.550	1.850	0.750	
1975	II		1.450	1.390	1.300			0.910	0.910	1.190	1.550	1.750	1.620
	III		1.400	1.300	1.230			1.180	1.330	1.490	1.440	1.400	1.320
1976	I	1.510	1.440	1.400	1.350	1.330	1.150	1.200	1.460	1.510	1.470	1.420	1.360
	II	1.540	1.460	1.410	1.370	1.350	1.280	1.000	1.200	1.460	1.380	1.370	1.300
	III	1.460	1.420	1.380	1.340	1.280	1.000	0.850	1.160	1.470	1.510	1.610	1.550
1977	I	1.290	1.220	1.130	1.000	1.000	0.870	1.000	1.420	1.500	1.630	1.640	1.580
	II	1.320	1.290	1.180	1.070	1.000	0.960	0.800	1.000	1.420	1.490	1.580	1.510
	III	1.270	1.180	1.070	0.950	0.960	0.800	1.080	1.270	1.260	1.170	1.090	1.050
1978	I	1.470	1.370	1.330	1.270	1.200	1.010	1.180	1.320	1.300	1.220	1.100	1.070
	II	1.510	1.410	1.360	1.320	1.260	1.090	1.010	1.180	1.230	1.100	1.070	1.020
	III	1.420	1.340	1.320	1.250	1.000	0.920	0.770	0.940			0.980	0.880
1979	I	1.010	1.000	0.900	0.840	0.800	0.830	0.840	1.000			1.000	0.940
	II	1.040	1.040	0.940	0.880	0.890	0.880	0.740	0.850			0.940	0.840
	III	1.000	0.940	0.880	0.770	0.770	0.780	0.140	0.140	0.100			
1980	I	0.790	0.730	0.700	0.590	0.350	0.220	0.170	0.170	0.110			
	II	0.830	0.740	0.730	0.640	0.460	0.270	0.120	0.100	0.080			
	III	0.740	0.720	0.640	0.460	0.280	0.180						
1982	I	0.290	0.240	0.240	0.140	0.060							
	II	0.300	0.260	0.230	0.160	0.100							
	III	0.260	0.220	0.150	0.100	0.020							0.82
1991	I												0.85
	II												

	III												0.78
1992	I	0.74	0.68	0.59	0.48	0.4	0.24	0.1	0.34	0.7	0.73	0.68	0.64
	II	0.78	0.71	0.64	0.54	0.45	0.33	0.15	0.58	0.73	0.75	0.7	0.66
	III	0.71	0.64	0.55	0.42	0.33	0.17	0.05	0.13	0.6	0.71	0.65	0.63
1993	I	0.63	0.57	0.51	0.6	0.68			0.74	0.86	0.82	0.7	0.58
	II	0.66	0.6	0.54	0.66	0.7			0.78	0.89	0.85	0.77	0.64
	III	0.6	0.54	0.44	0.5	0.66			0.7	0.85	0.77	0.64	0.54
1994	I	0.48	0.38	0.28	0.18	0.11	0	0	0.5	0.98	1	1	0.99
	II	0.54	0.43	0.32	0.23	0.16	0.02	0.1	0.94	1	1	1	1
	III	0.43	0.33	0.23	0.16	0.03	0	0	0.12	0.98	1	1	0.96
1995	I	0.94	0.86	0.82	0.78	0.76	0.65	0.53	0.89	1			
	II	0.96	0.88	0.86	0.81	0.79	0.75	0.69	1	1			
	III	0.89	0.84	0.78	0.76	0.75	0.6	0.48	0.59	1			
1997	I							1.81					
	II							1.87					
	III							1.71					
1998	I			2.14	2.06	2.04	1.9	1.88	2.55	3.2	3.28	3.24	3.17
	II			2.17	2.1	2.07	1.98	2.06	2.88	3.3	3.3	3.28	3.21
	III			2.11	2.04	1.98	1.83	1.8	2.13	2.96	3.27	3.21	3.14
1999	I	3.14	3.1	3.04	2.94	2.88	2.77	2.8	3.07	3.51	3.53	3.39	3.3
	II	3.14	3.12	3.07	3	2.91	2.82	2.86	3.41	3.54	3.56	3.54	3.33
	III	3.12	3.07	3	2.9	2.83	2.72	2.72	2.86	3.44	3.52	3.34	3.27
2000	I	3.23	3.14	3.01	2.89	2.93	2.8	2.84	3.64	3.92	3.98	3.98	3.93
	II	3.27	3.19	3.07	2.93	2.98	2.88	3.15	3.88	3.98	3.99	4	3.99
	III	3.2	3.07	2.94	2.86	2.88	2.74	2.74	3.22	3.87	3.98	3.96	3.95
2001	I	3.96	3.91	3.86	3.86	3.79	3.69	3.74	4.26	4.72	4.71	4.65	4.57
	II	3.98	3.94	3.91	3.90	3.82	3.74	3.95	4.65	4.75	4.74	4.69	4.60
	III	3.94	3.87	3.85	3.82	3.75	3.65	3.67	3.95	4.68	4.69	4.60	4.54

Note:- **I:** Monthly average water level reading, **II:** Maximum water level reading, **III:** Minimum water level reading

Annex-E

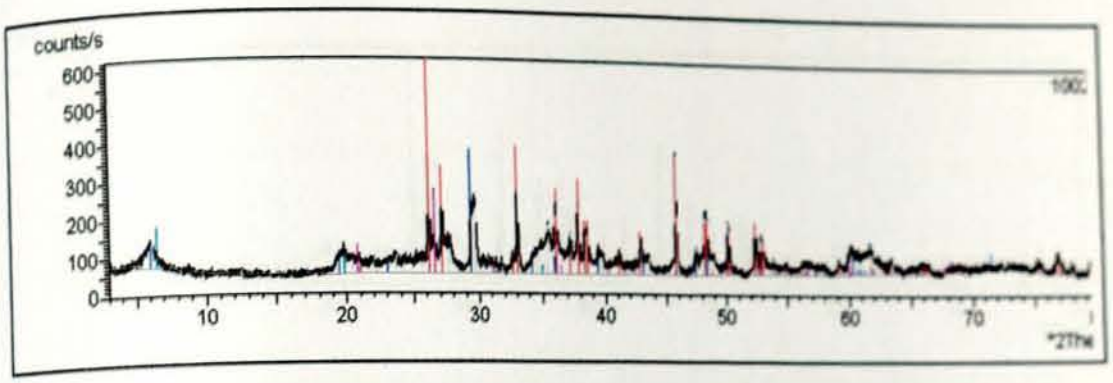

A	-	+	Name	Formula	Score	Score * Rel	Rel. Score	Scale Factor	Displacement	Reference Code	Line Type
✔			Aragonite	CaCO3	37.97	23.63	0.62	174.0	-98	41-1475	
✔			Quartz, low	SiO2	10.96	4.81	0.44	69.0	-68	85-0490	
✔			CALCITE	CaCO3	8.97	3.22	0.36	100.0	15	77-141	
✔			Montmorillonite-15A	Na0.3(Al,Mg)2Si4O10(OH)2l4H2	1.90	0.60	0.32	33.0	-59	29-1498	
✔		✔	Nontronite?	2(Mg,Fe)Ol(Fe,Al)2O3l5H2O	0.20	0.01	0.03	23.0	110	12-0222	

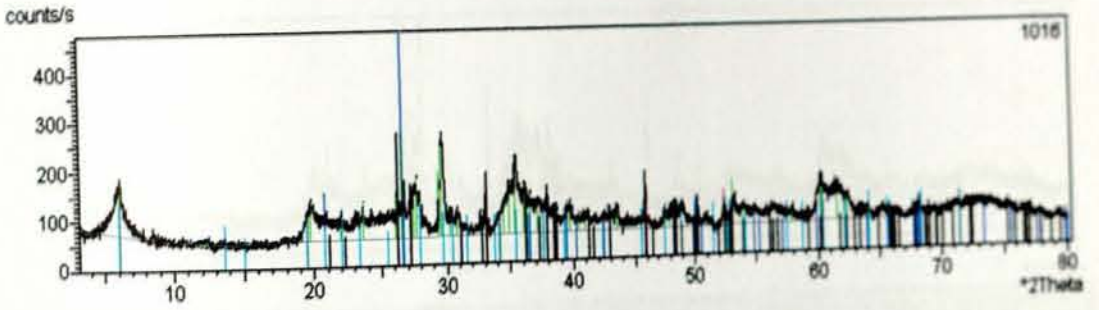

A	-	+	Name	Formula	Score	Score * Rel	Rel. Score	Scale Factor	Displacement	Reference Code	Line Type	Line Col
✔			Aragonit	CaCO3	16.97	11.07	0.65	69.0	-92	77- 17		
✔			ALPHA QUARTZ	SiO2	15.06	9.07	0.60	209.0	10	77-135		
✔			Orthoclase	KAlSi3O8	9.45	2.79	0.30	33.0	-123	09-0462		
✔		✔	Nontronite?	2(Mg,Fe)Ol(Fe,Al)2O3l5H2O	0.56	0.05	0.09	28.0	93	12-0222		
			Aragonite	CaCO3	33.23	18.10	0.54	100.0	-27	41-1475		

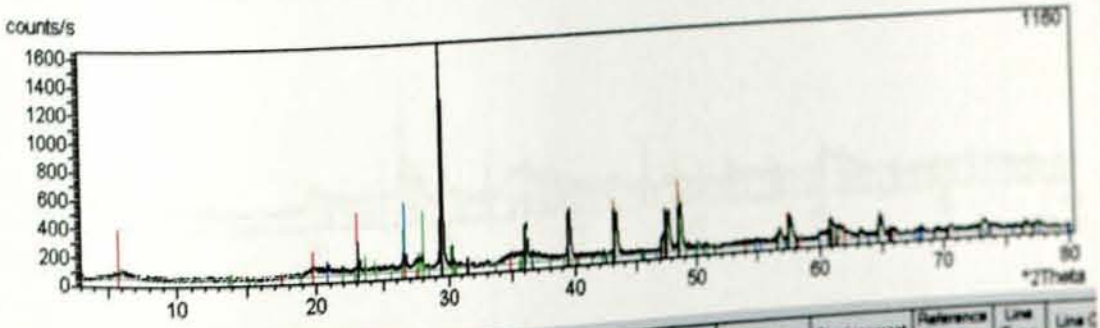

A	-	+	Name	Formula	Score	Score * Rel	Rel. Score	Scale Factor	Displacement	Reference Code	Line Type	Line C
✔			Calcite	CaCO3	14.69	11.98	0.82	100.0	123	24-0027		
✔			ALPHA QUARTZ	SiO2	16.96	11.50	0.68	33.0	10	77-135		
✔			Albite, disordered	Na(Si3Al)O8	6.10	0.88	0.15	28.0	-40	10-0393		
✔		✔	Montmorillonit,trock	Ca.24Na.01Mg.36Fe.02	2.13	0.45	0.21	23.0	41	77- 29		
			CALCITE	CaCO3	18.95	14.37	0.76	120.0	208	77-141		

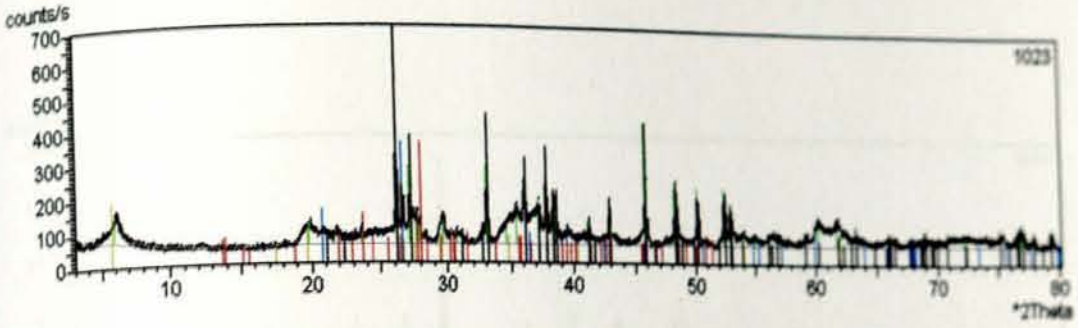

A	-	+	Name	Formula	Score	Score * Rel.	Rel. Score	Scale Factor	Displacement	Reference Code	Line Type	Line
✔			Aragonite	CaCO3	39,77	25,93	0,65	174,0	-65	41-1475		
✔			Quartz, low	SiO2	11,50	5,29	0,46	83,0	15	05-0490		
✔			Albite, disordered	Na(Si3Al)O8	5,57	0,74	0,13	83,0	-80	10-0393		
✔		✔	Montmorillonit,trock	Ca.24Na.01Mg.36Fe.02	1,54	0,24	0,15	33,0	206	??- 20		
			Aragonite, syn	CaCO3	28,06	21,88	0,78	145,0	-93	05-0453		

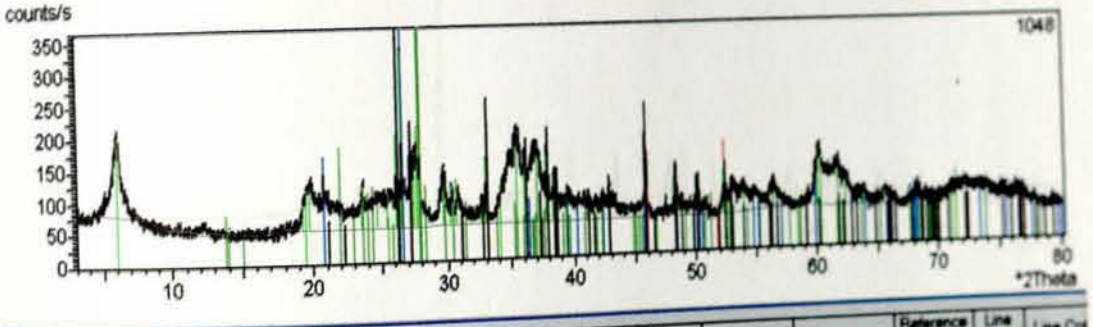

A	-	+	Name	Formula	Score	Score * Rel.	Rel. Score	Scale Factor	Displacement	Reference Code	Line Type	Line Col
✔			Aragonit	CaCO3	18,96	13,83	0,73	83,0	-160	??- 17		
✔			Quartz, low	SiO2	13,72	7,53	0,55	120,0	-23	05-0490		
✔			Albite, calcian, ordered	(Na,Ca)Al(Si,Al)3O8	17,20	4,48	0,26	174,0	-118	41-1480		
✔		✔	Nontronite?	2(Mg,Fe)Ol(Fe,Al)2O3l5H2O	1,84	0,57	0,31	28,0	15	12-0222		
			Aragonite	CaCO3	36,22	21,50	0,59	120,0	-83	41-1475		

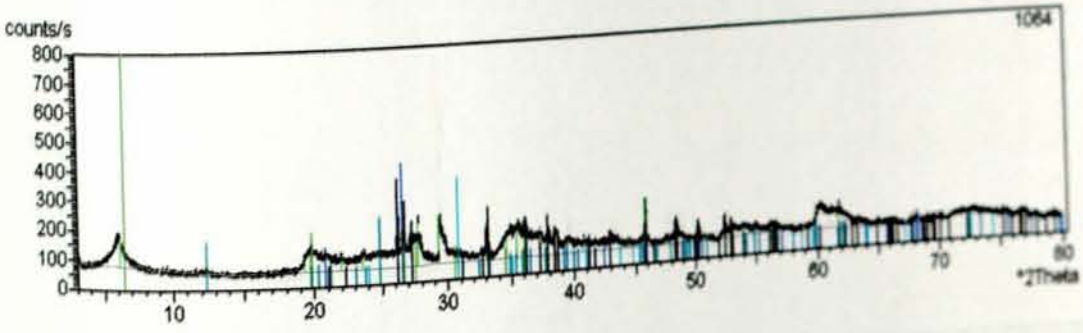

A	-	+	Name	Formula	Score	Score * Rel.	Rel. Score	Scale Factor	Displacement	Reference Code	Line Type	Line
✔			Aragonite	CaCO3	34,25	19,23	0,56	120,0	-40	41-1475		
✔			ALPHA QUARTZ	SiO2	11,91	5,68	0,48	145,0	18	??- 135		
✔			Dolomite, ferroan	Ca(Mg,Fe)(CO3)2	8,59	3,08	0,36	120,0	-177	34-0517		
✔			Kaolin	Al2Si2O5(OH)4	7,21	1,73	0,24	68,0	27	??- 14		
✔			Montmorillonite-14A	Na0.3(Al,Mg)2Si4O10(OH)2bH2	2,81	1,13	0,40	302,0	-12	13-0259		

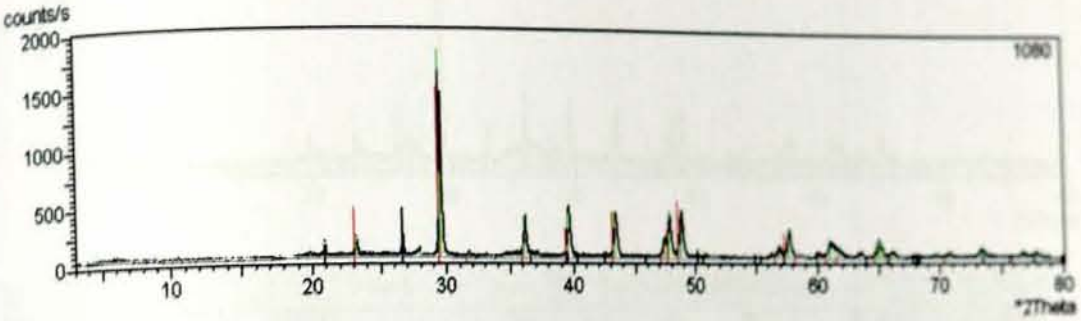

A	-	+	Name	Formula	Score	Score * Rel.	Rel. Score	Scale Factor	Displacement	Reference Code	Line Type	Line
✔			ALPHA QUARTZ	SiO2	14.79	8.75	0.59	23.0	30	??-135		
✔			Calcite	CaCO3	12.46	8.63	0.69	83.0	259	24-0027		
			ALPHA QUARTZ	SiO2	14.79	8.75	0.59	23.0	30	??-127		
			ALPHA QUARTZ	SiO2	14.79	8.75	0.59	23.0	30	??- 2		
			Quartz, syn	SiO2	14.68	8.62	0.59	23.0	76	33-1161		

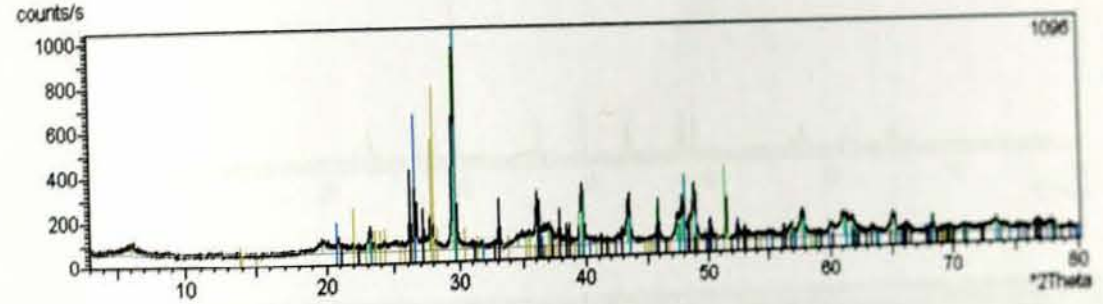

A	-	+	Name	Formula	Score	Score * Rel.	Rel. Score	Scale Factor	Displacement	Reference Code	Line Type	Line
✔			Aragonite	CaCO3	37.09	22.56	0.61	40.0	-30	41-1475		
✔		✔	Calcite, magnesian	(Ca,Mg)CO3	17.25	12.41	0.72	120.0	-259	43-0697		
✔			ALPHA QUARTZ	SiO2	14.54	8.45	0.58	69.0	10	??-135		
✔			Albite, calcian, ordered	(Na,Ca)Al(Si,Al)3O8	12.94	2.54	0.20	83.0	-79	41-1480		
			Aragonite, syn	CaCO3	24.34	16.46	0.68	33.0	-60	05-0453		

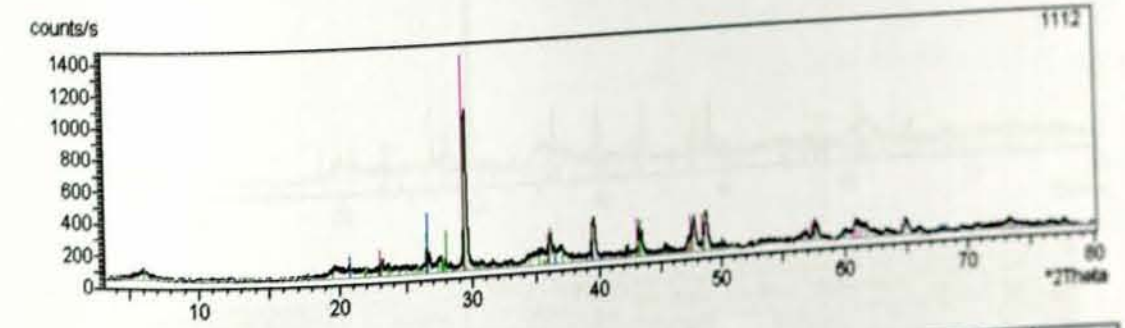

-	+	Name	Formula	Score	Score * Rel.	Rel. Score	Scale Factor	Displacement	Reference Code	Line Type	Line Col
		CALCITE	CaCO3	15.56	9.68	0.62	145.0	256	??-141		
		Quartz, low	SiO2	14.90	8.88	0.60	40.0	-60	05-0490		
		Albite, disordered	Na(Si3Al)O8	5.00	0.59	0.12	28.0	-195	10-0393		
		CALCITE	CaCO3	15.56	9.68	0.62	145.0	256	??-133		
		CALCITE	CaCO3	15.56	9.68	0.62	145.0	256	??- 8		

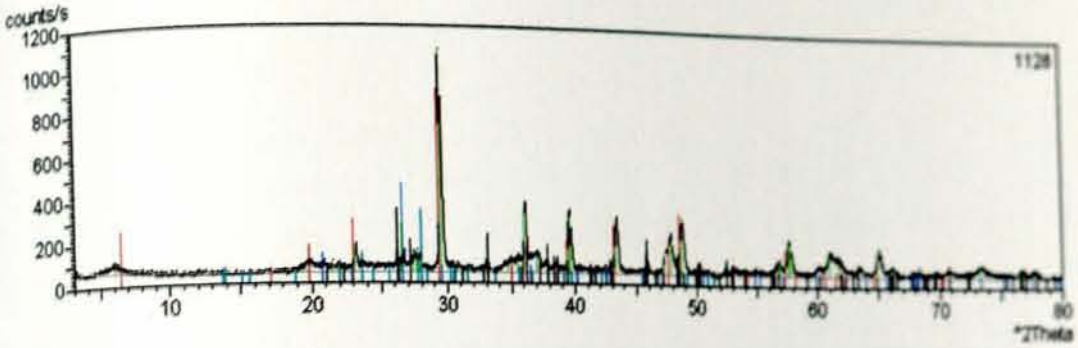

A	-	+	Name	Formula	Score	Score * Rel.	Rel. Score	Scale Factor	Displacement	Reference Code	Line Type	Line Col
✔			Aragonite	CaCO3	29,80	14,56	0,49	26,0	-85	41-1475		
✔			Calcite	CaCO3	12,07	8,09	0,67	83,0	231	24-0027		
✔			ALPHA QUARTZ	SiO2	13,59	7,39	0,54	40,0	18	77-1 35		
✔			Albite, disordered	Na(Si3Al)O8	6,30	0,94	0,15	28,0	-118	10-0393		
✔			Montmorillonite-15A	Na0.3(Al,Mg)2Si4O10(OH)2[4H2	0,33	0,02	0,05	19,0	-263	29-1498		

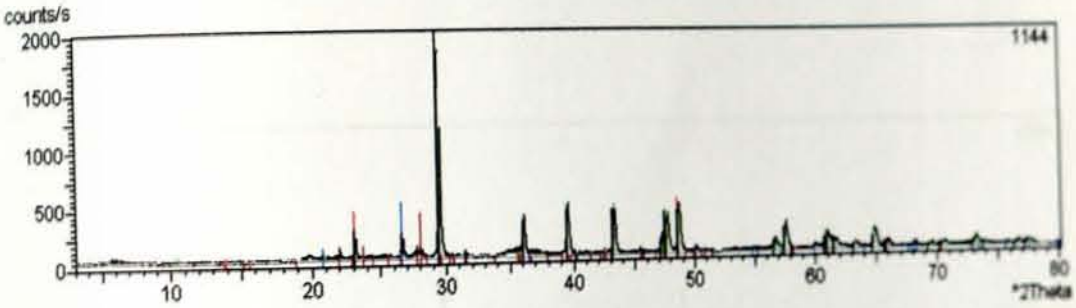

A	-	+	Name	Formula	Score	Score * Rel.	Rel. Score	Scale Factor	Displacement	Reference Code	Line Type	Line
✔			Calcite	CaCO3	14,56	11,77	0,81	83,0	177	24-0027		
✔			ALPHA QUARTZ	SiO2	16,59	11,01	0,66	28,0	15	77-1 35		
✔			Albite, disordered	Na(Si3Al)O8	5,42	0,70	0,13	23,0	-27	10-0393		

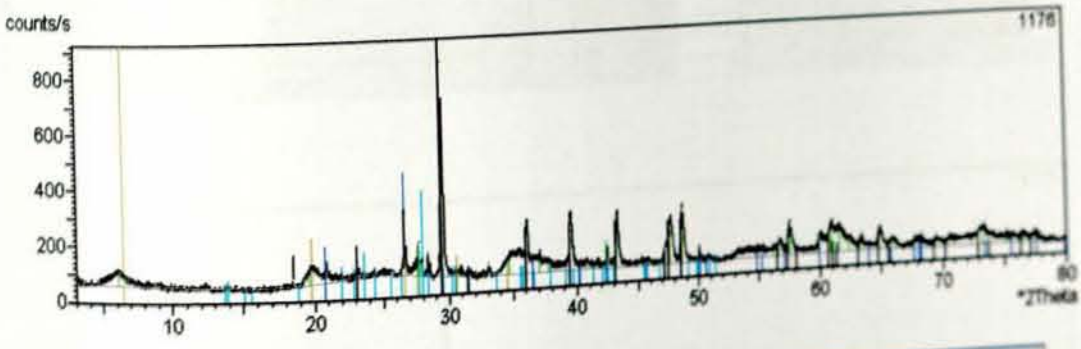

A	-	+	Name	Formula	Score	Score * Rel.	Rel. Score	Scale Factor	Displacement	Reference Code	Line Type	Line
✔			CALCITE	CaCO3	17,58	12,50	0,71	120,0	208	71-141		
✔			Quartz, low	SiO2	16,67	11,12	0,67	48,0	10	85-0490		
✔			Albite, disordered	Na(Si3Al)O8	6,66	1,06	0,16	40,0	-115	10-0393		
✔		✔	Montmorillonite-14A	Na0.3(Al,Mg)2Si4O10(OH)2bH2	1,43	0,29	0,20	120,0	-62	13-0259		
			CALCITE	CaCO3	17,68	12,50	0,71	120,0	208	71-133		

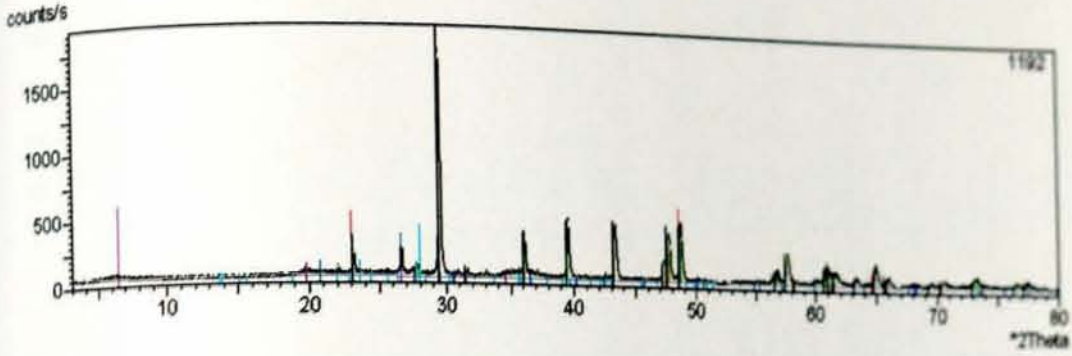

A	-	+	Name	Formula	Score	Score * Rel.	Rel. Score	Scale Factor	Displacement	Reference Code	Line Type	Line Col
✔			Calcite	CaCO3	13,75	10,50	0,76	100,0	177	24-0027		
✔			Quartz, low	SiO2	15,83	10,02	0,63	19,0	70	05-0490		
✔			Montmorillonite-14A	Na0.3(Al,Mg)2Si4O10(OH)2xH2	2,06	0,60	0,29	33,0	-16	13-0259		
✔			Albite, disordered	Na(Si3Al)O8	3,56	0,30	0,08	23,0	-62	10-0393		

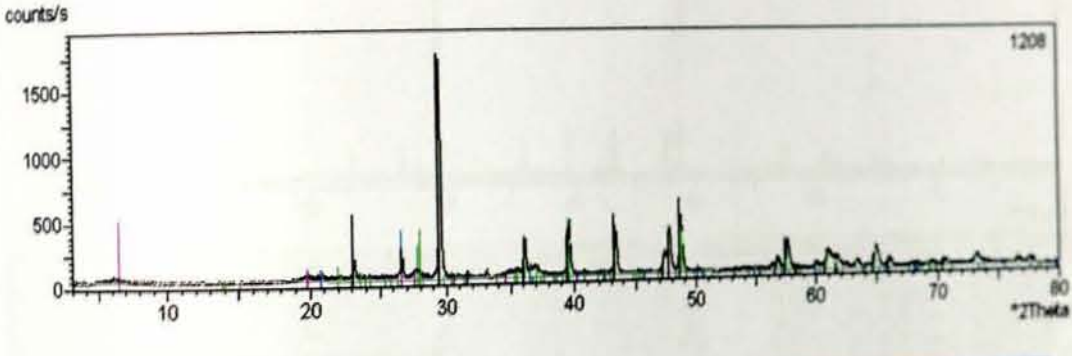

A	-	+	Name	Formula	Score	Score * Rel.	Rel. Score	Scale Factor	Displacement	Reference Code	Line Type	Line Col
✔			Calcite	CaCO3	14,70	12,00	0,82	100,0	206	24-0027		
✔			Quartz, syn	SiO2	14,64	8,58	0,59	23,0	35	33-1161		
✔			Albite, calcian, ordered	(Na,Ca)Al(Si,Al)3O8	14,84	3,34	0,22	23,0	123	41-1480		
✔			Montmorillonite-14A	Na0.3(Al,Mg)2Si4O10(OH)2xH2	2,65	1,00	0,38	28,0	-12	13-0259		
			Calcit	CaCO3	13,79	11,18	0,81	100,0	258	71- 48		

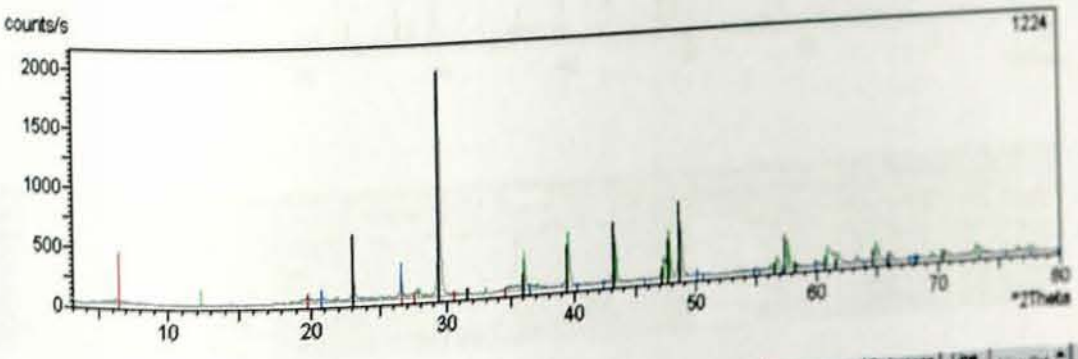

-	+	Name	Formula	Score	Score * Rel.	Rel. Score	Scale Factor	Displacement	Reference Code	Line Type	Line Col
		Calcite	CaCO3	13,61	10,29	0,76	100,0	241	24-0027		
		Quartz, low	SiO2	14,01	7,85	0,56	16,0	23	05-0490		
		Montmorillonite-14A	Na0.3(Al,Mg)2Si4O10(OH)2xH2	0,24	0,01	0,03	23,0	-14	13-0259		

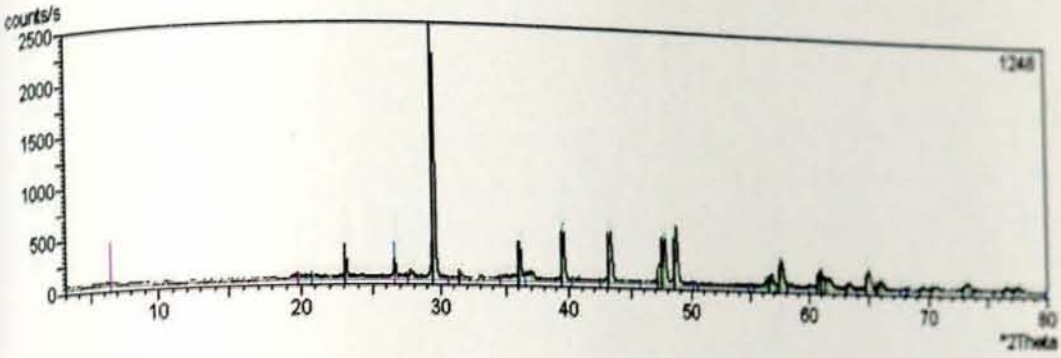

A	-	+	Name	Formula	Score	Score * Rel.	Rel. Score	Scale Factor	Displacement	Reference Code	Line Type	Line Co
✔			CALCITE	CaCO3	18.93	14.33	0.76	120.0	259	77-141		
✔			Quartz, syn	SiO2	14.56	8.48	0.58	16.0	27	33-1161		
✔			Montmorillonite-14A	Na0.3(Al,Mg)2Si4O10(OH)2bxH2	2.36	0.79	0.34	19.0	-16	13-0259		

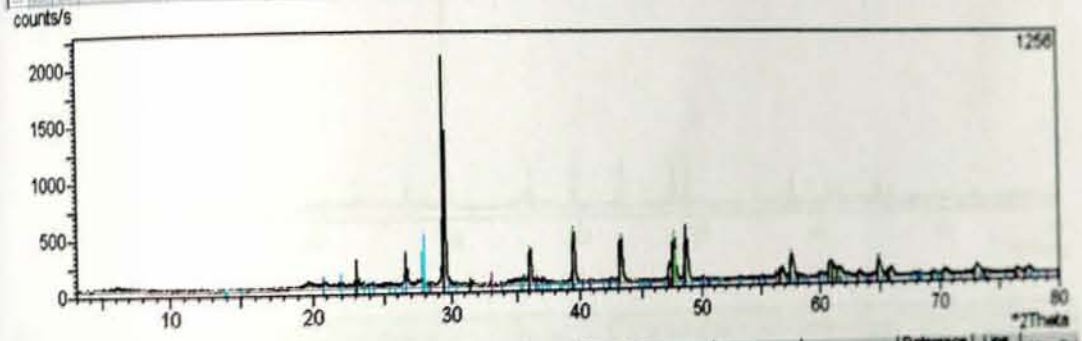

A	-	+	Name	Formula	Score	Score * Rel.	Rel. Score	Scale Factor	Displacement	Reference Code	Line Type	Line Co
✔			CALCITE	CaCO3	20.62	17.01	0.82	100.0	206	77-141		
✔			Quartz, low	SiO2	17.55	12.31	0.70	16.0	10	05-0490		
✔			Pyrite	FeS2	9.59	6.14	0.64	6.0	-90	42-1340		
✔			Albite, calcian, ordered	(Na,Ca)Al(Si,Al)3O8	12.46	2.35	0.19	23.0	30	41-1480		
			CALCITE	CaCO3	20.62	17.01	0.82	100.0	206	77-133		

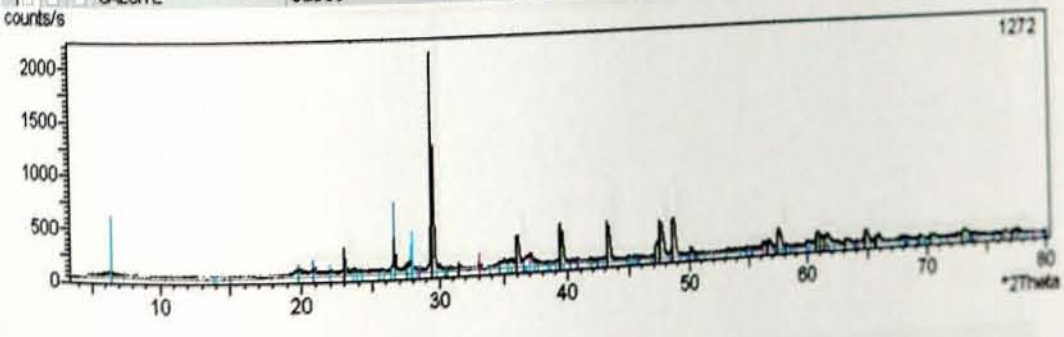

A	-	+	Name	Formula	Score	Score * Rel.	Rel. Score	Scale Factor	Displacement	Reference Code	Line Type	Line C
✔			CALCITE	CaCO3	18.76	14.08	0.75	145.0	208	77-141		
✔			Quartz, syn	SiO2	14.62	8.55	0.58	48.0	43	33-1161		
✔			Pyrite	FeS2	10.58	7.46	0.71	11.0	-48	42-1340		
✔			Albite, calcian, ordered	(Na,Ca)Al(Si,Al)3O8	14.94	3.38	0.23	28.0	58	41-1480		
✔			Montmorillonite-14A	Na0.3(Al,Mg)2Si4O10(OH)2bxH2	2.66	1.01	0.38	40.0	-57	13-0259		

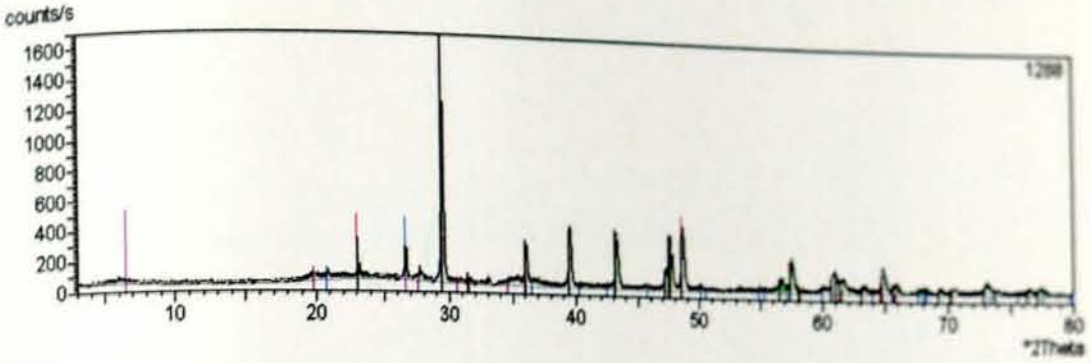

A	-	+	Name	Formula	Score	Score * Rel	Rel. Score	Scale Factor	Displacement	Reference Code	Line Type	Line Col...
✔			Calcite	CaCO3	15.10	12.67	0.84	100.0	110	24-0027		
✔			Quartz, syn	SiO2	14.98	8.97	0.60	28.0	-27	33-1161		
✔			Montmorillonite-14A	Na0.3(Al,Mg)2Si4O10(OH)2xH2	0.94	0.13	0.13	33.0	-65	13-0259		

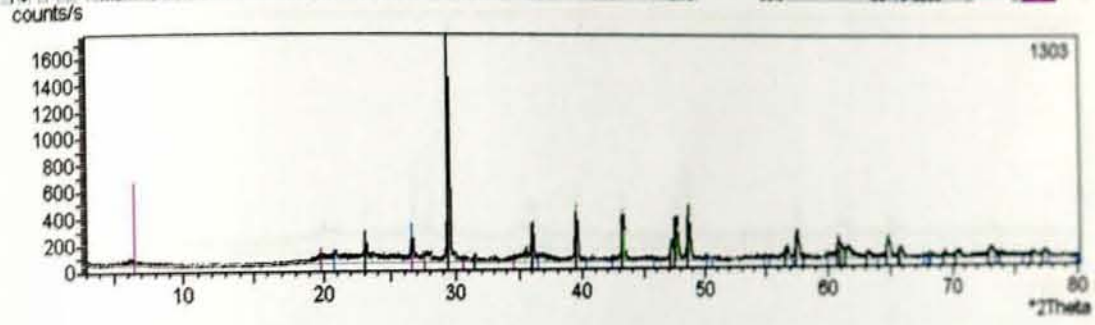

A	-	+	Name	Formula	Score	Score * Rel	Rel. Score	Scale Factor	Displacement	Reference Code	Line Type	Line Col
✔			CALCITE	CaCO3	21.09	17.78	0.84	120.0	145	77-1141		
✔			Quartz, low	SiO2	12.93	6.69	0.52	19.0	18	85-0490		
✔			Montmorillonite-14A	Na0.3(Al,Mg)2Si4O10(OH)2xH2	2.06	0.60	0.29	40.0	-48	13-0259		

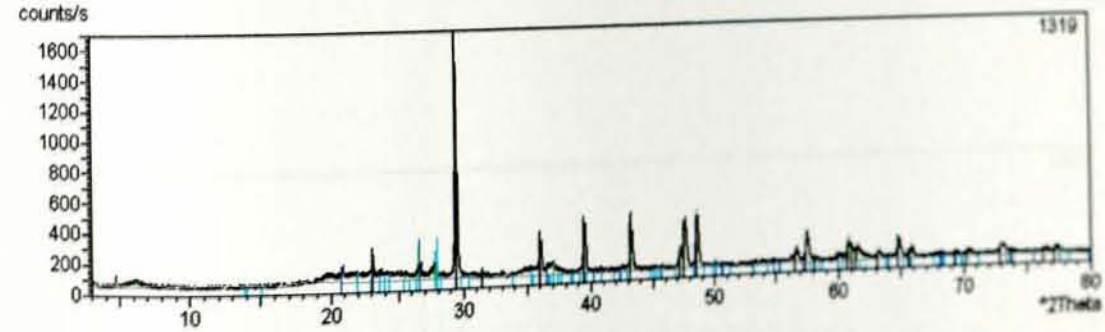

A	-	+	Name	Formula	Score	Score * Rel	Rel. Score	Scale Factor	Displacement	Reference Code	Line Type	Line Cl
✔			CALCITE	CaCO3	20.65	17.05	0.83	120.0	143	77-141		
✔			Quartz, low	SiO2	12.77	6.52	0.51	19.0	-17	85-0490		
✔			Albite, calcian, ordered	(Na,Ca)Al(Si,Al)3O8	12.71	2.45	0.19	19.0	-115	41-1480		
			CALCITE	CaCO3	20.65	17.05	0.83	120.0	143	77-133		
			CALCITE	CaCO3	20.65	17.05	0.83	120.0	143	77-8		

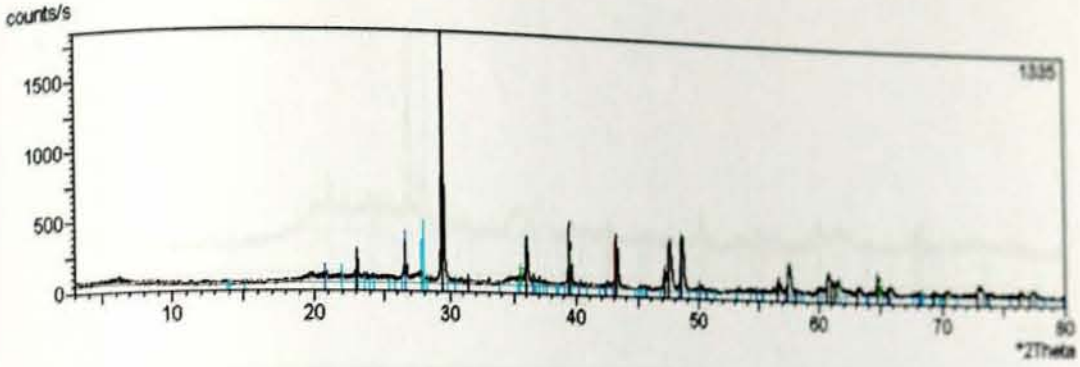

A	-	+	Name	Formula	Score	Score * Rel.	Rel. Score	Scale Factor	Displacement	Reference Code	Line Type	Line Col
✔			CALCITE	CaCO3	21,12	17,85	0,84	120,0	93	71-141		
✔			Quartz, low	SiO2	15,31	9,38	0,61	23,0	-32	05-0490		
✔			Albite, calcian, ordered	(Na,Ca)Al(Si,Al)3O8	13,07	2,59	0,20	28,0	-17	41-1480		

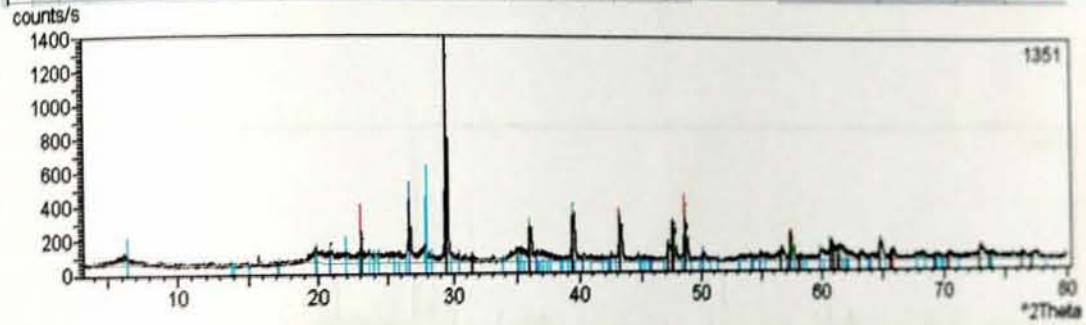

A	-	+	Name	Formula	Score	Score * Rel.	Rel. Score	Scale Factor	Displacement	Reference Code	Line Type	Line
✔			Calcite	CaCO3	15,56	13,45	0,86	100,0	45	24-0027		
✔			Quarz	SiO2	10,84	9,04	0,83	40,0	10	71- 32		
✔			Albite, calcian, ordered	(Na,Ca)Al(Si,Al)3O8	7,25	0,80	0,11	48,0	-145	41-1480		
✔			Montmorillonite-15A	Na0.3(Al,Mg)2Si4O10(OH)2l4H2	1,87	0,58	0,31	13,0	-224	29-1498		

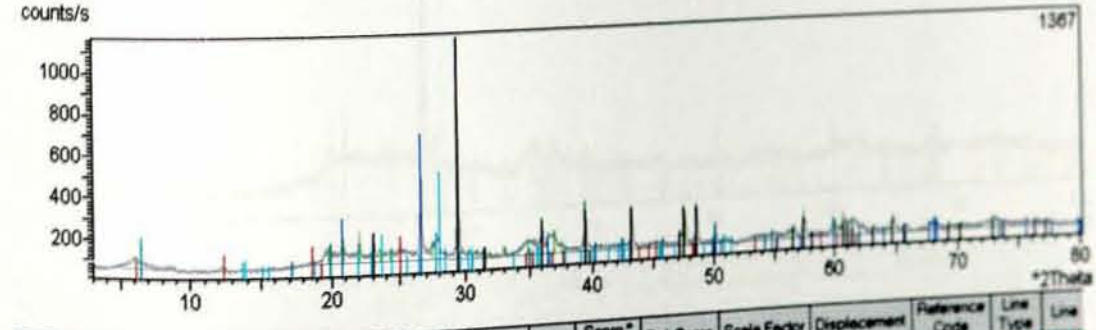

A	-	+	Name	Formula	Score	Score * Rel.	Rel. Score	Scale Factor	Displacement	Reference Code	Line Type	Line
✔			CALCITE	CaCO3	20,45	16,73	0,82	145,0	145	71-141		
✔			Quartz, low	SiO2	17,05	11,62	0,68	83,0	58	05-0490		
✔			Chlorit	(Mg,Al,Fe,Si)xO10OH8	7,73	2,72	0,35	16,0	58	71- 12		
✔			Albite, disordered	Na(Si3Al)O8	7,52	1,35	0,18	58,0	-23	19-0393		

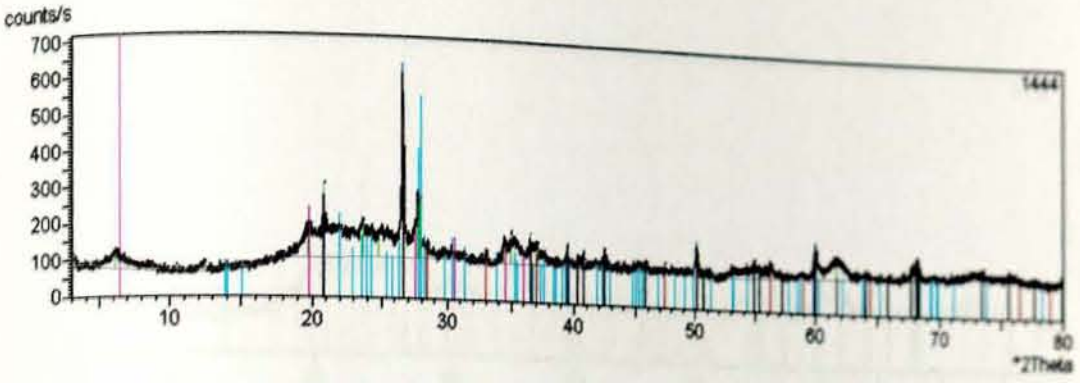

A	-	+	Name	Formula	Score	Score * Rel.	Rel. Score	Scale Factor	Displacement	Reference Code	Line Type	Line Col.
✔			Quarz	SiO2	11,82	10,74	0,91	100,0	10	77- 32		
✔			Pyrite, syn	FeS2	8,23	5,65	0,69	9,0	27	06-0710		
✔			Albite, calcian, ordered	(Na,Ca)Al(Si,Al)3O8	14,61	3,23	0,22	83,0	38	41-1480		
✔			Montmorillonite-14A	Na0.3(Al,Mg)2Si4O10(OH)2bH2	0,35	0,02	0,05	145,0	-133	13-0259		

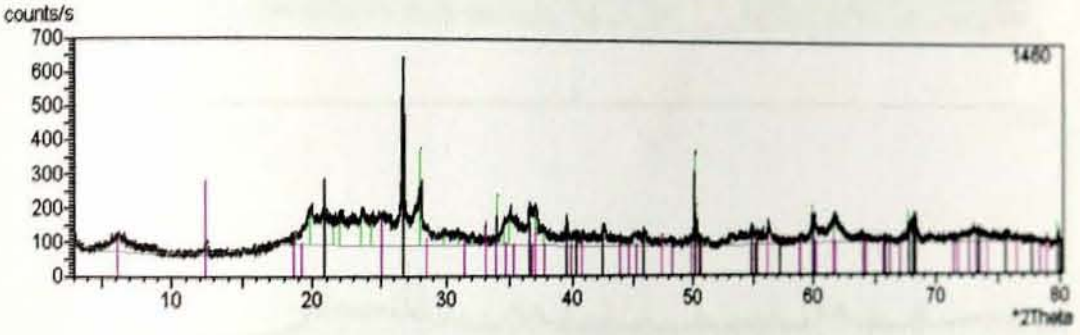

A	-	+	Name	Formula	Score	Score * Rel.	Rel. Score	Scale Factor	Displacement	Reference Code	Line Type	Line
✔			Quartz, low	SiO2	17,55	12,31	0,70	100,0	23	05-0490		
✔			Pyrite	FeS2	9,76	6,36	0,65	13,0	-48	42-1340		
✔			Nimite-1Mllb	(Ni,Mg,Al)6(Si,Al)4O10(OH)8	8,81	2,68	0,30	40,0	146	22-0712		

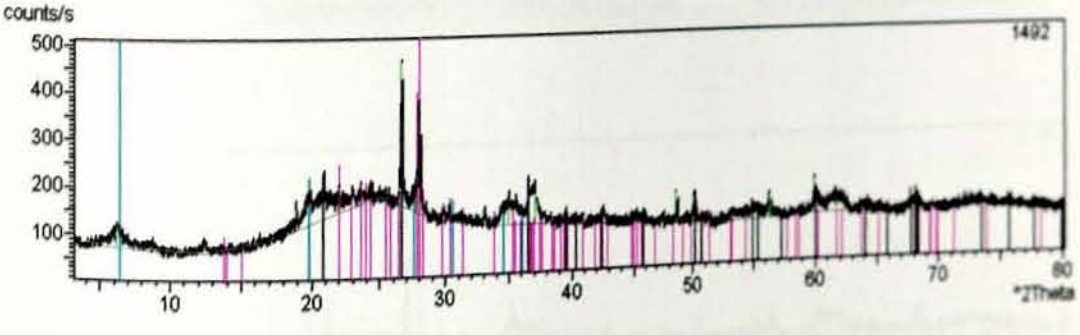

A	-	+	Name	Formula	Score	Score * Rel.	Rel. Score	Scale Factor	Displacement	Reference Code	Line Type	Line
✔			Quartz, low	SiO2	17,01	11,57	0,68	93,0	27	05-0490		
✔			Albite, calcian, ordered	(Na,Ca)Al(Si,Al)3O8	12,22	2,26	0,19	120,0	-17	41-1480		
✔		✔	Montmorillonite-14A	Na0.3(Al,Mg)2Si4O10(OH)2bH2	0,76	0,08	0,11	174,0	180	13-0259		

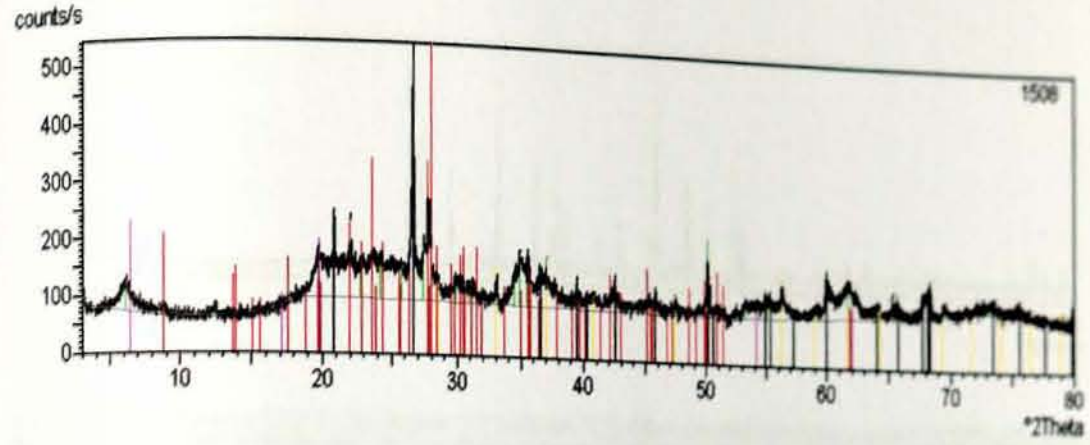

A	-	+	Name	Formula	Score	Score * Rel.	Rel. Score	Scale Factor	Displacement	Reference Code	Line Type	Line C
✔			Quartz, syn	SiO2	16,62	11,05	0,66	174,0	-23	33-1161		
✔			Pyrite, syn	FeS2	9,89	6,51	0,66	19,0	-23	26-0801		
✔			Illite-2M1	(K,H3O)Al2Si3AlO10(OH)2	7,27	2,94	0,40	40,0	-60	26-0911		
✔			Montmorillonite-15A	Na0.3(Al,Mg)2Si4O10(OH)2l4H2	1,80	0,54	0,30	40,0	-208	29-1498		

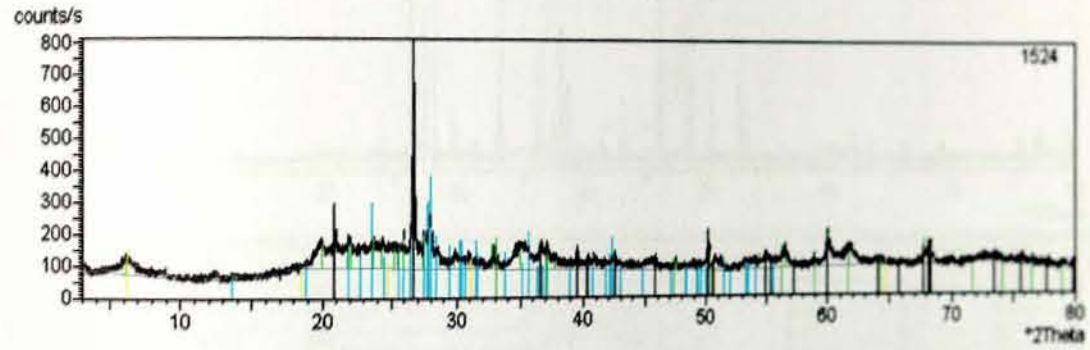

A	-	+	Name	Formula	Score	Score * Rel.	Rel. Score	Scale Factor	Displacement	Reference Code	Line Type	Line C
✔			ALPHA QUARTZ	SiO2	19,62	15,40	0,78	145,0	73	??-127		
✔			Pyrite	FeS2	11,31	8,53	0,75	16,0	35	42-1340		
✔			Anorthite, sodian,	(Ca,Na)(Si,Al)4O8	10,85	2,26	0,21	48,0	77	18-1202		
✔		✔	Vermiculit	Mg3(MgFe)3(SiAl)4O18	1,96	0,77	0,39	13,0	-88	??-24		

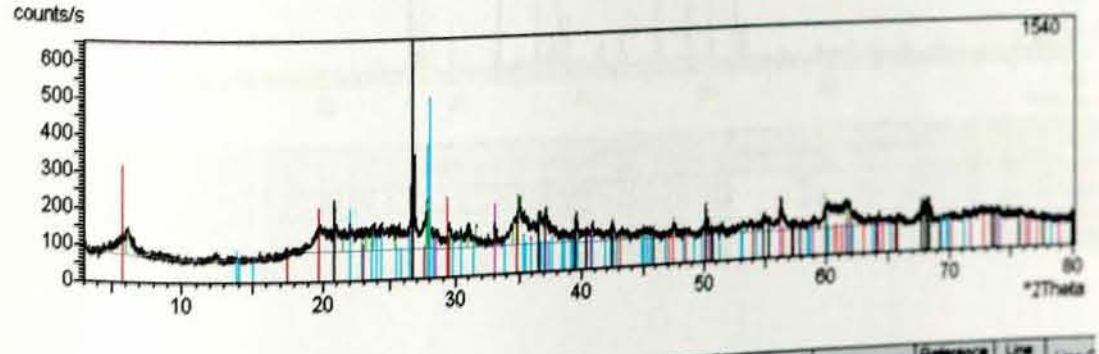

A	-	+	Name	Formula	Score	Score * Rel.	Rel. Score	Scale Factor	Displacement	Reference Code	Line Type	Line C
✔			Quartz, syn	SiO2	17,33	12,02	0,69	120,0	57	33-1161		
✔			Pyrite	FeS2	10,07	6,76	0,67	23,0	15	42-1340		
✔			CALCITE	CaCO3	11,56	5,35	0,46	28,0	184	??-141		
✔			Albite, calcian, ordered	(Na,Ca)Al(Si,Al)3O8	14,80	3,32	0,22	83,0	-17	41-1480		

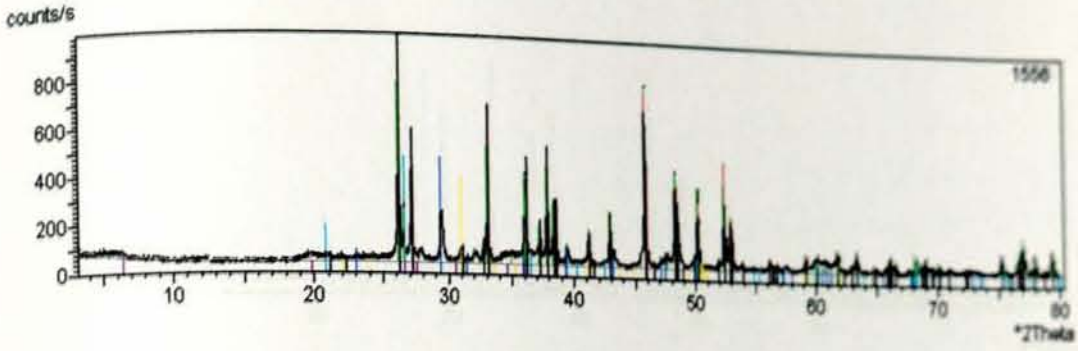

A	-	+	Name	Formula	Score	Score Rel.	Rel. Score	Scale Factor	Displacement	Reference Code	Line Type	Line Cl
✔			Aragonit	CaCO3	24,72	23,50	0,95	120,0	-145	71- 17		
✔			CALCITE	CaCO3	14,87	8,85	0,59	58,0	48	71- 141		
✔			Quartz, low	SiO2	10,50	4,41	0,42	58,0	-30	85-0490		
✔			Dolomit	CaMg(CO3)2	4,49	1,12	0,25	46,0	-213	71- 10		

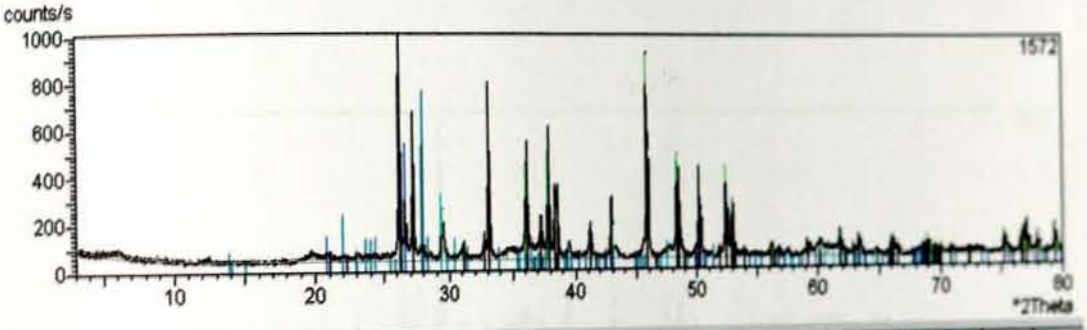

A	-	+	Name	Formula	Score	Score * Rel.	Rel. Score	Scale Factor	Displacement	Reference Code	Line Type	Line C
✔			Aragonite	CaCO3	49,07	39,48	0,80	145,0	-23	41-1475		
✔			Calcit	CaCO3	9,10	4,87	0,54	33,0	80	71- 49		
✔			ALPHA QUARTZ	SiO2	10,93	4,78	0,44	58,0	15	71-1.35		
✔		✔	Albite, calcian, ordered	(Na,Ca)Al(Si,Al)3O8	12,18	2,25	0,18	83,0	91	41-1480		

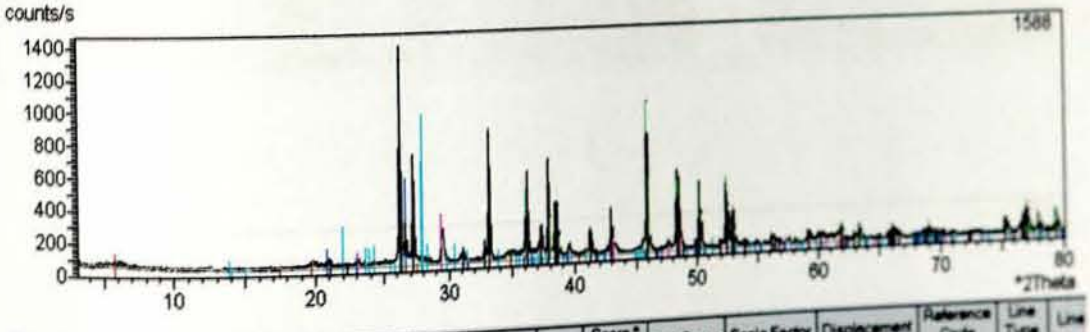

A	-	+	Name	Formula	Score	Score * Rel.	Rel. Score	Scale Factor	Displacement	Reference Code	Line Type	Line
✔			Aragonite	CaCO3	48,89	39,19	0,80	145,0	35	41-1475		
✔			ALPHA QUARTZ	SiO2	13,27	7,04	0,53	58,0	43	71-1.35		
✔			Calcite	CaCO3	9,77	5,31	0,54	33,0	48	24-0027		
✔			Montmorillonit,trock	Ca.24Na.01Mg.36Fe.02	5,02	2,52	0,50	9,0	24	71- 28		

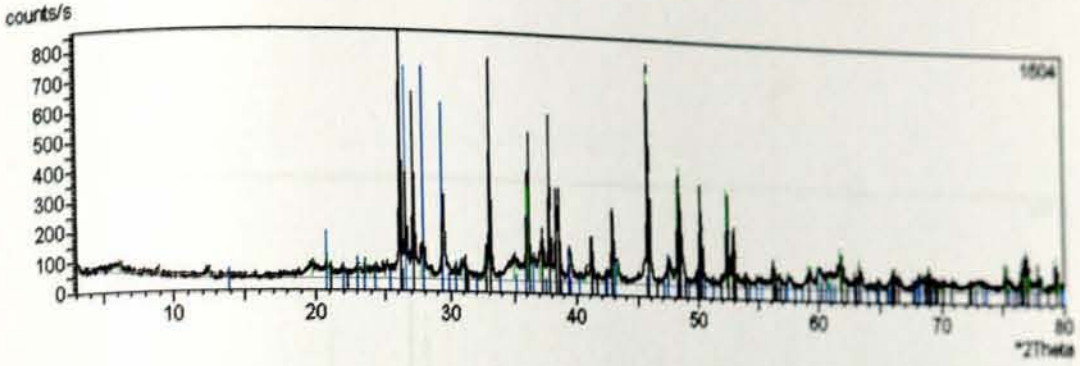

A	-	+	Name	Formula	Score	Score * Rel	Rel. Score	Scale Factor	Displacement	Reference Code	Line Type	Line Cl
✔			Aragonite	CaCO3	46.05	34.76	0.75	174.0	-58	41-1475		
✔			ALPHA QUARTZ	SiO2	15.61	9.75	0.62	100.0	15	??-135		
✔			CALCITE	CaCO3	13.30	7.07	0.53	83.0	81	??-141		
✔			Albit	NaAlSi3O8	7.07	1.79	0.25	100.0	-66	??-51		

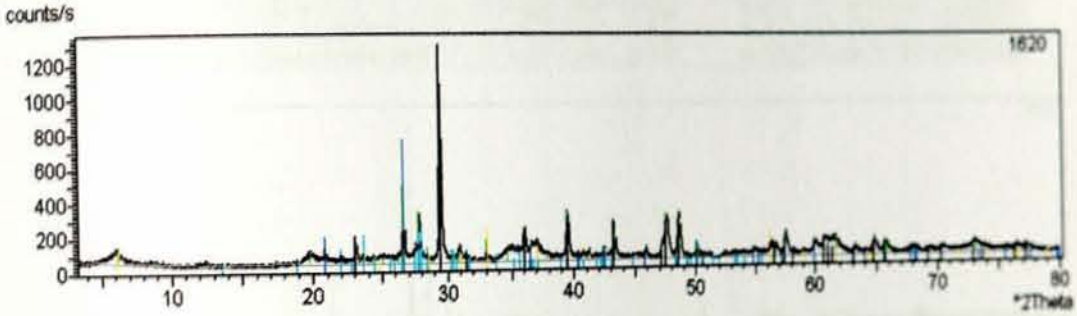

A	-	+	Name	Formula	Score	Score * Rel.	Rel. Score	Scale Factor	Displacement	Reference Code	Line Type	Line
✔			CALCITE	CaCO3	19.39	15.04	0.78	120.0	77	??-141		
✔			Quartz, syn	SiO2	17.10	11.70	0.68	69.0	10	33-1161		
✔			Pyrite	FeS2	10.56	7.43	0.70	19.0	-70	42-1340		
✔			Anorthite, sodian,	(Ca,Na)(Si,Al)4O8	15.31	4.51	0.29	23.0	-23	18-1202		

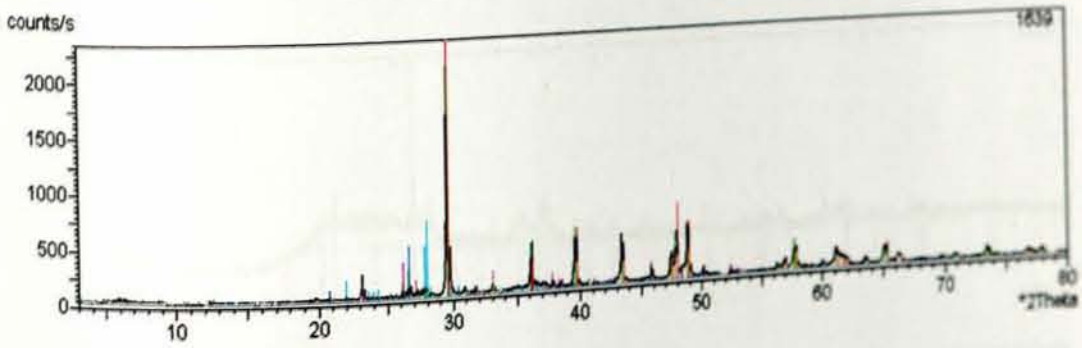

A	-	+	Name	Formula	Score	Score * Rel.	Rel. Score	Scale Factor	Displacement	Reference Code	Line Type	Line Col
✔			Aragonite	CaCO3	36.53	21.87	0.60	16.0	-27	41-1475		
✔		✔	Calcite, magnesian	(Ca,Mg)CO3	18.38	14.07	0.77	120.0	-259	43-0697		
✔			Pyrite	FeS2	11.50	8.82	0.77	6.0	-48	42-1340		
✔			Quartz, syn	SiO2	13.50	7.29	0.54	23.0	10	33-1161		

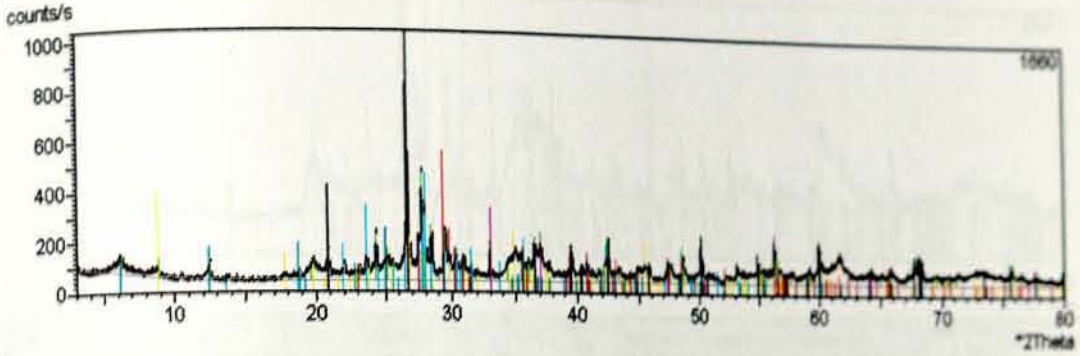

A	-	+	Name	Formula	Score	Score * Rel.	Rel. Score	Scale Factor	Displacement	Reference Code	Line Type	Line Col.
✔			Quartz, low	SiO2	19,04	14,50	0,76	120,0	15	05-0490		
✔			Pyrite	FeS2	11,95	9,52	0,80	33,0	-65	42-1340		
✔			Muscovite-2M1	KAl2(Si3Al)O10(OH,F)2	22,48	6,83	0,30	40,0	10	06-0263		
✔			Chlorit	(Mg,Al,Fe,Si)xO10OH8	12,11	6,67	0,55	23,0	186	??- 12		

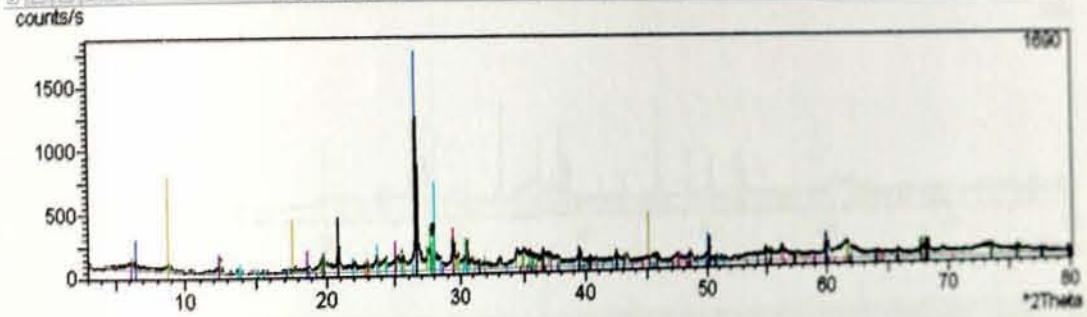

A	-	+	Name	Formula	Score	Score * Rel.	Rel. Score	Scale Factor	Displacement	Reference Code	Line Type	Line Cl
✔			ALPHA QUARTZ	SiO2	19,78	15,65	0,79	120,0	10	??- 135		
✔			Pyrit	FeS2	7,89	6,92	0,88	9,0	-241	??- 33		
✔			Calcite	CaCO3	10,60	6,24	0,59	23,0	48	24-0027		
✔			Chlorit	(Mg,Al,Fe,Si)xO10OH8	9,96	4,51	0,45	16,0	116	??- 12		

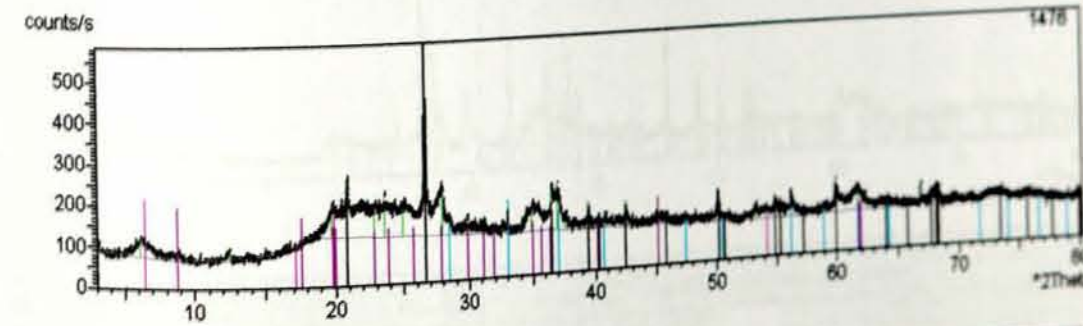

A	-	+	Name	Formula	Score	Score * Rel.	Rel. Score	Scale Factor	Displacement	Reference Code	Line Type	Line
✔			ALPHA QUARTZ	SiO2	17,25	11,91	0,69	120,0	10	??- 135		
✔			Pyrite	FeS2	11,24	8,42	0,75	19,0	-60	42-1340		
✔			Illite-2M1	(K,H3O)Al2Si3AlO10(OH)2	5,71	1,81	0,32	33,0	-95	26-0911		
✔			Montmorillonite-15A	Na0.3(Al,Mg)2Si4O10(OH)2l4H2	1,91	0,61	0,32	33,0	-206	29-1498		

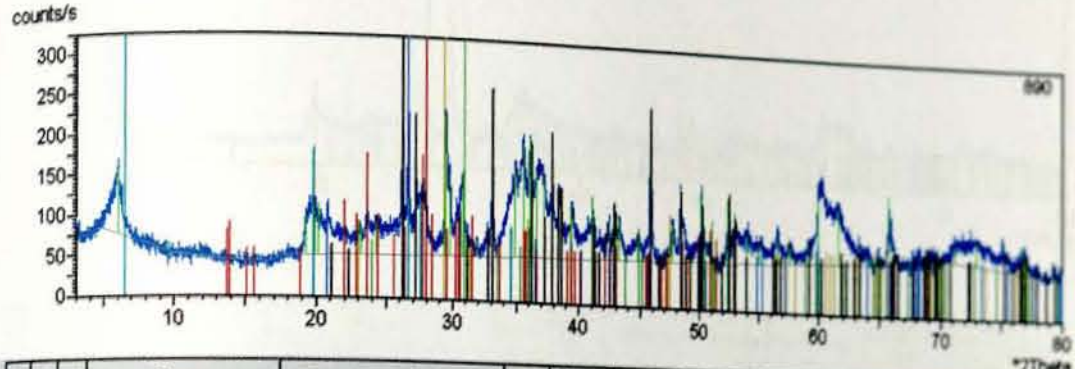

A	-	+	Name	Formula	Score	Score * Rel.	Rel. Score	Scale Factor	Displacement	Reference Code	Line Type	Line Col.
✔			Aragonite	CaCO3	33,82	18,75	0,55	145,0	18	41-1475		
✔			ALPHA QUARTZ	SiO2	13,51	7,30	0,54	120,0	58	??-127		
✔			CALCITE	CaCO3	12,95	6,70	0,52	145,0	241	??-141		
✔			Dolomite	CaMg(CO3)2	12,57	4,78	0,38	174,0	-177	36-0426		

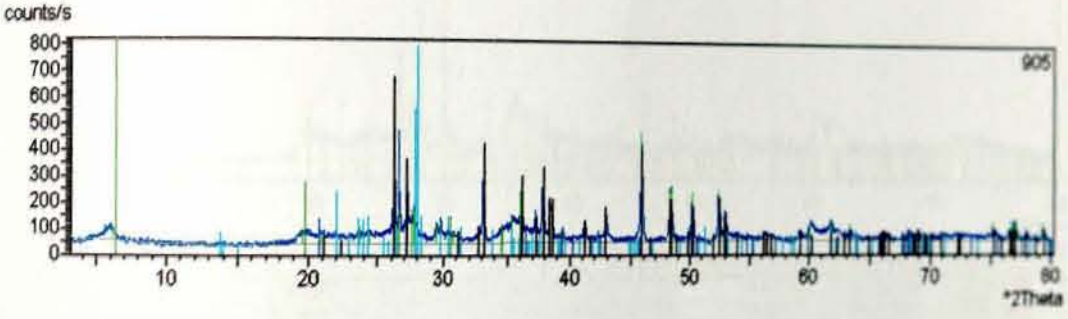

A	-	+	Name	Formula	Score	Score * Rel.	Rel. Score	Scale Factor	Displacement	Reference Code	Line Type	Line Col.
✔			Aragonite	CaCO3	47,04	36,27	0,77	145,0	48	41-1475		
✔			ALPHA QUARTZ	SiO2	11,41	5,21	0,46	100,0	127	??-127		
✔			Albite, calcian, ordered	(Na,Ca)Al(Si,Al)3O8	10,02	1,52	0,15	174,0	-48	41-1480		
✔			Montmorillonite-14A	Na0.3(Al,Mg)2Si4O10(OH)2xH2	2,21	0,70	0,32	302,0	182	13-0259		

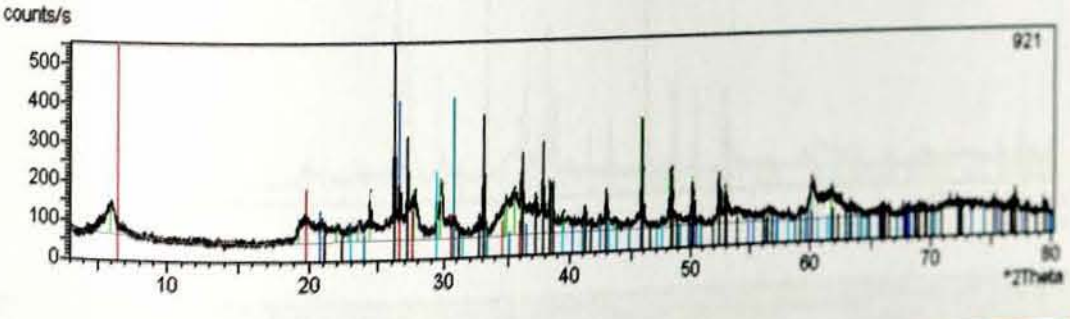

A	-	+	Name	Formula	Score	Score * Rel.	Rel. Score	Scale Factor	Displacement	Reference Code	Line Type	Line Col.
✔			Aragonite	CaCO3	37,07	22,53	0,61	174,0	-24	41-1475		
✔			Dolomite, ferroan	Ca(Mg,Fe)(CO3)2	9,61	3,85	0,40	120,0	17	34-0517		
✔			ALPHA QUARTZ	SiO2	9,42	3,55	0,38	120,0	-18	??-136		
✔			Calcite	CaCO3	5,49	1,67	0,30	58,0	72	24-0027		

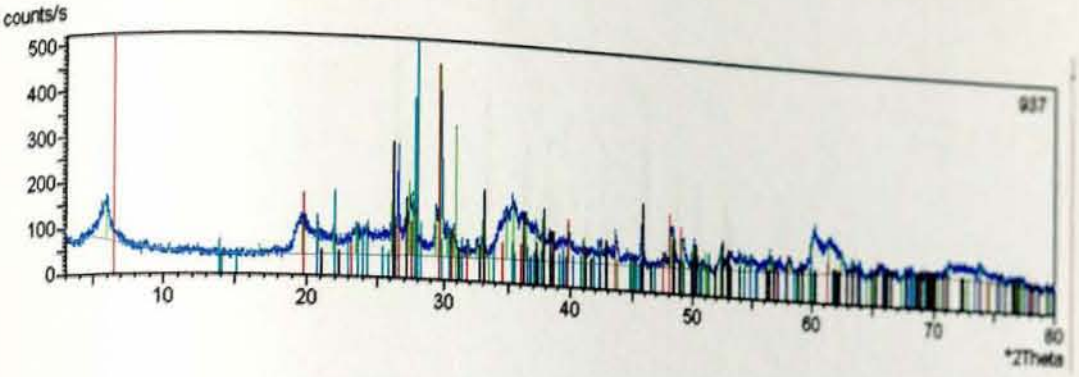

A	-	+	Name	Formula	Score	Score * Rel.	Rel. Score	Scale Factor	Displacement	Reference Code	Line Type	Line Col.
✔			Aragonite	CaCO3	30,19	14,94	0,49	58,0	-92	41-1475		
✔			Calcite, magnesian	(Ca,Mg)CO3	16,02	10,69	0,67	100,0	146	43-0697		
✔			Quartz, low	SiO2	14,39	8,28	0,58	58,0	-30	05-0490		
✔			Dolomite	CaMg(CO3)2	12,89	5,04	0,39	69,0	-155	36-0426		

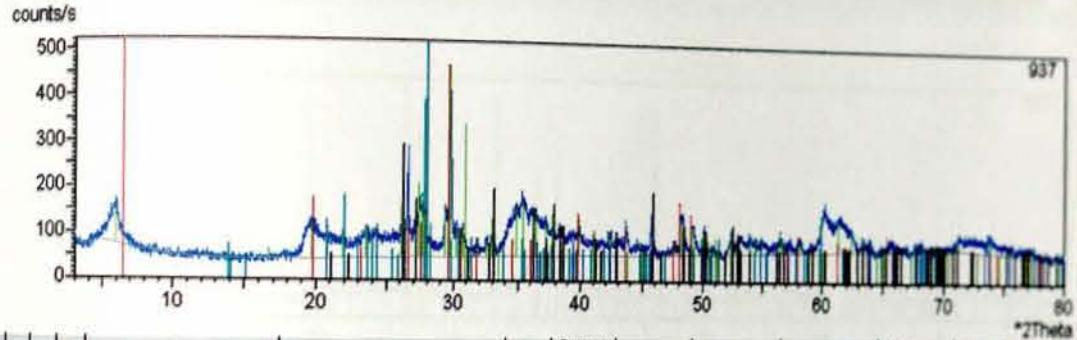

A	-	+	Name	Formula	Score	Score * Rel.	Rel. Score	Scale Factor	Displacement	Reference Code	Line Type	Line Col.
✔			Aragonite	CaCO3	30,19	14,94	0,49	58,0	-92	41-1475		
✔			Calcite, magnesian	(Ca,Mg)CO3	16,02	10,69	0,67	100,0	146	43-0697		
✔			Quartz, low	SiO2	14,39	8,28	0,58	58,0	-30	05-0490		
✔			Dolomite	CaMg(CO3)2	12,89	5,04	0,39	69,0	-155	36-0426		

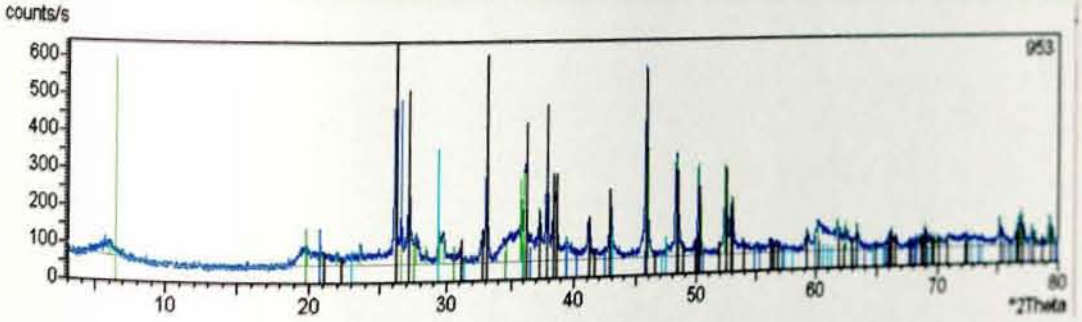

A	-	+	Name	Formula	Score	Score * Rel.	Rel. Score	Scale Factor	Displacement	Reference Code	Line Type	Line Col.
✔			Aragonite	CaCO3	43,25	30,67	0,71	174,0	10	41-1475		
✔			ALPHA QUARTZ	SiO2	9,15	3,35	0,37	83,0	56	??-135		
✔			CALCITE	CaCO3	7,42	2,20	0,30	58,0	18	??-141		
✔			Montmorillonite-14A	Na0.3(Al,Mg)2Si4O10(OH)2bd•2	3,28	1,54	0,47	100,0	129	13-0259		

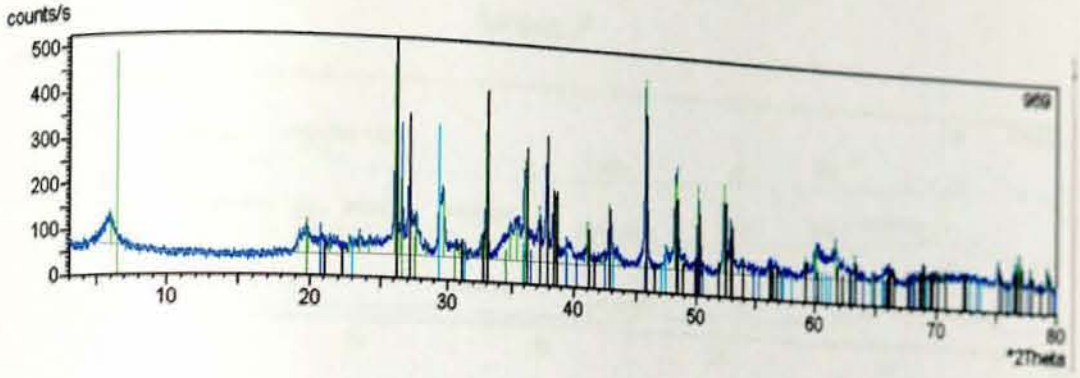

A	-	+	Name	Formula	Score	Score * Rel.	Rel. Score	Scale Factor	Displacement	Reference Code	Line Type	Line Col...
✔			Aragonite	CaCO3	44,05	31,81	0,72	145,0	-57	41-1475		
✔			ALPHA QUARTZ	SiO2	10,51	4,42	0,42	69,0	-23	??-135		
✔			Calcite, syn	CaCO3	7,53	2,27	0,30	69,0	48	05-0586		
✔			Montmorillonite-14A	Na0.3(Al,Mg)2Si4O10(OH)2bH2	2,19	0,68	0,31	100,0	186	13-0259		

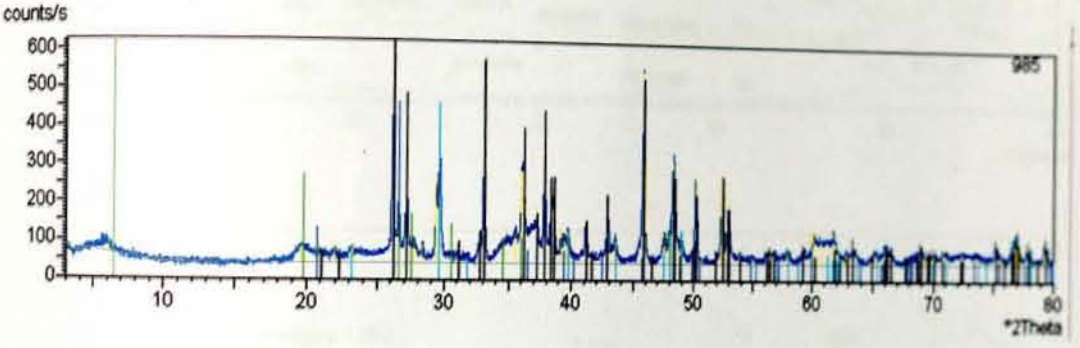

A	-	+	Name	Formula	Score	Score * Rel.	Rel. Score	Scale Factor	Displacement	Reference Code	Line Type	Line Col...
✔			Aragonite	CaCO3	43,74	31,36	0,72	174,0	38	41-1475		
✔			Calcite, magnesian	(Ca,Mg)CO3	15,08	9,48	0,63	83,0	-140	43-0697		
✔			ALPHA QUARTZ	SiO2	7,23	2,09	0,29	83,0	56	??-135		
✔			Montmorillonite-14A	Na0.3(Al,Mg)2Si4O10(OH)2bH2	1,65	0,39	0,24	251,0	72	13-0259		

Annex-F

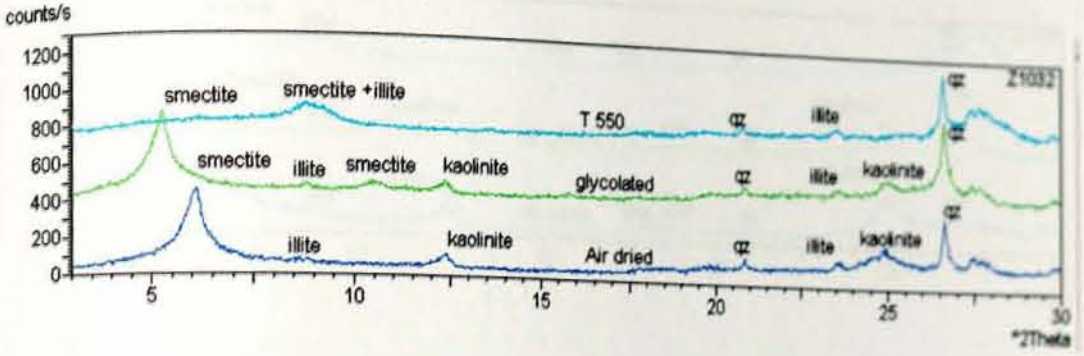
counts/s
smectite
smectite +illite
T 550
qz
illite
smectite
illite
smectite
kaolinite
glycolated
kaolinite
illite
kaolinite
Air dried
*2Theta

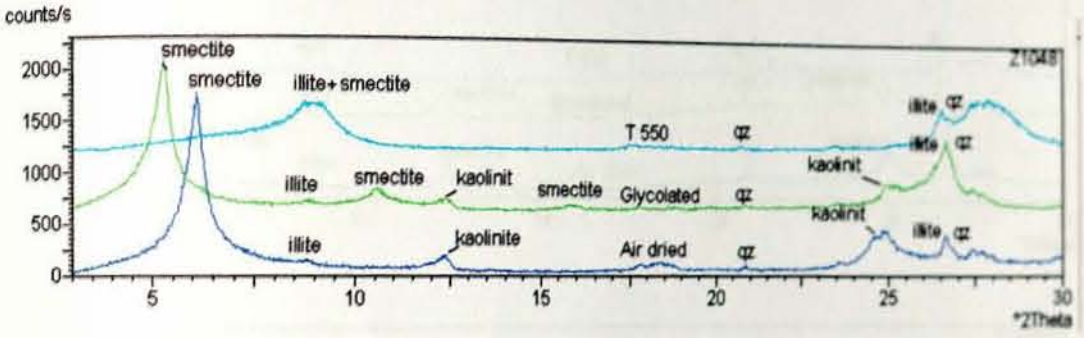
counts/s
smectite
smectite
illite+ smectite
T 550
qz
illite
smectite
kaolinit
smectite
Glycolated
kaolinit
illite
kaolinite
Air dried
*2Theta

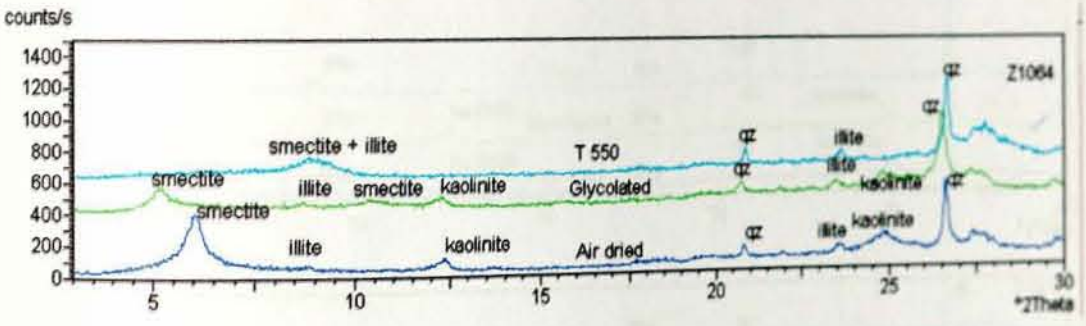
counts/s
smectite + illite
T 550
qz
illite
smectite
illite
smectite
kaolinite
Glycolated
kaolinite
smectite
illite
kaolinite
Air dried
*2Theta

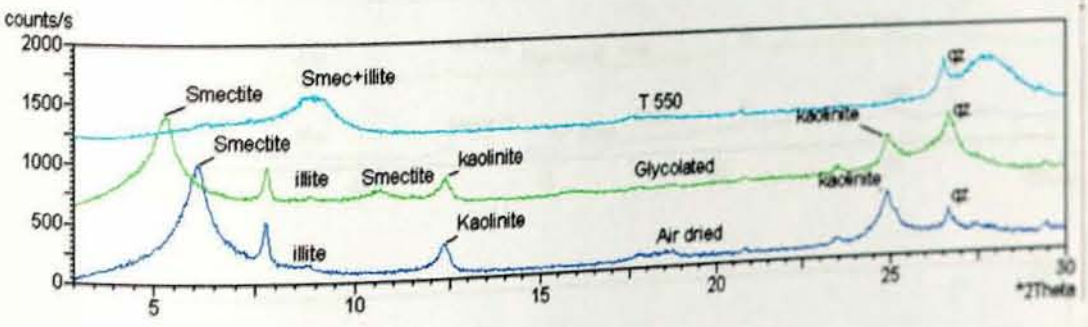
counts/s
Smectite
Smec+illite
T 550
kaolinite
qz
Smectite
illite
Smectite
kaolinite
Glycolated
kaolinite
Kaolinite
Air dried
illite
*2Theta

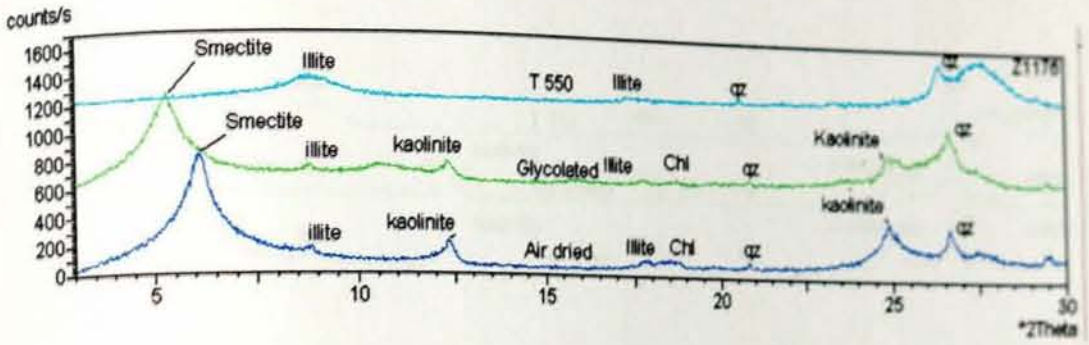
counts/s
Z1176
Smectite
Illite
T 550
Illite
qz
Smectite
illite
kaolinite
Glycolated
Illite
Chl
qz
Kaolinite
qz
illite
kaolinite
Air dried
Illite
Chl
qz
kaolinite
qz
*2Theta

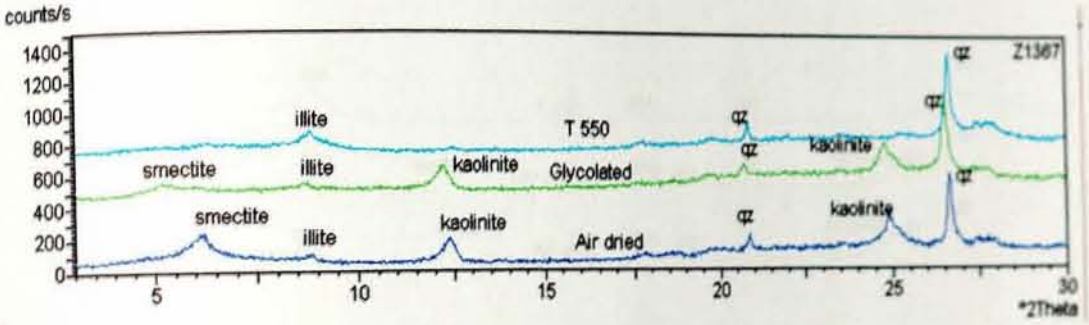
counts/s
Z1367
illite
T 550
qz
qz
qz
kaolinite
smectite
illite
kaolinite
Glycolated
qz
kaolinite
qz
smectite
illite
kaolinite
Air dried
qz
kaolinite
qz
*2Theta

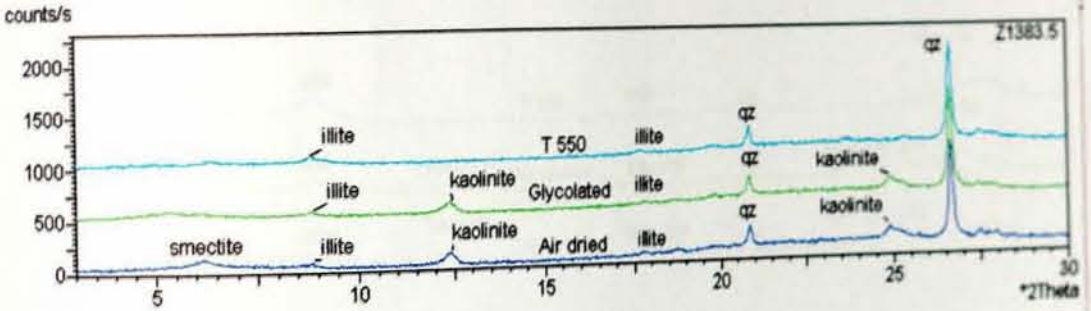
counts/s
Z1383.5
qz
illite
T 550
illite
qz
illite
kaolinite
Glycolated
illite
qz
kaolinite
smectite
illite
kaolinite
Air dried
illite
qz
kaolinite
*2Theta

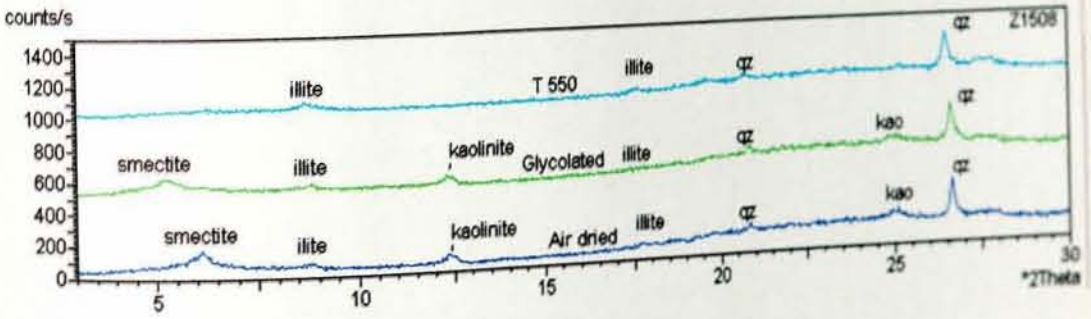
counts/s
Z1508
illite
T 550
illite
qz
qz
kao
smectite
illite
kaolinite
Glycolated
illite
qz
qz
kao
smectite
illite
kaolinite
Air dried
illite
qz
*2Theta

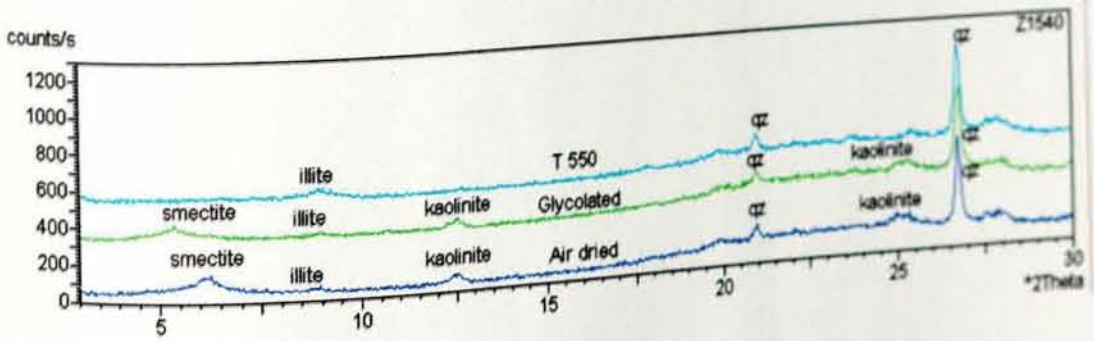
counts/s
Z1540
qz
illite
T 550
qz
kaolinite
qz
smectite
illite
kaolinite
Glycolated
qz
kaolinite
smectite
illite
kaolinite
Air dried
*2Theta

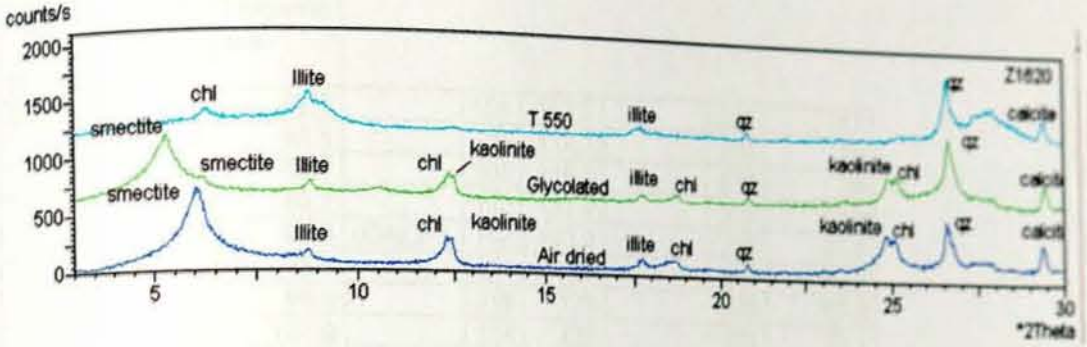
counts/s
2000
1500
1000
500
0
chl
Illite
smectite
T 550
ilite
qz
Z1620
calcite
smectite
illite
chl
kaolinite
Glycolated
kaolinite
chl
smectite
Illite
chl
kaolinite
Air dried
ilite
chl
qz
5
10
15
20
25
30
°2Theta

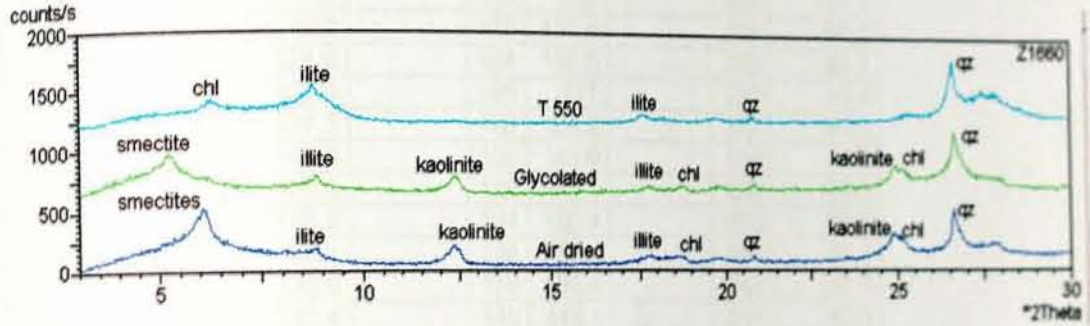
counts/s
2000
1500
1000
500
0
chl
ilite
T 550
ilite
qz
Z1660
smectite
illite
kaolinite
Glycolated
ilite
chl
qz
kaolinite
chl
smectites
ilite
kaolinite
Air dried
ilite
chl
qz
kaolinite
chl
5
10
15
20
25
30
°2Theta

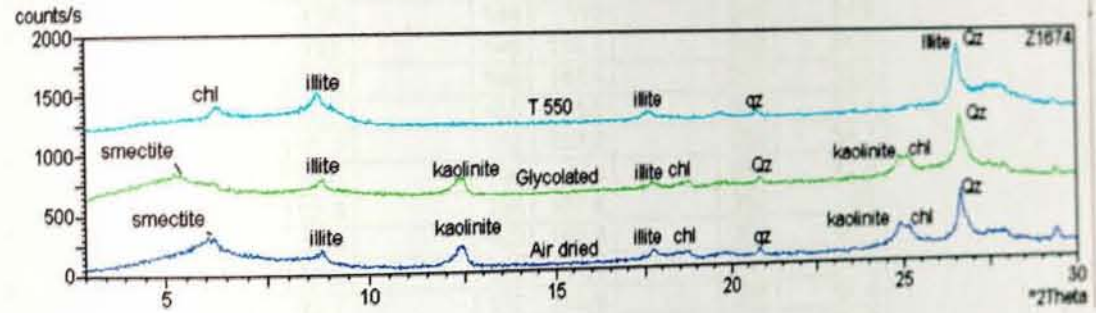
counts/s
2000
1500
1000
500
0
chl
illite
T 550
ilite
qz
Illite
Qz
Z1674
smectite
illite
kaolinite
Glycolated
illite
chl
Qz
kaolinite
chl
smectite
illite
kaolinite
Air dried
ilite
chl
qz
kaolinite
chl
5
10
15
20
25
30
°2Theta

Annex-G

Seg no.	depth of sed	Magnetic sus.							
03AL3 - 1	0	83.3		104	112.2		208	27
	2	92.1		106	112.7		210	28
	4	89.2		108	119.2		212	28
	6	89.7		110	121.9		214	32.9
	8	90.3	03AL2-1	112	123.2		216	40.5
	10	93.1		114	125		218	50.9
	12	98.9		116	126		220	63.9
	14	107.9		118	127		222	71.1
	16	117.3		120	130		224	81.1
	18	123		122	131.4		226	90.2
	20	128.5		124	135.5		228	86.3
	22	131.5		126	127		230	85.4
	24	137.3		128	132.2		232	84.3
	26	146.5		130	143.9		234	78
	28	150.1		132	148.5		236	73.3
	30	145.2		134	160.4		238	62.4
	32	137.1		136	167.1		240	52.9
	34	133.9		138	160.4		242	47.9
	36	132.4		140	144.1		244	43.1
	38	130.9		142	124.9		246	38.4
	40	130		144	119		248	34.9
	42	128		146	133.1		250	34.5
	44	127.2		148	146.1		252	35.3
	46	121.6		150	158.9		254	33.4
	48	115.9		152	157.2		256	34.7
	50	112.6		154	155		258	41.4
	52	112.3		156	157.8		260	52
	54	109		158	152.4		262	59.6
	56	102.2		160	141.5		264	63.5
	58	92.7		162	142.6		266	67.4
	60	86.5		164	145.2		268	63.3
	62	83.3		166	151.5		270	49.9
	64	80.5		168	147		272	46
	66	79.1		170	134.4		274	51.6
	68	78.8		172	125.9		276	62.2
	70	77.9		174	109.7		278	84.1
	72	75.4		176	93.6		280	95.2
	74	73.1		178	91.9		282	103.2
	76	72.7		180	79.8		284	97.8
	78	73.9		182	68.7		286	88.7
	80	76		184	50.1		288	85
	82	77.8		186	35.1		290	91.9
	84	78.7		188	30.6		292	95.6
	86	80		190	26.7		294	91.5
	88	80.4		192	24.7		296	79.1
	90	83.9		194	27.1		298	51.8
	92	79.9		196	29.3	03AL2-3	300	32.7
	94	94.4		198	29		302	27.1
	96	100.7	03AL2-2	200	28.4		304	28.2
	98	104.7		202	27.5		306	32.5
	100	111.4		204	28.4		308	33
	102	112.9		206	27.7		310	34
	312	35.3		438	30.1			
	314	34.5		440	28.4			
	316	32.7		442	26.7			
	318	34		444	29.9			

	320	36.9		446	31.4			
	322	36.2		448	31.9		560	8.5
	324	29.7		450	28.6		562	8.5
	326	27.1		452	24.5		564	9.1
	342	17.3		454	20.8		566	8.7
	344	16.7		456	17.3		568	10
	346	15.4		458	14.7		570	10.6
	348	13.2		460	15.6		572	10.2
	350	10.6		462	15.4		574	8.7
	352	10.6		464	14.7		576	6.9
	354	10		466	13.2		578	5.9
	356	10		468	13.4		580	4.6
	358	10		470	13.4		582	4.3
	360	10.8		472	12.4		584	4.3
	362	13.2		474	11.5		586	4.6
	364	14.5		476	12.8		588	5.4
	366	15.6		478	12.6		590	5.9
	368	18.9		480	11.7		592	6.1
	370	21.9		482	10.8		594	6.9
	372	23		484	10.8		596	7.2
	374	23		486	10.6		598	7.2
	376	21		488	10.2	03AL2-6	600	10
	378	19.9		490	9.3		602	13.7
	380	19.1		492	9.3		604	15
	382	18.9		494	9.3		606	15.6
	384	22.8		496	9.5		608	16.7
	386	27.1		498	9.3		610	18
	388	31.6	03AL2-5	500	9.5		612	17.6
	390	32.3		502	9.3		614	19.3
	392	28.6		504	9.1		616	24.5
	394	25.4		506	8		618	36.9
	396	23.4		508	9.1		620	57
	398	22.3		510	10.4		622	75
03AL2-4	400	24.7		512	11.1		624	48.1
	402	25.4		514	11.5		626	22.8
	404	26.7		516	11.1		628	15.2
	406	25.8		518	9.3		630	15
	408	21.7		520	9.3		632	16
	410	21.7		522	9.3		634	14.5
	412	24.3		524	9.8		636	13.2
	414	24.9		526	10		638	13
	416	24.5		528	9.1		640	14.3
	418	24.5		530	8.7		642	18.9
	420	23.8		532	8.9		644	26.7
	422	21		534	10.2		646	29.9
	424	18.4		536	11.5		648	22.3
	426	18.9		538	12.6		650	17.3
	428	22.8		540	12.4		652	13.9
	430	26		542	11.9		654	11.1
	432	28		544	11.3		656	7.8
	434	29.9		546	9.8		658	6.1
	436	30.6		548	8.7		660	4.6
	662	4.1		774	377.8			
	664	3.5		776	367.6			
	666	3.5		778	390.6			
	668	3.7		780	425.3			
	670	4.1		782	435.5			
	672	4.8		784	398.4			
	674	5.2		786	395.8			

	676	4.8
	678	4.8
	680	5.2
	682	4.8
	684	4.6
	686	4.8
	688	5
	690	5
	692	4.6
	694	4.8
	696	5
	698	5
03AL2-7	700	5.2
	702	6.3
	704	5
	706	5.6
	708	6.5
	710	7.2
	712	8
	714	8.7
	716	8.7
	718	9.8
	720	12.4
	722	15
	724	18.4
	726	20.2
	728	21
	730	21.7
	732	24.5
	734	31.4
	736	38.4
	738	41.6
	740	42.7
	742	40.5
	744	41.4
	746	42.5
	748	43.8
	750	40.8
	752	34.7
	754	39.2
	756	48.8
	758	63.3
	760	90.2
	762	137.4
	764	213.5
	766	306.7
	768	356.1
	770	372
	772	378
	788	411
	790	392.8
	792	387
	794	381
	796	376
	798	371
	800	368

Annex-H

Ashange core 03AL2								
Clay mineralogy								
Sample no	depth from water sur	sediment depth	smectite%	illite%	I/S%	chlorite%	kaolinite%	Smec/Kaol
Z1032	1032	142	92,92	4,33	0	0	2,73	33.95
Z1064	1064	174	69,10	23,94	0	0	6,95	9.94
Z1128	1128	238	95,06	0	0	0	4,93	19.26
Z1176	1176	286	89,80	5,49	0	0	4,70	19.10
Z1367.5	1367.5	477.5	43,34	34,37	0	0	22,28	1.94
Z1383.5	1383.5	493.5	35,10	36,99	0	0	27,90	1.25
Z1508	1508	618	19,88	78,21	0	0	1,90	10.44
Z1524	1524	634	86,65	8,21	0	0	5,13	16.88
Z1540	1540	650	6,63	26,31	0	0	11,05	0.600
Z1620	1620	730	71,22	19,68	0	5,63	3,45	20.62
Z1660	1660	770	92,48	0	0	2,91	4,6	20.06
Z1674	1674	784	87,43	0	0	7,82	4,74	18.41

Annex-I

Loss On Ignition
Core: 03AL2 & 03AL2
Sampling interval 5cm

Depth	Deptyhsed	Weight of crucible	Crucible + wet sample	Crucible + Dry 105 °c	water contient	weight at 550 °c	weight at 950°c	Dry weight	Wt. Loss 550(om)	Wt loss 950(car)	%OM	%CAR	% MIN RES
890	0	24.522	26.0752	24.9707	1.105	24.928	24.892	0.448	0.042	0.0361	9.43143813	8.0490524	82.5195095
895	5	15.223	16.394	15.4806	0.913	15.453	15.431	0.257	0.027	0.0223	10.6531882	8.67029549	80.6765163
900	10	11.056	12.2172	11.4694	0.748	11.45	11.434	0.413	0.02	0.0164	4.71698113	3.96710208	91.3159168
905	15	23.342	24.7813	24.0393	0.742	24.01	23.993	0.698	0.029	0.0168	4.21444954	2.40825688	93.3772936
910	20	24.325	25.3871	24.5492	0.838	24.524	24.504	0.224	0.025	0.0197	11.1804009	8.77505568	80.0445434
915	25	25.172	26.1731	25.4172	0.756	25.392	25.369	0.245	0.025	0.0229	10.2407181	9.34312525	80.4161567
920	30	15.618	16.8185	15.9205	0.898	15.889	15.862	0.302	0.031	0.0275	10.353953	9.09692359	80.5491234
925	35	20.922	22.1526	21.1979	0.955	21.171	21.148	0.276	0.027	0.0228	9.81173063	8.25488776	81.9333816
930	40	16.491	17.6673	16.7114	0.956	16.691	16.677	0.221	0.021	0.0141	9.42883046	6.39165911	84.1795104
935	45	19.067	20.4285	19.3254	1.103	19.298	19.281	0.259	0.027	0.0171	10.5486862	6.60741886	82.8438949
940	50	23.065	24.5519	23.3166	1.235	23.289	23.272	0.251	0.028	0.0161	11.1863057	6.40923567	82.4044586
945	55	11.097	12.4357	11.3759	1.06	11.335	11.305	0.279	0.041	0.0299	14.6437522	10.7053348	74.650913
950	60	22.324	23.6654	22.5569	1.109	22.52	22.486	0.232	0.037	0.0335	16	14.4086022	69.5913978
955	65	16.593	18.0533	16.8313	1.222	16.79	16.755	0.238	0.041	0.0352	17.1776564	14.7837043	68.0386392
960	70	21.688	23.1655	21.9408	1.225	21.897	21.862	0.252	0.044	0.0352	17.3465347	13.9405941	68.7128713
965	75	22.003	23.3271	22.2186	1.109	22.174	22.139	0.215	0.044	0.0356	20.6223874	16.5350673	62.8425453
970	80	24.104	25.7111	24.3902	1.321	24.342	24.291	0.286	0.049	0.0505	17.0041899	17.6326816	65.3631285
975	85	24.845	26.3027	25.1627	1.14	25.114	25.051	0.318	0.049	0.0624	15.4814349	19.6349906	64.8835746
980	90	21.327	22.6679	21.5601	1.108	21.51	21.484	0.233	0.051	0.0257	21.6981132	11.0205832	67.2813036
985	95	24.201	25.4297	24.4463	0.983	24.406	24.377	0.245	0.04	0.0295	16.4556962	12.045733	71.4985708
990	100	22.964	24.5529	23.3411	1.212	23.299	23.238	0.377	0.042	0.0615	11.1405836	16.3129973	72.5464191
995	105	20.674	21.8583	20.9812	0.877	20.954	20.901	0.308	0.027	0.0526	8.87227819	17.0945726	74.0331492
1000	110	17.2	18.6686	18.05	0.619	17.92	17.863	0.85	0.13	0.057	15.2941176	6.70588235	78
1005	115	17.83	19.0605	18.41	0.651	18.33	18.26	0.58	0.08	0.07	13.7931034	12.0689655	74.137931
1010	120	18.9	20.0315	19.35	0.682	19.28	19.249	0.45	0.07	0.031	15.5555556	6.88888889	77.5555556
1015	125	18.05	19.1165	18.66	0.457	18.57	18.558	0.61	0.09	0.012	14.7540984	1.96721311	83.2786885
1020	130	17.23	18.6476	17.81	0.838	17.72	17.698	0.58	0.09	0.022	15.5172414	3.79310345	80.6896552

1025	135	17.18	18.4479	17.67	0.778	17.6	17.589	0.49	0.07	0.011	14.2857143	2.24489796	83.4693878
1030	140	18.43	19.7232	18.9	0.823	18.82	18.819	0.47	0.08	0.001	17.0212766	0.21276596	82.7659574
1035	145	19.01	20.4552	19.63	0.825	19.54	19.485	0.62	0.09	0.055	14.516129	8.87096774	76.6129032
1040	150	17.73	19.1952	18.43	0.765	18.31	18.294	0.7	0.12	0.016	17.1428571	2.28571429	80.5714286
1045	155	19.43	20.6811	20.13	0.551	20.03	20.013	0.7	0.1	0.017	14.2857143	2.42857143	83.2857143
1050	160	17.43	19.1258	18.28	0.846	18.14	18.088	0.85	0.14	0.052	16.4705882	6.11764706	77.4117647
1055	165	19.64	21.7015	20.97	0.732	20.61	20.548	1.33	0.36	0.062	27.0676692	4.66165414	68.2706767
1060	170	18.21	19.7867	19.23	0.557	19.09	19.045	1.02	0.14	0.045	13.7254902	4.41176471	81.8627451
1065	175	16.19	17.8674	17.23	0.637	17.06	16.983	1.04	0.17	0.077	16.3461538	7.40384615	76.25
1070	180	19.51	21.6362	20.83	0.806	20.69	20.366	1.32	0.14	0.324	10.6060606	24.5454545	64.8484848
1075	185	16.42	18.1407	17.39	0.751	17.15	16.99	0.97	0.24	0.16	24.742268	16.4948454	58.7628866
1080	190	16.42	18.1317	17.39	0.742	17.15	16.99	0.97	0.24	0.16	24.742268	16.4948454	58.7628866
1085	195	18.71	20.2407	19.46	0.781	19.28	19.169	0.75	0.18	0.111	24	14.8	61.2
1090	200	19.2	20.8237	19.97	0.854	19.73	19.594	0.77	0.24	0.136	31.1688312	17.6623377	51.1688312
1095	205	18.75	20.5249	19.68	0.845	19.46	19.344	0.93	0.22	0.116	23.655914	12.4731183	63.8709677
1100	210	17.31	18.7068	17.9	0.807	17.77	17.695	0.59	0.13	0.075	22.0338983	12.7118644	65.2542373
1105	215	17.93	19.5778	18.76	0.818	18.56	18.46	0.83	0.2	0.1	24.0963855	12.0481928	63.8554217
1110	220	17.66	19.6179	18.79	0.828	18.58	18.457	1.13	0.21	0.123	18.5840708	10.8849558	70.5309735
1115	225	18.85	20.4266	19.59	0.837	19.44	19.344	0.74	0.15	0.096	20.2702703	12.972973	66.7567568
1120	230	18.35	19.8501	18.99	0.86	18.85	18.739	0.64	0.14	0.111	21.875	17.34375	60.78125
1125	235	18.68	21.065	20.34	0.725	20.05	19.811	1.66	0.29	0.239	17.4698795	14.3975904	68.1325301
1130	240	18.9	20.5098	19.62	0.89	19.48	19.385	0.72	0.14	0.095	19.4444444	13.1944444	67.3611111
1135	245	19.24	20.6915	19.87	0.822	19.74	19.628	0.63	0.13	0.112	20.6349206	17.7777778	61.5873016
1140	250	19.06	20.4112	19.59	0.821	19.45	19.393	0.53	0.14	0.057	26.4150943	10.754717	62.8301887
1145	255	17.11	18.743	17.71	1.033	17.58	17.486	0.6	0.13	0.094	21.6666667	15.6666667	62.6666667
1150	260	19.16	20.4507	19.77	0.681	19.64	19.587	0.61	0.13	0.053	21.3114754	8.68852459	70
1155	265	17.89	19.2667	18.52	0.747	18.39	18.348	0.63	0.13	0.042	20.6349206	6.66666667	72.6984127
1160	270	16.43	18.0906	17.23	0.861	17.05	16.961	0.8	0.18	0.089	22.5	11.125	66.375
1165	275	19.35	20.9735	20.16	0.814	19.99	19.928	0.81	0.17	0.062	20.9876543	7.65432099	71.3580247
1170	280	22.45	24.0307	23.24	0.791	23.11	23.068	0.79	0.13	0.042	16.4556962	5.3164557	78.2278481
1175	285	16.36	17.8399	17.1	0.74	16.97	16.944	0.74	0.13	0.026	17.5675676	3.51351351	78.9189189
1180	290	22.63	24.3882	23.57	0.818	23.41	23.331	0.94	0.16	0.079	17.0212766	8.40425532	74.5744681
1185	295	19.43	21.1242	20.15	0.974	19.95	19.867	0.72	0.2	0.083	27.7777778	11.5277778	60.6944444
1190	300	16.77	18.1464	17.35	0.796	17.2	17.124	0.58	0.15	0.076	25.862069	13.1034483	61.0344828

1200	310	18.01	20.1223	19.2	0.922	18.93	18.764	1.19	0.27	0.166	22.6890756	13.9495798	63.3613445
1205	315	16.71	18.8638	17.88	0.984	17.64	17.439	1.17	0.24	0.201	20.5128205	17.1794872	62.3076923
1210	320	16.57	18.9937	18.18	0.814	17.83	17.595	1.61	0.35	0.235	21.7391304	14.5962733	63.6645963
1215	325	17.93	19.6189	18.77	0.849	18.56	18.482	0.84	0.21	0.078	25	9.28571429	65.7142857
1220	330	17.28	19.1488	18.3	0.849	18.07	17.933	1.02	0.23	0.137	22.5490196	13.4313725	64.0196078
1225	335	16.99	18.5043	17.63	0.874	17.44	17.349	0.64	0.19	0.091	29.6875	14.21875	56.09375
1230	340	16.59	18.1072	17.2	0.907	17.04	16.96	0.61	0.16	0.08	26.2295082	13.1147541	60.6557377
1235	345	16.8	18.4198	17.57	0.85	17.37	17.261	0.77	0.2	0.109	25.974026	14.1558442	59.8701299
1240	350	16.73	18.1064	17.65	0.456	17.43	17.291	0.92	0.22	0.139	23.9130435	15.1086957	60.9782609
1245	355	16.18	17.863	17	0.863	16.75	16.632	0.82	0.25	0.118	30.4878049	14.3902439	55.1219512
1250	360	17.2	18.7511	17.92	0.831	17.72	17.598	0.72	0.2	0.122	27.7777778	16.9444444	55.2777778
1255	365	21.32	22.269	21.573	0.696	21.52	21.484	0.253	0.053	0.036	20.9486166	14.229249	64.8221344
1260	370	24.622	25.282	24.85	0.432	24.795	24.769	0.228	0.055	0.026	24.122807	11.4035088	64.4736842
1265	375	29.681	30.608	29.917	0.691	29.86	29.827	0.236	0.057	0.033	24.1525424	13.9830508	61.8644068
1270	380	11.364	12.4	11.608	0.792	11.555	11.519	0.244	0.053	0.036	21.7213115	14.7540984	63.5245902
1275	385	24.202	25.159	24.431	0.728	24.382	24.35	0.229	0.049	0.032	21.3973799	13.9737991	64.628821
1280	390	18.134	19.173	18.414	0.759	18.365	18.326	0.28	0.049	0.039	17.5	13.9285714	68.5714286
1285	395	24.523	25.503	24.772	0.731	24.724	24.69	0.249	0.048	0.034	19.2771084	13.6546185	67.0682731
1290	400	24.523	25.503	24.772	0.731	24.724	24.69	0.249	0.048	0.034	19.2771084	13.6546185	67.0682731
1295	405	20.923	21.939	21.208	0.731	21.157	21.12	0.285	0.051	0.037	17.8947368	12.9824561	69.122807
1300	410	24.057	25.069	24.34	0.729	24.29	24.252	0.283	0.05	0.038	17.6678445	13.4275618	68.9045936
1305	415	16.301	17.274	16.556	0.718	16.511	16.478	0.255	0.045	0.033	17.6470588	12.9411765	69.4117647
1310	420	22.666	23.67	22.915	0.755	22.864	22.832	0.249	0.051	0.032	20.4819277	12.8514056	66.6666667
1315	425	10.097	12.12	11.357	0.763	11.308	11.27	1.26	0.049	0.038	3.88888889	3.01587302	93.0952381
1320	430	11.527	12.57	11.776	0.794	11.728	11.698	0.249	0.048	0.03	19.2771084	12.0481928	68.6746988
1325	435	21.69	22.722	21.92	0.802	21.872	21.844	0.23	0.048	0.028	20.8695652	12.173913	66.9565217
1330	440	11.056	12.088	11.354	0.734	11.318	11.291	0.298	0.036	0.027	12.0805369	9.06040268	78.8590604
1335	445	17.318	18.35	17.586	0.764	17.534	17.495	0.268	0.052	0.039	19.4029851	14.5522388	66.0447761
1340	450	23.066	24.086	23.336	0.75	23.283	23.245	0.27	0.053	0.038	19.6296296	14.0740741	66.2962963
1345	455	23.047	24.043	23.247	0.796	23.187	23.164	0.2	0.06	0.023	30	11.5	58.5
1350	460	23.047	24.043	23.247	0.796	23.187	23.164	0.2	0.06	0.023	30	11.5	58.5
1355	465	15.816	16.783	15.993	0.79	15.94	15.928	0.177	0.053	0.012	29.9435028	6.77966102	63.2768362
1360	470	20.107	21.035	20.264	0.771	20.214	20.204	0.157	0.05	0.01	31.8471338	6.36942675	61.7834395
1365	475	16.594	17.559	16.766	0.793	16.714	16.704	0.172	0.052	0.01	30.2325581	5.81395349	63.9534884

1370	480	24.269	25.225	24.445	0.78	24.391	24.38	0.176	0.054	0.011	30.6818182	6.25	63.0681818
1375	485	25.174	26.116	25.344	0.772	25.295	25.288	0.17	0.049	0.007	28.8235294	4.11764706	67.0588235
1380	490	23.343	24.275	23.495	0.78	23.446	23.439	0.152	0.049	0.007	32.2368421	4.60526316	63.1578947
1385	495	22.325	23.268	22.478	0.79	22.423	22.42	0.153	0.055	0.003	35.9477124	1.96078431	62.0915033
1390	500	15.62	16.568	15.776	0.792	15.724	15.717	0.156	0.052	0.007	33.3333333	4.48717949	62.1794872
1395	505	24.617	25.509	24.766	0.743	24.714	24.711	0.149	0.052	0.003	34.8993289	2.01342282	63.0872483
1400	510	22.965	23.898	23.132	0.766	23.074	23.071	0.167	0.058	0.003	34.7305389	1.79640719	63.4730539
1405	515	21.806	22.673	21.947	0.726	21.889	21.884	0.141	0.058	0.005	41.1347518	3.54609929	55.3191489
1410	520	24.326	25.267	24.486	0.781	24.431	24.427	0.16	0.055	0.004	34.375	2.5	63.125
1415	525	24.618	25.543	24.769	0.774	24.716	24.712	0.151	0.053	0.004	35.0993377	2.64900662	62.2516556
1420	530	20.584	21.505	20.731	0.774	20.681	20.677	0.147	0.05	0.004	34.0136054	2.72108844	63.2653061
1425	535	15.955	16.771	16.085	0.686	16.04	16.04	0.13	0.045	0	34.6153846	0	65.3846154
1430	540	24.672	25.603	24.834	0.769	24.786	24.783	0.162	0.048	0.003	29.6296296	1.85185185	68.5185185
1435	545	24.809	25.65	24.952	0.698	24.908	24.904	0.143	0.044	0.004	30.7692308	2.7972028	66.4335664
1440	550	20.674	21.616	20.828	0.788	20.775	20.771	0.154	0.053	0.004	34.4155844	2.5974026	62.987013
1445	555	14.542	15.507	14.718	0.789	14.661	14.655	0.176	0.057	0.006	32.3863636	3.40909091	64.2045455
1450	560	23.34	24.274	23.502	0.772	23.444	23.44	0.162	0.058	0.004	35.8024691	2.4691358	61.7283951
1455	565	23.713	24.674	23.875	0.799	23.824	23.817	0.162	0.051	0.007	31.4814815	4.32098765	64.1975309
1460	570	22.744	23.727	22.927	0.8	22.87	22.863	0.183	0.057	0.007	31.147541	3.82513661	65.0273224
1465	575	20.355	21.311	20.527	0.784	20.475	20.468	0.172	0.052	0.007	30.2325581	4.06976744	65.6976744
1470	580	16.36	17.228	16.516	0.712	16.461	16.45	0.156	0.055	0.011	35.2564103	7.05128205	57.6923077
1475	585	16.852	17.823	17.011	0.812	16.954	16.947	0.159	0.057	0.007	35.8490566	4.40251572	59.7484277
1480	590	18.492	19.433	18.644	0.789	18.59	18.585	0.152	0.054	0.005	35.5263158	3.28947368	61.1842105
1485	595	18.492	19.433	18.644	0.789	18.59	18.585	0.152	0.054	0.005	35.5263158	3.28947368	61.1842105
1490	600	20.9	21.803	21.055	0.748	21.001	20.998	0.155	0.054	0.003	34.8387097	1.93548387	63.2258065
1495	605	28.94	29.914	29.133	0.781	29.08	29.07	0.193	0.053	0.01	27.4611399	5.18134715	67.357513
1500	610	19.43	20.39	19.633	0.757	19.581	19.58	0.203	0.052	0.001	25.6157635	0.49261084	73.8916256
1505	615	17.66	18.639	17.855	0.784	17.806	17.8	0.195	0.049	0.006	25.1282051	3.07692308	71.7948718
1510	620	17.333	18.309	17.522	0.787	17.47	17.463	0.189	0.052	0.007	27.5132275	3.7037037	68.7830688
1515	625	19.251	20.184	19.42	0.764	19.387	19.384	0.169	0.033	0.003	19.5266272	1.77514793	78.6982249
1520	630	17.924	18.814	18.072	0.742	18.025	18.015	0.148	0.047	0.01	31.7567568	6.75675676	61.4864865
1525	635	17.855	18.845	18.035	0.81	17.988	17.979	0.18	0.047	0.009	26.1111111	5	68.8888889
1530	640	17.225	18.16	17.389	0.771	17.343	17.328	0.164	0.046	0.015	28.0487805	9.14634146	62.804878
1535	645	17.225	18.16	17.389	0.771	17.343	17.328	0.164	0.046	0.015	28.0487805	9.14634146	62.804878

DECLARATION

I the undersigned declare that this Thesis is my original work and has not been presented for any degree in any University and all the sources of materials used for the Thesis has been duly acknowledged.

Name Zelalem Kubsa

Signature